Master Thesis

in

Computer Simulation in Science

by

Alois Grimbach

Improvement of the static-light axial current on the lattice

February 19, 2008

Referees:
Prof. Dr.F.Knechtli
Dr. Ch.Hölbling

Bergische Universitaet Wuppertal
FB-C
Institut fuer Theoretische Physik

Contents

1 Introduction

Since Democritus and Anaxagoras proposed smallest particles called *atoms*, the idea of the existence of basic constituents of matter has led to more and more sophisticated and exact descriptions of nature. Today, elementary particles are described by the Standard Model of Particle Physics which has evolved in the 1970's. The basic constituents are fermions, namely quarks and leptons, carrying spin $\frac{1}{2}$ and gauge bosons carrying spin 1 which act as intermediaries for the interactions between particles. The interactions can be described by gauge field theories. Electromagnetism is described by QED which is invariant under the symmetry group $U(1)$. Glashow, Salam and Weinberg showed that the weak interaction together with Quantum Electrodynamics (QED) can be described by the theory of electro-weak interaction. The remaining strong interaction can be described by Quantum Chromodyamics (QCD) which is locally invariant under transformations of the $SU(3)$ colour group. The formulation of QCD as a $SU(3)$ group implies 3 chromatic degrees of freedom for the quarks and 8 different gluons as gauge bosons according to the number of generators of the Lie Algebra.

QCD is an asymptotic free theory, i.e. the coupling constant is dependent on the distance and quarks become quasi free particles at very small distances. One can then speak about a high energy regime (HER), because small distances correspond to large momenta in momentum space. In this HER, perturbation theory (PT) is very successful. On the other hand, at large distances the coupling constant is believed to become that strong to cause a confinement which aligns with not observing any free quarks. In this low energy regime, pertubation theory breaks down. However, in 1974 Wilson developed a powerful non-pertubative method called *Lattice Gauge Theory* or *Lattice QCD*. It allows computer-based numerical simulations which work out a Monte Carlo integration of the Euclidean path integral. Those simulations in fact show a quark confinement. Non-pertubative calculations allow also to determine hadronic spectra and matrix elements between hadronic states. Due to the usage of Euclidean time, the price for this elegant solution is that direct calculations are limited to static properties of QCD. Considerations in Minkowski spacetime have to be deducted and are much more involved. But open questions like the quark masses, spontaneous chiral symmetry breaking, quark-gluon plasma, phase transitions, etc. can be investigated.

In Lattice QCD, the spacetime continuum is discretised on a 4-dimensional Euclidean hypercubic lattice. The gauge action is then described by a sum over oriented plaquettes on the lattice. Those plaquettes are elementary squares and consist of closed loops of gauge links which are members of the $SU(3)$ group and which are denoted by $U_\mu(x)$. The link $U_\mu(x)$ connects the point x with the neighbour point $x + a\hat{\mu}$, where $\hat{\mu}$ defines a direction in the μ-th lattice direction. The crucial point is that this formulation is both gauge invariant and reproduces the Yang-Mills theory in the continuum limit.

In contrast to the gauge fields, the situation for fermions becomes more involved. The naive formulation of a gauge invariant action leads to the non-physical effect of fermion doubling on the lattice. One possible and here adopted method to avoid those doublers are Wilson fermions which suppress the emerging poles by a counterterm that vanishes in the continuum limit. This is only

possible by the price of sacrifying chiral symmetry for massless fermions[1]. The Wilson fermions have corrections of order a which deteriorate the convergence to the continuum limit. However, these $\mathcal{O}(a)$ corrections can be eliminated by an improvement scheme which was first proposed by Symanzik [24] [25]. The action may then be improved by an additional term, the Sheikoleslami-Wohlert clover term, which cancels the $\mathcal{O}(a)$ corrections of the fermionic action. We have then arrived at an $\mathcal{O}(a)$ improved action without fermion doublers. When computing correlators on the lattice, according to Symanzik, complete $\mathcal{O}(a)$ improvement is achieved by improving operators separately in order avoid additional $\mathcal{O}(a)$ corrections. Counterterms can be won by examining symmetries, merely the according coefficients have to be determined to achieve the desired improvement.

In this master thesis, the $\mathcal{O}(a)$ improvement of the static-light axial current is investigated.

The static-light axial current is induced by a meson consisting of a light and a static quark. For the light quark, the above introduced description of a Wilson fermion is adopted whereas the static quark is treated in Heavy quark effective theory (HQET), following a proposal of Eichten and Hill for the static quark action ([15], EH action). The improvement coefficient for the static-light axial current can be determined non-pertubatively, but for a first guess one may be interested in computing the coefficients in pertubation theory. Such a calculation also provides a non-trivial check of the Symanzik programme for the improved fields and the improved action. The pertubative expansion of the improvement coefficient of the EH action enters also in the estimation of smeared actions like the HYP action via hybrid methods [13]. These hybrid methods can be treated as effective estimators neither giving a purely one-loop nor a fully non-pertubative value. They are affected by $\mathcal{O}(g_0^4)$ systematic errors. This error can more precisely be estimated only when the one-loop coefficient of at least one specific choice of HYP parameters is known.

The HYP action arises from smearing the original (thin) link $U_\mu(x)$ by decorating it with staples in each direction. The smeared HYP links stay within the attached hypercubes, i.e. staples that would overstep the borders of the hypercubes during contruction are disregarded. Thus, HYP smearing looks superior to other techniques in that it preserves locality to a high degree. This was first proved to be remarkably effective when studying the quark/anti-quark potential with improved statistical precision [10]. The use of HYP links to measure the static potential from Wilson loops reduced the statistical errors and improved the rotational invariance.

The origin of the statistical improvement has been subsequently identified as due to a strong reduction of the static-self energy for appropriate choices of the HYP parameters [13]. Since the binding energy of mesons consisting of a static and a light quark is amplified by self-energy contributions, the adoption of HYP links in the static action has allowed for lattice simulations with smaller binding energy, thus triggering an exponential improvement of the signal-to-noise ratio of the meson correlators at large time distances. This helped significantly in several applications of HQET, e.g. [4] to [9].

[1]The need of this sacrifice is theoretically stated by the Nielson-Ninomiya theorem.

The aim of this thesis is the analytical determination of the improvement coefficient for the HYP action in PT at one-loop order, i.e. $c_{\mathrm{A}}^{\mathrm{stat}\,(1)}$. The framework of the Schrödinger Functional (SF) is chosen. The SF allows to define a correlation function so that on the one hand, the sought improvement coefficient is contained, and on the other hand, unwelcome renormalisation constants like the divergent self-energy are cancelled. The SF imposes Dirichlet boundary conditions in the temporal direction. $\mathcal{O}(a)$ improvement of the action in the SF will therefore contain additional boundary contributions for the light quark which will have to be taken into account. Those of course do not affect the value of $c_{\mathrm{A}}^{\mathrm{stat}\,(1)}$ as it is independent of the chosen geometry to compute it. Hence, the work is organised as follows:

After this introduction, basic definitions are given in the second chapter and the HYP smearing is being formally introduced. Thereupon, the basic concept of $\mathcal{O}(a)$ improvement following the Symanzik improvement scheme is presented. In the third chapter, the Schrödinger Functional is described. Feynman rules in time momentum representation including $\mathcal{O}(a)$ improvement are derived for the needed correlators. After having reviewed some effects of $SU(3)$ projections used in the HYP smearing, the Feynman rules for HYP smearing are set up. This enables us to determine, $c_{\mathrm{A}}^{\mathrm{stat}\,(1)}$ for the EH action for reference and for various choices of the HYP parameters in chapter 4. Finally, in chapter 5 the self energy for different actions is determined. It is then investigated as a function of the HYP parameters and the global minimum is identified.

2 The Static-light Current on the Lattice

2.1 On Actions and Currents

In order to set up a coherent discussion, the underlying definitions shall be given in this chapter. Firstly, we restrict ourselves to a four dimensional infinite hypercubic lattice with lattice spacing a. The here used basic notations according to QCD on the lattice can be found in Appendix A.1.
The Grassmann-valued fields $\Psi(x)$ and $\bar{\Psi}(x)$ are associated with the lattice sites whereas the gauge links $U_\mu(x)$ reside on the nearest-neighbour links in direction μ. Gauge invariance is assured by the definitions given in Appendix A.1. This set-up allows us to consider the total action $S[U, \bar{\Psi}, \Psi]$ which can be split into a fermionic part $S_F[U, \bar{\Psi}, \Psi]$ and a gauge part $S_G[U]$

$$S[U, \bar{\Psi}, \Psi] = S_F[U, \bar{\Psi}, \Psi] + S_G[U] \tag{2.1}$$

with the gauge action

$$S_G[U] = \frac{1}{g_0^2} \sum_p \mathrm{tr}\left\{1 - \mathrm{U(p)}\right\} \tag{2.2}$$

and with g_0 being the bare coupling constant. $U(p)$ denotes the parallel transporter around the oriented plaquette p.

As we want to deal with the static-light current, the fermionic action $S_F[U, \bar{\Psi}, \Psi]$ consists of a static and a relativistic contribution which we need to consider separately. The relativistic (=light) fermionic action on the lattice is described by the Wilson action

$$S_l[\psi_l, \bar{\psi}_l] = a^4 \sum_x \bar{\Psi}_l(x)(D + m_0)\Psi_l(x) \tag{2.3}$$

with m_0 being the bare quark mass. D denotes the Wilson-Dirac operator and is given by

$$D = \frac{1}{2}\left\{\gamma_\mu(\nabla_\mu^* + \nabla_\mu) - a\nabla_\mu^*\nabla_\mu\right\} \tag{2.4}$$

It contains the covariant lattice derivative operators owing to the gauge invariance of the theory. The second term in Eq. (2.4) is called the Wilson term which cancels in the continuum limit $a \to 0$. It is introduced to avoid fermion doublers arising from the lattice discretisation by shifting the spurious poles of the propagator by an amount proportional to $\frac{1}{a}$. This is achieved by the price of breaking chiral symmetry on the lattice for vanishing quark masses. The above appearing covariant derivatives ∇_μ and $\nabla_\mu*$ are defined in Appendix A.1.

Considering heavy quarks, i.e. quarks whose mass are large compared to the intrinsic scale of QCD, relativistic physics does not yield much input. Let us e.g. consider a b-quark with a mass m_b. We are then faced with a restriction $a < \frac{1}{m_b}$ [7] for describing a b-quark by the standard relativistic QCD Lagrangian. In terms of computational effort, this seems to be far out of reach for dynamical simulations. Heavy quarks are therefore described by a so called Heavy Quark Effective Theory (HQET). This theory starts from the static approximation describing the asymptotics at $m_0 \to \infty$. The higher contributions are organised as powers of the inverse quark mass. This leads to an existing

continuum limit independent of the chosen regularisation. For a further description of this procedure, pls. refer to e.g. [5].
Static quarks are represented by a decoupled pair of fermion fields $(\psi_{\mathrm{h}}, \psi_{\bar{\mathrm{h}}})$, propagating forward and backward in time, respectively. There is no spatial dynamics since the heavy quark does not move in space. The temporal dynamics of the fields is governed by the lattice actions [15]

$$S_h[\psi_{\mathrm{h}}, \overline{\psi}_{\mathrm{h}}] = a^4 \sum_x \overline{\psi}_{\mathrm{h}}(x) \nabla_0^* \psi_{\mathrm{h}}(x) \tag{2.5}$$

$$S_{\bar{h}}[\psi_{\bar{\mathrm{h}}}, \overline{\psi}_{\bar{\mathrm{h}}}] = -a^4 \sum_x \overline{\psi}_{\bar{\mathrm{h}}}(x) \nabla_0 \psi_{\bar{\mathrm{h}}}(x) \tag{2.6}$$

The field $\psi_{\mathrm{h}}(\overline{\psi}_{\mathrm{h}})$ can be thought of as the annihilator (creator) of a heavy quark. Similarly, $\psi_{\bar{\mathrm{h}}}(\overline{\psi}_{\bar{\mathrm{h}}})$ creates (annihilates) a heavy antiquark. Each field is represented by a four-component Dirac vector, yet only half of the components play a dynamical role. In order to refelect this fact, the projectors P_+ and P_- are introduced:

$$\begin{aligned} P_+ &= \frac{1}{2}(1 + \gamma_0) \\ P_- &= \frac{1}{2}(1 - \gamma_0) \end{aligned} \tag{2.7}$$

leading to the static projection constraints

$$\begin{aligned} P_+ \psi_{\mathrm{h}} &= \psi_{\mathrm{h}} \ , \quad & P_- \psi_{\mathrm{h}} &= 0 \\ \overline{\psi}_{\mathrm{h}} P_+ &= \overline{\psi}_{\mathrm{h}} \ , \quad & \overline{\psi}_{\mathrm{h}} P_- &= 0 \\ P_- \psi_{\bar{\mathrm{h}}} &= \psi_{\bar{\mathrm{h}}} \ , \quad & P_+ \psi_{\bar{\mathrm{h}}} &= 0 \\ \overline{\psi}_{\bar{\mathrm{h}}} P_- &= \overline{\psi}_{\bar{\mathrm{h}}} \ , \quad & \overline{\psi}_{\bar{\mathrm{h}}} P_+ &= 0 \end{aligned} \tag{2.8}$$

This set-up provides the basic ingredients to treat the static effective theory in the Schrödinger functional.
Hereafter, the axial current and vector current shall be defined. Especially the axial current will help to define the correlation functions which we will need later. In the case of SU(2) isopsin, the local isovector axial current is defined by

$$A_\mu^\alpha(x) = \overline{\Psi}(x) \gamma_\mu \gamma_5 \frac{1}{2} \tau^\alpha \Psi(x) \tag{2.9}$$

whereby the Pauli matrix τ^α acts on the flavour indices of the quark field only. The light-light current is partially conserved, e.g it satisfies the PCAC relation [4], [5]

$$\frac{1}{2}(\partial_\mu^* + \partial_\mu) A_\mu^\alpha(x) = 2 m_p P^\alpha(x) \tag{2.10}$$

with m_p being the PCAC mass and the axial density P^α defined as

$$P^\alpha(x) = \overline{\Psi}(x) \gamma_5 \frac{1}{2} \tau^\alpha \Psi(x) \tag{2.11}$$

The static axial current is defined through a path integral with the total action (Eq. (2.1)) as [1]

$$A_0^{stat} = \overline{\Psi}_l(x)\gamma_0\gamma_5\Psi_h(x) \tag{2.12}$$

It consists of a heavy quark and a relativistic anti-quark field. Due to missing isospin, no Pauli matrices appear.

For the sake of completeness, the definition of the relativistic vector current shall be given as

$$V_\mu^\alpha(x) = \overline{\Psi}(x)\gamma_\mu\frac{1}{2}\tau^\alpha\Psi(x) \tag{2.13}$$

as well as for the static vector current

$$V_0^{stat} = \overline{\Psi}_l(x)\gamma_0\Psi_h(x) \tag{2.14}$$

2.2 Extension to HYP smearing

The static action (see Eq. (2.5),Eq. (2.6)) has a functional dependence upon the parallel transporter U_0. Extending the EH action to the HYP action [14], this temporal link shall be substituted by a temporal HYP link W_0.

According to the original definition [10], the HYP link is obtained through a three-step recursive APE smearing projected onto $SU(3)$ after each step. The original thin link is then decorated with staples belonging to its surrounding hypercubes, i.e.

$$W_\mu(x) \equiv W_\mu^{(3)}(x) = \mathcal{P}_{\mathrm{SU(3)}}[(1-\alpha_1)U_\mu(x)+ \\ + \frac{\alpha_1}{6}\sum_{\pm\nu\neq\mu} W_{\nu;\mu}^{(2)}(x)W_{\mu;\nu}^{(2)}(x+a\hat{\nu})W_{\nu;\mu}^{(2)}(x+a\hat{\mu})^\dagger]\,, \tag{2.15}$$

$$W_{\mu;\nu}^{(2)}(x) = \mathcal{P}_{\mathrm{SU(3)}}[(1-\alpha_2)U_\mu(x)+ \\ + \frac{\alpha_2}{4}\sum_{\pm\rho\neq\nu,\mu} W_{\rho;\nu\mu}^{(1)}(x)W_{\mu;\rho\nu}^{(1)}(x+a\hat{\rho})W_{\rho;\nu\mu}^{(1)}(x+a\hat{\mu})^\dagger]\,, \tag{2.16}$$

$$W_{\mu;\nu\rho}^{(1)}(x) = \mathcal{P}_{\mathrm{SU(3)}}[(1-\alpha_3)U_\mu(x)+ \\ + \frac{\alpha_3}{2}\sum_{\pm\eta\neq\rho,\nu,\mu} U_\eta(x)\; U_\mu(x+a\hat{\eta})U_\eta(x+a\hat{\mu})^\dagger]\,, \tag{2.17}$$

where $U_{-\mu}(x) = U_\mu^\dagger(x-a\hat{\mu})$. In Eq. (2.15), U_μ denotes the fundamental gauge link and the index ν in $W_{\mu;\nu}^{(2)}$ indicates that the fat link at location x and direction μ is not decorated with staples extending in direction ν. The decorated link $W_{\mu;\nu}^{(2)}$ is then constructed in Eq. (2.16) with a modified APE blocking from an other set of decorated links, where the indices $\rho\,\nu$ indicate that the fat link $W_{\mu;\rho\,\nu}^{(1)}$ in direction μ is not decorated with staples extending in the ρ or ν directions. Finally, the decorated link $W_{\mu;\rho\,\nu}^{(1)}$ is constructed in Eq. (2.17) from the original thin links with a modified APE blocking step where only the two staples orthogonal to μ, ν and ρ are used. After each smearing step the new fat link is projected onto $SU(3)$.

The coefficients $\vec{\alpha} = (\alpha_1, \alpha_2, \alpha_3)$ need to be specified to define the combination of differently smeared links in the construction of the HYP link. In the following we will discuss two possible the choices which we will refer to

as the HYP1 action:

$$\vec{\alpha}_{HYP1} = (0.75, 0.6, 0.3) \tag{2.18}$$

and the HYP2 action:

$$\vec{\alpha}_{HYP2} = (1.0, 1.0, 0.5) \tag{2.19}$$

HYP smearing is constructed by three steps of APE smearing which is characterised by a link not projected onto SU(3). Therefore, the APE action cannot be generated for any choice of the HYP parameters Nevertheless, SU(3) projection is ineffective at one-loop order of pertubation theory [22] which will play a role at a later step when describing the Feynman diagrams at one-loop order. Therefore, the APE action can be written as choice of HYP parameters

$$\vec{\alpha}_{APE} = (1, 0, 0) \tag{2.20}$$

The Eichten Hill action obviously does not contain any smearing and is decribed by

$$\vec{\alpha}_{EH} = (0, 0, 0) \tag{2.21}$$

2.3 O(a) improvement

Due to the disretisation on the lattice, cutoff effects in lattice QCD are inevitable and can be rather large on the accessible lattices. These effects are proportional to the lattice spacing a. However, an improvement to order $\mathcal{O}(a^2)$ is possible by adding local counterterms both to lattice action and axial current cancelling the $\mathcal{O}(a)$ part of the cutoff effects. This concept is called $\mathcal{O}(a)$ improvement and was first introduced by Symanzik [24], [25]. For a pedagogical introduction see e.g. [5]. The counterterms have to be adjusted with adequate coefficients to achieve the desired improvement. Those coefficients can be expanded in pertubation theory. Through the complete improvement of the theory, one achieves that renormalised on-shell quantities like matrix elements of the axial current approach the continuum limit with a rate proportional to a^2, i.e. the discretisation error is scaled down from $\mathcal{O}(a)$ to $\mathcal{O}(a^2)$.

2.3.1 Actions

As stated above, a momentum cutoff arises when bringing a field theory on the lattice. One may consider this momentum cutoff in a purely mathematical sense as a scale of new physics and describe it by a continuum effective theory. This means, the lattice theory is described by a continuum theory containing interaction terms which depend on polynomials in a. The lowest order term of this continuum effective theory describes the continuum field theory. By adjusting the lattice action, one can cancel the higher interaction terms and the desired continuum description survives. This approach might become more evident by having a look at the effective action

$$S_{eff} = \int d^4x \left[\mathcal{L}_0(x) + \sum_{k=1}^{\infty} a^k \mathcal{L}_k(x) \right] \tag{2.22}$$

$\mathcal{L}_0(x)$ denotes the continuum Lagrangian, whereas $\mathcal{L}_k(x)$ consists of linear combinations of operators of dimension $4+k$. We restrict ourselves on $\mathcal{L}_1(x)$ since all other terms $\mathcal{L}_k(x)$, $k > 1$ vanish faster than $\mathcal{L}_1(x)$ when approaching the continuum limit. Taking into account all symmetries of the lattice action, $\mathcal{L}_1(x)$ might be represented as a linear combination of the fields

$$\mathcal{O}_1 = \overline{\Psi}\, i\sigma_{\mu\nu} F_{\mu\nu} \Psi \tag{2.23}$$

$$\mathcal{O}_2 = \overline{\Psi} D_\mu D_\mu \Psi + \overline{\Psi} \overleftarrow{D}_\mu \overleftarrow{D}_\mu \Psi \tag{2.24}$$

$$\mathcal{O}_3 = m \ \mathrm{tr}\left\{ \mathrm{F}_{\mu\nu} \mathrm{F}_{\mu\nu} \right\} \tag{2.25}$$

$$\mathcal{O}_4 = m \left\{ \overline{\Psi} \gamma_\mu D_\mu \Psi - \overline{\Psi} \overleftarrow{D}_\mu \gamma_\mu \Psi \right\} \tag{2.26}$$

$$\mathcal{O}_5 = m^2 \overline{\Psi} \Psi \tag{2.27}$$

Here, D_μ and $\overleftarrow{D}_\mu$ denote the right and left covariant derivatives in the continuum as defined by

$$D_\mu \Psi(x) = (\partial_\mu + i g_0 A_\mu) \Psi(x) \tag{2.28}$$

$$\overline{\Psi}(x) \overleftarrow{D}_\mu = \overline{\Psi}(x) (\overleftarrow{\partial}_\mu - i g_0 A_\mu) \tag{2.29}$$

The above basis of fields can be further simplified. One may thereby distinguish between the actions for the light and static fermions which will lead to different $\mathcal{O}(a)$ improvement terms.

For the light action, one can follow the argumentation of [5] and construct a minimal independent basis by applying the equations of motion, i.e. it holds

$$\mathcal{O}_1 - \mathcal{O}_2 + 2\mathcal{O}_5 = 0, \qquad \mathcal{O}_4 + 2\mathcal{O}_5 = 0 \tag{2.30}$$

which allows to cancel e.g. $\mathcal{O}_2$ and $\mathcal{O}_4$. For the $\mathcal{O}(a)$ improvement, we want to eliminate the contribution of the effective Lagrangian $\mathcal{L}_1$ which is a linear combination of the reduced basis of fields $\mathcal{O}_1$, $\mathcal{O}_3$ and $\mathcal{O}_5$. The local counterterm we will have to add on the lattice then obviously takes the form:

$$\delta S = a^5 \sum_x \left\{ c_1 \hat{\mathcal{O}}_1(x) + c_3 \hat{\mathcal{O}}_3(x) + c_5 \hat{\mathcal{O}}_5(x) \right\} \tag{2.31}$$

with $\hat{\mathcal{O}}_1$, $\hat{\mathcal{O}}_3$ and $\hat{\mathcal{O}}_5$ being some lattice representation of the fields $\mathcal{O}_1$, $\mathcal{O}_3$ and $\mathcal{O}_5$. In pertubation theory, the coefficients c_i are calculable polynomials of gauge coupling constant g_0 [2] und thus of the logarithmic lattice spacing ln(a) whereas the fields are independent on a.
The discretisation $\hat{\mathcal{O}}_i(x)$ of the fields $\mathcal{O}_i$ has discretisation ambiguities of order a^2. Especially, we may choose the discretised counterparts $\hat{\mathcal{O}}_3(x)$ and $\hat{\mathcal{O}}_5(x)$ of the fields $\mathcal{O}_3$ and $\mathcal{O}_5(x)$ by the plaquette field and the local scalar density that appear in the action for Wilson fermions Eq. (2.3). The consideration of this terms can therefore be achieved by rescaling the bare coupling and mass by a factor $1 + \mathcal{O}(am)$, i.e.

$$\tilde{g}_0^2 = (1 + b_g a m_q) g_0^2 \tag{2.32}$$

$$\tilde{m}_q = (1 + b_m a m_q) m_q \tag{2.33}$$

The remaining improvement contribution arises from $\mathcal{O}_1(x)$. On the lattice, it may be represented by

$$\hat{\mathcal{O}}_1(x) = \overline{\Psi}(x) i\, \sigma_{\mu\nu} \hat{F}_{\mu\nu}(x) \Psi(x) \tag{2.34}$$

with the discretised field strength tensor

$$\hat{F}_{\mu\nu}(x) = \frac{1}{8a^2} \left\{ Q_{\mu\nu}(x) - Q_{\nu\mu}(x) \right\} \tag{2.35}$$

The improved action for light fermions thus reads

$$S_{impr} = S_l[\psi_l, \bar{\psi}_l] + a^5 \sum_x c_{sw} \overline{\Psi}(x) \frac{i}{4} \sigma_{\mu\nu} \hat{F}_{\mu\nu}(x) \Psi(x) \tag{2.36}$$

and is is known as Sheikoleslami-Wohlert action. It contains the clover terms $\sigma_{\mu\nu}\hat{F}_{\mu\nu}(x)$. $Q_{\mu\nu}(x)$ denotes the sum of the four adjacent plaquette loops.

[2] The gauge coupling in turn is dependent on the lattice spacing a, due to the asymptotic freedom it holds $a \propto exp\left\{-const/g_0^2\right\}$

For the heavy quark, the resulting basis of fields is a different one because one can find additional symmetries in HQET. Furthermore, the equations of motion lead to different relations for the on-shell variables.
Additional symmetries for the static theory comprise firstly the heavy quark spin symmetry [1]. The action is invariant under the transformation

$$\Psi_h \to V\Psi_h \tag{2.37}$$
$$\overline{\Psi}_h \to \overline{\Psi}_h V^{-1} \tag{2.38}$$

with

$$V = e^{-i\Phi_i \epsilon_{ijk}\sigma_{jk}} \tag{2.39}$$

and transfomation parameters Φ_i. $T^i = \epsilon_{ijk}T^k$ form generators of the $SU(2)$ group and fulfil the commutation relations $\left[T^i, T^j\right] = \epsilon_{ijk}T^k$. This symmetry makes spatial clover contributions according to Eq. (2.23) to a static improvement term vanish, i.e., terms of the form $\overline{\Psi}_h\sigma_{jk}F_{jk}\Psi_h$ do not fulfil the heavy quark spin symmetry. Moreover, the temporal clover term $\overline{\Psi}_h\sigma_{oj}F_{oj}\Psi_h$ vanishes due to $P_+\sigma_{oj}P_+ = 0$.
The spatial part $\overline{\Psi}_h D_j D_j \Psi_h + \overline{\Psi}_h \overleftarrow{D}_j \overleftarrow{D}_j \Psi_h$ of $\mathcal{O}_2$ in Eq. (2.24) does not fulfil the local conservation of the heavy quark flavour number. This is may be formulated as the invariance of the action under

$$\Psi_h \to e^{i\eta(\mathbf{x})}\Psi_h \tag{2.40}$$
$$\overline{\Psi}_h \to \overline{\Psi}_h e^{-i\eta(\mathbf{x})} \tag{2.41}$$

with an arbitrary space dependent parameter $\eta(\mathbf{x})$. Physically, this conservation claims that the static quark does not move in space. Accordingly, the spatial parts of $\mathcal{O}_2$ do not contribute.
Finally, the application of the equations of motion

$$\begin{aligned} D_0\Psi_h(x) &= 0 \\ \overline{\Psi}_h(x)\overleftarrow{D}_0 &= 0 \end{aligned} \tag{2.42}$$

make the temporal parts of $\mathcal{O}_2$ and $\mathcal{O}_4$ vanish.
We are then left with the contribution of the field $\mathcal{O}_3$ and get for the improved action for the heavy quark fields

$$S_{impr,h} = S_h[\psi_h, \bar{\psi}_h] + a^5 \sum_x b_h m_q^2 \overline{\Psi}_h(x)\Psi_h(x) \tag{2.43}$$

The coefficient b_h is a function of the bare coupling g_0. m_q denotes the subtracted bare quark mass (see section 4.1). The improvement of the static action thus results in the addition of a mass counterterm to the unimproved heavy action.
In the Schrödinger functional (SF), an additional boundary improvement term will arise for the improved light action which will be given in the next chapter. The improved static action in the SF does not obtain a boundary term and thus does not change its form in the SF.

2.3.2 Axial Current

After having improved the actions, one needs, to improve the fields to achieve complete $\mathcal{O}(a)$ improvement. The basis that fulfils the appropriate dimension and symmetry properties for the definition of the static-light axial current (see Eq. (2.12)) consists of

$$(\delta A_0^{stat})_1 = \overline{\Psi}_l \overleftarrow{D}_j \gamma_j \gamma_5 \Psi_h \tag{2.44}$$

$$(\delta A_0^{stat})_2 = \overline{\Psi}_l \gamma_5 D_0 \Psi_h \tag{2.45}$$

$$(\delta A_0^{stat})_3 = \overline{\Psi}_l \overleftarrow{D}_0 \gamma_5 \Psi_h \tag{2.46}$$

$$(\delta A_0^{stat})_4 = m \overline{\Psi}_l \gamma_0 \gamma_5 \Psi_h \tag{2.47}$$

Like for the quark fields, local conservation of the flavour number can be applied to the axial current, i.e.

$$A_0^{stat}(x) \to e^{i\eta(\mathbf{x})} A_0^{stat}(x) \tag{2.48}$$

with some space dependent parameter $\eta(\mathbf{x})$. This makes the terms containing $D_j \Psi_h$ vanish as they violate Eq. (2.48). The equations of motion Eq. (2.42) eliminate $(\delta A_0^{stat})_2$. $(\delta A_0^{stat})_1$, $(\delta A_0^{stat})_3$ and $(\delta A_0^{stat})_4$ are connected by the Dirac field equations for the light quark. Therefore one more field, e.g.$(\delta A_0^{stat})_3$ can be eliminated. $(\delta A_0^{stat})_4$ may be absorbed in the renormalisation constant. We are then left with the contribution related to $(\delta A_0^{stat})_1$. Writing $D_j = \frac{1}{2}(\overleftarrow{\nabla}_j + \overleftarrow{\nabla}_j^*)$ on the lattice, the final expression for the improved axial current on the lattice is

$$\begin{aligned}(A_I^{stat})_0 &= A_0^{stat} + a c_{\mathrm{A}}^{\mathrm{stat}} \delta A_0^{stat} \\ &= A_0^{\mathrm{stat}} + a c_{\mathrm{A}}^{\mathrm{stat}} \overline{\Psi}_l \gamma_j \gamma_5 \frac{1}{2} (\overleftarrow{\nabla}_j + \overleftarrow{\nabla}_j^*) \Psi_h\end{aligned} \tag{2.49}$$

$(A_I^{stat})_0$ may be renormalised as

$$(A_R^{stat})_0 = Z_{\mathrm{A}}^{\mathrm{stat}} (1 + b_{\mathrm{A}}^{\mathrm{stat}} a m_q)(A_I^{stat})_0 \tag{2.50}$$

3 The Static-light Current in the Schrödinger Functional

3.1 A very first look at the Schrödinger Functional

This introductory section shall describe the idea of the Schrödinger Functional (SF) at a glance. A formal description of the SF can be found in the original papers [21] and [2]. One should not expect formal completeness at this point as the focus is set onto the basic and for our case interesting properties of the SF.

The SF is a construction of a field theory with fixed boundary conditions in Euclidean time. It consists of a hypercubic lattice $L^3 \times T$ with periodic boundary conditions in spatial directions but with a finite extent in temporal direction. L and T are integer multiples of the lattice spacing a. PBC can be described by a phase shift Θ_k in spatial directions like defined in Eq. (A.15) to Eq. (A.17) in Appendix A. Different angles Θ_k are going to be used in the simulations for the determination of $c_{\mathrm{A}}^{\mathrm{stat}}$. We impose Dirichlet boundary conditions in the temporal direction by demanding fixed values for the fermionic boundary fields $\rho(\mathbf{x})$ and $\bar{\rho}(\mathbf{x})$ at $x_0 = 0$ as well as $\rho'(\mathbf{x})$ and $\bar{\rho}'(\mathbf{x})$ at $x_0 = T$. One can extend the definition of fields to an infinite lattice by demanding $\Psi(x) = \overline{\Psi}(x) = 0$ if $x_0 < 0$ or $x_0 > T$. The gauge links for $x_0 < 0$ or $x_0 > T$ fulfil $U_\mu(x) = \mathbb{1}$, i.e. no gauge fields are present. [3]. Fermion and gauge fields are defined in the same manner as on the full torus.

The projectors P_+ and P_- select the components that are used when applying the Dirac Wilson operator, i.e. two of the four spinor components $\Psi_i(x), i \in [1..4]$ at the boundaries. For consistency reasons, the complementary projections are set to zero. This gives us for the light quark fields

$$\begin{aligned} &P_+\Psi_l(x)|_{x_0=0} = \rho(\mathbf{x}) \quad \text{fixes } \Psi_{\mathrm{l},1}(\mathrm{x}), \Psi_{\mathrm{l},2}(\mathrm{x}) \text{ at } \mathrm{x}_0 = 0 \\ &P_-\Psi_l(x)|_{x_0=0} = 0 \\ &P_-\Psi_l(x)|_{x_0=T} = \rho'(\mathbf{x}) \quad \text{fixes } \Psi_{\mathrm{l},3}(\mathrm{x}), \Psi_{\mathrm{l},4}(\mathrm{x}) \text{ at } \mathrm{x}_0 = \mathrm{T} \\ &P_+\Psi_l(x)|_{x_0=T} = 0 \end{aligned} \tag{3.1}$$

and for the light anti-quark fields

$$\begin{aligned} &\overline{\Psi}_l(x)P_-|_{x_0=0} = \bar{\rho}(\mathbf{x}) \quad \text{fixes } \overline{\Psi}_{\mathrm{l},3}(\mathrm{x}), \overline{\Psi}_{\mathrm{l},4}(\mathrm{x}) \text{ at } \mathrm{x}_0 = 0 \\ &\overline{\Psi}_l(x)P_+|_{x_0=0} = 0 \\ &\overline{\Psi}_l(x)P_+|_{x_0=T} = \bar{\rho}'(\mathbf{x}) \quad \text{fixes } \overline{\Psi}_{\mathrm{l},1}(\mathrm{x}), \overline{\Psi}_{\mathrm{l},2}(\mathrm{x}) \text{ at } \mathrm{x}_0 = \mathrm{T} \\ &\overline{\Psi}_l(x)P_-|_{x_0=T} = 0 \end{aligned} \tag{3.2}$$

For the static quark fields, the boundaries are fixed accordingly. There are no projectors necessary due to Eq. (2.8). Also here the components relevant to the Dirac Wilson operator are fixed by

$$\Psi_h(x)|_{x_0=0} = \rho_h(\mathbf{x}) \tag{3.3}$$

and for the adjoint fields by

$$\overline{\Psi}_h(x)|_{x_0=T} = \bar{\rho}'_h(\mathbf{x}) \tag{3.4}$$

[3] This follows from Eq. (3.43) with vanishing local gauge fields $q_\mu = 0$

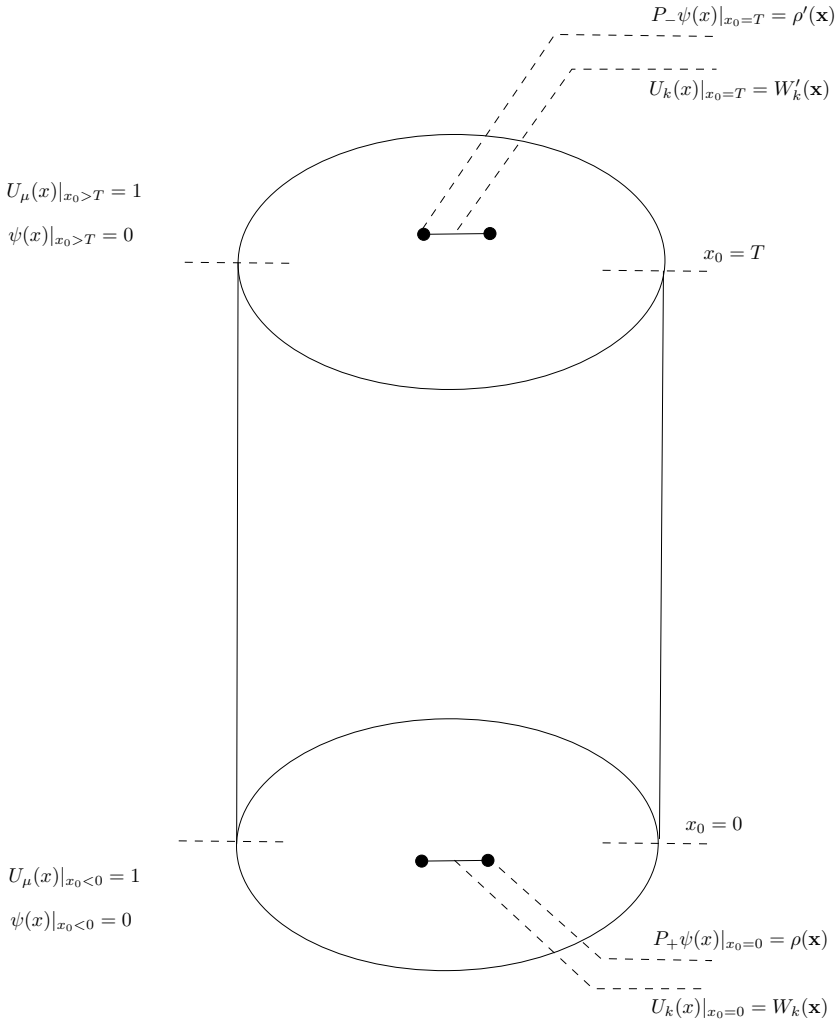

Figure 1: Sketch of the Schrödinger Functional for light quark fields

Figure 1 shows a sketch of the basic SF construction for light quark fields.

3.2 Light and Heavy Fermions in the lattice SF

For a more formal description of the SF consider the generating functional

$$\mathcal{Z}\left[U,\rho',\bar{\rho}',\rho,\bar{\rho},\eta,\bar{\eta}\right]=\frac{1}{Z}\int D\Psi D\overline{\Psi}DU e^{-\left(S_F\left[U,\overline{\Psi},\Psi\right]+S_G(U)+a^4\sum\limits_x\left(\bar{\eta}(x)\Psi(x)+\overline{\Psi}(x)\eta(x)\right)\right)} \tag{3.5}$$

The fields η and $\bar{\eta}$ are the source fields for the quark and anti-quark fields, ρ', $\bar{\rho}'$, $\rho,\bar{\rho}$ denote the boundary fields as introduced in the former section. As known from standard methods [19], [18], the generating functional is evaluated at vanishing sources and thus allows to compute expectation values of the operators in question. This prodecure will be explained more in detail in the next section when computing the basic correlation functions. The SF, however, is defined by the partition function at vanishing sources:

$$Z\left[\rho',\bar{\rho}',\rho,\bar{\rho},\eta,\bar{\eta}\right]_{\eta=\bar{\eta}=0}=\int D\Psi D\overline{\Psi}e^{-S_F\left[U,\overline{\Psi},\Psi\right]+S_G[U]} \tag{3.6}$$

For of a heavy and a light quark, the fermionic action can be divided into

$$S_F\left[U,\overline{\Psi},\Psi\right]=S_l\left[U,\overline{\Psi},\Psi\right]+S_h\left[U,\overline{\Psi},\Psi\right] \tag{3.7}$$

In the following, the fermion actions shall be specified separately. We begin with the light action, namely according to the free theory without gluon fields. In this special case, the generating functional takes the form

$$\mathcal{Z}_f\left[\rho_l',\bar{\rho}_l',\rho,\bar{\rho}_l,\eta_l,\bar{\eta}_l\right]=\frac{1}{Z_f}\int D\Psi_l D\overline{\Psi}_l e^{-\left(S_F\left[\overline{\Psi}_l,\Psi_l\right]+a^4\sum\limits_x\left(\bar{\eta}(x)\Psi_l(x)+\overline{\Psi}_l(x)\eta(x)\right)\right)} \tag{3.8}$$

Now the following considerations can be simplified by having defined the fields $\Psi_l(x)$ and $\overline{\Psi}_l(x)$ for all times x_0,i.e. it allows us to write down the light quark action like on the four-dimensional torus as

$$S_l\left[\overline{\Psi}_l,\Psi_l\right]=a^4\sum_x\overline{\Psi}_l(x)(D+m)\Psi_l(x) \tag{3.9}$$

We can now fall back upon the classical solution $\Psi_{cl}(x)$ of the Dirac equation $(D+m)\Psi_{cl}(x)=0$ for $0<x_0<T$ with prescribed boundary values given by Eq. (3.1) and Eq. (3.2). For a description in the SF, the fields $\chi(x)$ and $\bar{\chi}(x)$ are introduced with vanishing arguments at the boundaries, i.e. $\chi(x)|_{x_0=0}=\chi(x)|_{x_0=T}=0$. $\Psi_l(x)$ is then written as

$$\Psi_l(x)=\Psi_{cl}(x)+\chi(x) \tag{3.10}$$

$$\overline{\Psi}_l(x)=\overline{\Psi}_{cl}(x)+\overline{\chi}(x) \tag{3.11}$$

$\chi(x)$ and $\bar{\chi}(x)$ can be interpreted as quantum fluctuations around $\Psi_{cl}(x)$ with prescribed values at $x_0=0$ and $x_0=T$. This allows us to write $\Psi_l(x)$ as

$$\begin{aligned}\Psi_l(x)&=a^4\sum_x(\overline{\Psi}_{cl}(x)+\overline{\chi}(x))(D+m)(\Psi_{cl}(x)+\chi(x))\\&=a^4\sum_x\overline{\Psi}_{cl}(x)(D+m)\Psi_{cl}(x)+a^4\sum_x\overline{\chi}(x)(D+m)\chi(x)\\&\quad+a^4\sum_x\overline{\chi}(x)(D+m)\Psi_{cl}(x)+a^4\sum_x\overline{\Psi}_{cl}(x)(D+m)\chi(x)\end{aligned} \tag{3.12}$$

The third term in Eq. (3.12) is zero due to the Dirac equation $(D+m)\Psi_{cl}(x) = 0$ for $0 < x_0 < T$ and $\overline{\chi}(x) = 0$ for $x_0 \in [0, T]$. The same argument can be applied to the last term if we write $\overline{\Psi}_{cl}(x)(D+m)\chi(x)$ as $\overline{\Psi}_{cl}(x)(\overleftarrow{D}^\dagger + m)\chi(x) = 0$ for $0 < x_0 < T$ [4]. Then the entire expression vanishes beacuse $\chi(x) = 0$ for $x_0 \in [0, T]$. We can therefore decompose the light action $S_l[\overline{\Psi}_l, \Psi_l]$ into

$$S_l[\overline{\Psi}_l, \Psi_l] = S_l[\overline{\Psi}_{cl}, \Psi_{cl}] + S_l[\overline{\chi}, \chi] \tag{3.13}$$

which allows to determine the generating functional for the SF with new integration variables χ and $\bar{\chi}$ as [3], [18]

$$\begin{aligned} \ln \mathcal{Z}_f &= -S_l[\overline{\Psi}_{cl}, \Psi_{cl}] + (\bar{\eta}(x)\Psi_{cl}(x)) + (\overline{\Psi}_{cl}(x)\eta(x)) + (\bar{\eta}, (D+m)^{-1}\eta) \\ &= -S_l[\overline{\Psi}_{cl}, \Psi_{cl}] + a^4 \sum_x (\bar{\eta}(x)\Psi_{cl}(x) + \overline{\Psi}_{cl}(x)\eta(x)) \\ &+ a^8 \sum_{0<x_0,y_0<T} \sum_{\mathbf{x},\mathbf{y}} \bar{\eta}(x) S(x,x) \eta(y) \end{aligned} \tag{3.14}$$

Above, the notation $(\bar{\eta}(x)\Psi_{cl}(x)) = a^4 \sum_x \bar{\eta}(x)\Psi_{cl}(x)$ is used for the scalar product of $\bar{\eta}(x)$ and $\Psi_{cl}(x)$. One can now compute the SF explicitly by calculating the first term in above equation. For the SF in the free theory, this is being done in detail in Appendix A.4 and results in

$$\begin{aligned} S_l[\overline{\Psi}_{cl}, \Psi_{cl}] = a^4 \sum_x \frac{1}{2} \big(\bar{\rho}(\mathbf{x})\gamma_k(\nabla_k + \nabla_k^*)\rho(\mathbf{x}) + \bar{\rho}'(\mathbf{x})\gamma_k(\nabla_k + \nabla_k^*)\rho'(\mathbf{x}) \big) \\ - a^3 \sum_x \bar{\rho}(\mathbf{x})\Psi_{cl}(x)|_{x_0=a} - a^3 \sum_x \bar{\rho}'(\mathbf{x})\Psi_{cl}(x)|_{x_0=T-a} \end{aligned} \tag{3.15}$$

Taking into account the gluon fields and the improvement of the action, the solution of the SF can be found in complete analogy to the free solution. Only the fermionic part of the generating functional will play a role for our interests since we are going to expand the gluonic expectation value in pertubation theory. Accordingly, the fermionic part of the SF for light quark fields with improved action reads

$$Z_F\left[\rho_l', \bar{\rho}_l', \rho_l, \bar{\rho}_l, \eta_l, \bar{\eta}_l, U\right]_{\eta=\bar{\eta}=0} = \int D\Psi_l D\overline{\Psi}_l e^{-S_{F,impr}\left[U, \overline{\Psi}_l, \Psi_l\right]} \tag{3.16}$$

As well as in the case for free quarks, we are able to compute the fermionic part of the SF explicitly. The first term can be computed in analogy to Eq. (3.15) and thus be determined as [9]

$$\begin{aligned} S_{F,impr}[U, \overline{\Psi}_{cl}, \Psi_{cl}] = a^4 \sum_x \frac{\tilde{c}_s}{2} \big(\bar{\rho}(\mathbf{x})\gamma_k(\nabla_k + \nabla_k^*)\rho(\mathbf{x}) + \bar{\rho}'(\mathbf{x})\gamma_k(\nabla_k + \nabla_k^*)\rho'(\mathbf{x}) \big) \\ - \tilde{c}_t a^3 \sum_x \bar{\rho}(\mathbf{x}) U(x - a\hat{0}, 0)\Psi_{cl}(x)|_{x_0=a} - \tilde{c}_t a^3 \sum_x \bar{\rho}'(\mathbf{x})\Psi_{cl}(x)U(x,0)^{-1}|_{x_0=T-a} \end{aligned}$$

[4] In fact, it holds for the action [3]:

$$S[\Psi, \overline{\Psi}] = a^4 \sum_x \overline{\Psi}(x)(D+m)\Psi(x) = a^4 \sum_x \overline{\Psi}(x)(\overleftarrow{D}^\dagger + m)\Psi(x)$$

with the derivatives given by Eq. (A.18) and Eq. (A.19) in Appendix A. The coefficients $\tilde{c}_t$ and $\tilde{c}_s$ arise from the $\mathcal{O}(a)$ improvement and shall be treated in the next section.

For a descriptions of heavy fermions, one may consider the equations of motion a heavy quark field:

$$\nabla_0^* \Psi_{h,cl} = 0 \tag{3.17}$$

$$\overline{\Psi}_{h,cl} \overleftarrow{\nabla}_0 = 0 \tag{3.18}$$

which are solved by the classical solutions

$$\Psi_{h,cl}(x) = U_0(x - a\hat{0})^{-1} ... U_0(x - x_0\hat{0})^{-1} \rho_h(\mathbf{x}) \tag{3.19}$$

$$\overline{\Psi}_{h,cl}(x) = \bar{\rho}_h(\mathbf{x})' U_0(x)^{-1}|_{x_0 = T - a\hat{0}} ... U_0(x)^{-1} \tag{3.20}$$

The classical action for the heavy quark given by Eq. (2.5) vanishes due to the equations of motion Eq. (3.17) and Eq. (3.18), i.e.

$$S_h[U, \overline{\Psi}_{h,cl}, \Psi_{h,cl}] = 0$$

The entire fermionic part of the SF consisting of a light and a static quark including the gluon fields is given by

$$\begin{aligned} &Z_F\left[\rho_l', \bar{\rho}_l', \bar{\rho}_h', \rho_l, \rho_h, \bar{\rho}_l, \eta_l, \bar{\eta}_l, \eta_h, \bar{\eta}_h, U\right]_{\eta_l = \bar{\eta}_l = \eta_h = \bar{\eta}_h = 0} \\ &\quad = \int D\Psi_l D\overline{\Psi}_l D\Psi_h D\overline{\Psi}_h e^{-S_l\left[U, \overline{\Psi}_l, \Psi_l\right] - S_h\left[U, \overline{\Psi}_h, \Psi_h\right]} \end{aligned} \tag{3.21}$$

3.3 O(a) improvement in the lattice SF

Due to the boundary conditions of the SF, there are additional contributions to the $\mathcal{O}(a)$ counterterms to the light quark action and in principle to the static quark action. The static improvement terms at order a at the boundaries can be disregarded because all possible operators that are invariant under discrete 3-dimensional Euclidean rotations become zero either because of or of Eq. (2.8) or Eq. (2.42) [1]. Thus, the boundaries only affect the action improvement of the light quark. The Dirac Wilson operator hence has the structure

$$\delta D = \delta D_V + \delta D_b \tag{3.22}$$

where the volume improvement term δD_V consists of the clover term for the fermion action (see Eq. (2.36)). A possible form of the boundary improvement term is given by [6]

$$\begin{aligned} \delta D_b\left[\Psi, \overline{\Psi}, U\right] = a^4 \sum_{\mathbf{x}} \{&(\tilde{c}_s - 1)(\mathcal{L}_s(\mathbf{x}) + \mathcal{L}_s'(\mathbf{x})) \\ &+ (\tilde{c}_t - 1)(\mathcal{L}_t(\mathbf{x}) + \mathcal{L}_t'(\mathbf{x}))\} \end{aligned} \tag{3.23}$$

with

$$\mathcal{L}_s(\mathbf{x}) = \frac{1}{2} \bar{\rho}(\mathbf{x}) \gamma_k (\nabla_k^* + \nabla_k) \rho(\mathbf{x}) \tag{3.24}$$

$$\mathcal{L}_s'(\mathbf{x}) = \frac{1}{2} \bar{\rho}'(\mathbf{x}) \gamma_k (\nabla_k^* + \nabla_k) \rho'(\mathbf{x}) \tag{3.25}$$

$$\mathcal{L}_t(\mathbf{x}) = \left\{ \overline{\Psi}(y) P_+ \nabla_0^* \Psi(y) + \overline{\Psi}(y) \overleftarrow{\nabla}_0^* P_- \Psi(y) \right\} |_{y = (a, \mathbf{x})} \tag{3.26}$$

$$\mathcal{L}_t'(\mathbf{x}) = \left\{ \overline{\Psi}(y) P_- \nabla_0 \Psi(y) + \overline{\Psi}(y) \overleftarrow{\nabla}_0 P_+ \Psi(y) \right\} |_{y = (T - a, \mathbf{x})} \tag{3.27}$$

The improvement coefficients $\tilde{c}_s$ and $\tilde{c}_t$ in Eq. (3.23) must be chosen such that the time reversal invariance of the theory is preserved. The pertubative expansion of the improvement coefficients $\tilde{c}_s$ and $\tilde{c}_t$ reads

$$\tilde{c}_{s,t} = 1 + \sum_{k=1}^{\infty} \tilde{c}_{s,t}^{(k)} g_0^{2k} \tag{3.28}$$

Due to $c_{s,t}^{(0)} = 1$, the improvement coefficients do not appear explicitly for the free theory in Eq. (3.15). The reason for that is that the theory for free Wilson fermions is already $\mathcal{O}(a)$ improved [3]. For one-loop computations, one needs to consider only the first non-vanishing terms of volume and boundary improvement terms, i,.e. $\delta D_V^{(1)}$ and $\delta D_b^{(2)}$ where the upper index (k) here denotes the order of the expansion in g_0. $\delta D_V^{(1)}$ induces a magnetic colour moment and modifies the 3-point quark-gluon vertex. This results in additional definitions which can be read off Table 7 in Appendix B. The values $i \in [6..16]$ in Table 7 arise from the clover term of the improved action.
$\delta D_b^{(2)}$yields a contribution to the second order of the boundary to bulk propagator, i.e. $\Psi_{cl}^{(2)}$ is affected. It will appear as a matrix H_{bi} which has to be defined in the next section and which is based on Eq. (3.23). The explicit forms of the boundary improvement terms will not be given, they will be included in the final expressions for the Feynman diagrams.
There are no improvement contributions from the boundaries to the axial current. The reason for that is that the axial current is defined in the interior of the SF by the annihilation of a quark and an antiquark and thus is a pure volume term. Moreover, the SF offers the opportunity to compute the proportional constant $c_{\mathrm{A}}^{\mathrm{stat}}$ by choosing the involved correlation functions in a smart way.
In this work, the proportional constant $c_{\mathrm{A}}^{\mathrm{stat}}$ is determined to first loop order. To set up the notation, $c_{\mathrm{A}}^{\mathrm{stat}}$ may be epanded in pertubation theory by

$$c_{\mathrm{A}}^{\mathrm{stat}} = \sum_{k=0}^{\infty} c_{\mathrm{A}}^{\mathrm{stat}\,(k)} g_0^{2k} \tag{3.29}$$

with the upper index k being the loop order.
Due to the already given $\mathcal{O}(a)$ improvement of the free theory, there is no improvement term necessary for $U_\mu(x) = \mathbb{1}$, and

$$c_{\mathrm{A}}^{\mathrm{stat}\,(0)} = 0 \tag{3.30}$$

The first non-vanishing contribution to $c_{\mathrm{A}}^{\mathrm{stat}}$ therefore is $c_{\mathrm{A}}^{\mathrm{stat}\,(1)}$. It should be emphasized, that, although pertubation theory is set up in the SF in the following, the improvement coefficient $c_{\mathrm{A}}^{\mathrm{stat}}$ is not a property ofthe SF nor it is affected by the SF. The SF just offers a smart and elegant way to define the operators which are needed to extract $c_{\mathrm{A}}^{\mathrm{stat}\,(1)}$.

3.4 Correlation functions in the lattice SF

In Euclidean space, the expectation value of any product $\mathcal{O}$ of local composite fields is given by the functional integral

$$< \mathcal{O} >= \frac{1}{Z} \int_{fields} \mathcal{O} e^{-S} \tag{3.31}$$

That is, we will have to integrate over all gluonic and femionic fields. This procedure can be described seperately and gives us the fermionic expectation value $[]_F$ and the gluonic expectation value $<>_G$

$$< \mathcal{O} >=< [\mathcal{O}]_F >_G \tag{3.32}$$

After having integrated out the fermionic fields, the gauge field probability depends on Z_F and is described by the density function

$$p = Z_F \; e^{-S[U]} \tag{3.33}$$

The gluonic expectation value will appear in the definition of the axial current, e.g. it will have the form of $f_A =< .. >_G$ and will be evaluated in pertubation theory. At this point, we are only interested in an analytic computation of the fermionic expectation value $[\mathcal{O}]_F$.

Since the SF is a Gaussian function of the source fields η and $\bar{\eta}$ and the boundary fields ρ, $\bar{\rho}$, ρ' and $\bar{\rho}'$, correlation functions in the SF are typically obtained by taking variational derivatives with respect to those fields. To make this concept clearer, let $\mathcal{O}$ be a polynomial in the variational derivatives with respect to source and boundary fields. We define its fermionic expectation value through

$$[\mathcal{O}(\Psi, \overline{\Psi}, \zeta, \bar{\zeta}, \zeta', \bar{\zeta}')]_F = \left\{ \frac{1}{\mathcal{Z}_F} \mathcal{O}(\frac{\delta}{\eta}, \frac{\delta}{\delta\bar{\eta}}, \frac{\delta}{\delta\rho}, \frac{\delta}{\delta\bar{\rho}}, \frac{\delta}{\delta\rho'}, \frac{\delta}{\delta\bar{\rho}'}) \mathcal{Z}_F \left[\rho'; \bar{\rho}'; \rho; \bar{\rho}; \eta; \bar{\eta}\right] \right\}_{\rho'=..=\bar{\eta}=0} \tag{3.34}$$

In the notation of Eq. (3.34), the variational derivatives are associated with corresponding fields. For the light quark, this is done according to

$$-\overline{\Psi}_l(x) \leftrightarrow \frac{\delta}{\eta_l(x)} \tag{3.35}$$

$$\Psi_l(x) \leftrightarrow \frac{\delta}{\delta\bar{\eta}_l(x)} \tag{3.36}$$

$$-\bar{\zeta}_l(\mathbf{x}) \leftrightarrow \frac{\delta}{\delta\rho_l(\mathbf{x})} \tag{3.37}$$

$$\zeta_l(\mathbf{x}) \leftrightarrow \frac{\delta}{\delta\rho_l(\mathbf{x})} \tag{3.38}$$

$$-\bar{\zeta}'_l(\mathbf{x}) \leftrightarrow \frac{\delta}{\delta\rho_l(\mathbf{x})} \tag{3.39}$$

$$\zeta'_l(\mathbf{x}) \leftrightarrow \frac{\delta}{\delta\rho_l(\mathbf{x})}, \tag{3.40}$$

The boundary fields $\zeta_l, \bar{\zeta}_l, \zeta'_l$ and $\bar{\zeta}'_l$ are just symbolic notations whereas the fields $\overline{\Psi}_l$ and Ψ_l may be identified with the fields in Eq. (3.6).

One is now able to compute an arbitrary product of fields $\Psi_l, \overline{\Psi}_l, \zeta_l, \bar{\zeta}_l$ by applying Wick contractions and thus decomposing $[\mathcal{O}]_F$ into a sum of basic two-point functions. Therefore, we are left with deducing a basic set of two-point functions allowing to build a basis for arbitrary operators. In oder to write down the basic two-point functions, we need to consider the classical solution of the quark propagator fulfilling the boundary conditions imposed by the SF. For the light quark, it is given by [1]

$$\Psi_{cl,l}(x) = a^3 \sum_y \tilde{c}_t \big(S(x,y) U(y - a\hat{0})^{-1} \rho_l(\mathbf{y})|_{y_0=a} + S(x,y) U(y,0) \rho_l'(\mathbf{y})|_{y_0=T-a} \big)$$

Knowing that $\frac{\delta}{\delta \rho_l(\mathbf{y})} \rho_l(\mathbf{y}) = P_+$, this yields immediately

$$\frac{\delta}{\delta \rho_l(\mathbf{y})} \Psi_{cl,l}(x) = \tilde{c}_t S(x,y) U(y - a\hat{0}, 0)^{-1} P_+|_{y_0=a}$$

and with $\frac{\delta}{\delta \rho_l'(\mathbf{y})} \rho_l'(\mathbf{y}) = P_-$ one gets

$$\frac{\delta}{\delta \rho_l'(\mathbf{y})} \Psi_{cl,l}(x) = \tilde{c}_t S(x,y) U(y,0) P_-|_{y_0=T-a}$$

The adjoint equation

$$\overline{\Psi}_{cl,l}(x) = a^3 \sum_y \tilde{c}_t \big(\bar{\rho}_l(\mathbf{x}) U(x - a\hat{0}, 0) S(x,y)|_{x_0=a} + \bar{\rho}_l'(\mathbf{x}) U(x,0)^{-1} S(x,y)|_{x_0=T-a} \big)$$

with $\frac{\delta}{\delta \bar{\rho}_l(\mathbf{x})} \bar{\rho}_l(\mathbf{x}) = P_-$ leads to

$$\frac{\delta}{\delta \bar{\rho}_l(\mathbf{x})} \overline{\Psi}_{cl,l}(x) = \tilde{c}_t P_- U(x - a\hat{0}, 0) S(x,y)|_{x_0=a}$$

and with $\frac{\delta}{\delta \bar{\rho}_l'(\mathbf{x})} \bar{\rho}_l'(\mathbf{x}) = P_+$ to

$$\frac{\delta}{\delta \bar{\rho}_l'(\mathbf{x})} \overline{\Psi}_{cl,l}(x) = \tilde{c}_t P_+ U(x,0)^{-1} S(x,y)|_{x_0=T-a}$$

For the heavy quark, due to the choice of the boundary fields given by Eq. (3.3) and Eq. (3.4), only the fields $\bar{\zeta}_h(\mathbf{x})$ and ${\zeta'}_h(\mathbf{x})$ are defined analogously. With the classical solutions Eq. (A.37), one finds

$$\frac{\delta}{\delta \rho_h(\mathbf{x})} \overline{\Psi}_{cl,h}(x) = U_0(x - a\hat{0})^{-1} .. U_0(x - x_0\hat{0})^{-1} P_+ \tag{3.41}$$

$$\frac{\delta}{\delta \bar{\rho}_h'(\mathbf{x})} \overline{\Psi}_{cl,h}(x) = P_+ U_0(x)^{-1}|_{x_0=T-a\hat{0}} .. U_0(x)^{-1} \tag{3.42}$$

The basic light and static two-point functions can now be computed by applying above listed expressions. They are given in detail in Appendix A.2 and A.3.

3.5 Pertubation Theory in the lattice SF

Having evaluated the fermionic expectation values analytically, we are now left in determining the gluonic expectation values. In computer simulations, this is usually done by using Monte Carlo methods. For the computation of $c_{\mathrm{A}}^{\mathrm{stat}}$, we choose a different approach and evaluate them in pertubation theory. In concrete, this will lead to the task of determining $c_{\mathrm{A}}^{\mathrm{stat}}$ to first order, namely $c_{\mathrm{A}}^{\mathrm{stat}(1)}$.
Initially, we introduce a gauge vector field $q_\mu(x)$ fluctuating around a vanishing background gauge field. The link variable can then be written as

$$U_\mu(x) = e^{g_0 a q_\mu(x)} \tag{3.43}$$

A description of pertubation theory on the lattice now consists of expanding the gauge links in terms of the bare coupling g_0. In order to perform the calculation of $c_{\mathrm{A}}^{\mathrm{stat}}$, we are interested in two particular correlation functions, i.e. $f_{\mathrm{A}}^{\mathrm{stat}}$ and f_1^{stat}. The reason for this shall become clearer when performing the final computation of $c_{\mathrm{A}}^{\mathrm{stat}}$ in the next chapter.
The discretized version of the correlation function $f_{\mathrm{A}}^{\mathrm{stat}}(x_0)$ is given by

$$\begin{aligned} f_{\mathrm{A}}^{\mathrm{stat}}(x_0) &= -a^6 \sum_{\mathbf{y},\mathbf{z}} \frac{1}{2} \left\langle A_0^{stat}(x) \bar{\zeta}_h(\mathbf{y}) \gamma_5 \zeta_l(\mathbf{z}) \right\rangle \\ &= -\frac{1}{2} < \mathrm{tr}\left\{ \mathrm{H_l(x)} \gamma_0 \mathrm{H_h(x)} \right\} >_{\mathrm{G}} \end{aligned} \tag{3.44}$$

The trace is to be taken over Dirac and colour indices. In above equation, the definition

$$H(x) = a^3 \sum_{\mathbf{y}} \frac{\delta \Psi_{cl}(x)}{\delta \rho(\mathbf{y})} \tag{3.45}$$

is used. $H(x)$ can be expanded in pertubation theory by

$$H(x) = \sum_{k=0}^{\infty} H^{(k)} g_0^k \tag{3.46}$$

Please note that above formulae are based on the correlation functions which were derived in the former section. $f_{\mathrm{A}}^{\mathrm{stat}}(x_0)$ may now be expanded in terms of g_0. This gives us

$$f_{\mathrm{A}}^{\mathrm{stat}}(x_0) = \sum_{k=0}^{\infty} g_0^{2k} f_{\mathrm{A}}^{\mathrm{stat}\,(k)}(x_0)$$

or, in our notation using H-matrices:

$$\begin{aligned} f_A^{stat}(x_0) &= -\frac{1}{2} \left\langle \mathrm{tr}\left\{ \mathrm{H_l^\dagger(x)} \gamma_0 \mathrm{H_h^\dagger(x)} \right\} \right\rangle_G \\ &= -\frac{1}{2} \left\langle \mathrm{tr}\left\{ \mathrm{P} + \mathrm{q_0 Q} + \mathrm{q_0^2 R} \right\} \right\rangle_G \end{aligned} \tag{3.47}$$

with

$$\begin{aligned} P &= H_l^{(0)\dagger} \gamma_0 H_h^{(0)} \\ Q &= H_l^{(1)\dagger} \gamma_0 H_h^{(0)} + H_l^{(0)\dagger} \gamma_0 H_h^{(1)} \\ R &= H_l^{(1)\dagger} \gamma_0 H_h^{(1)} + H_l^{(0)\dagger} \gamma_0 H_h^{(2)} + H_l^{(2)\dagger} \gamma_0 H_h^{(0)} \end{aligned} \tag{3.48}$$

It follows for

$$f_A^{stat,(0)}(x_0) = -\frac{1}{2}\left\langle \mathrm{tr}\left\{ \mathrm{H_l^{(0)\dagger}}\gamma_0 \mathrm{H_h^{(0)}} \right\} \right\rangle_G \tag{3.49}$$
$$f_A^{stat,(1)}(x_0) = -\frac{1}{2}\left\langle \mathrm{tr}\left\{ \mathrm{H_l^{(1)\dagger}}\gamma_0 \mathrm{H_h^{(1)}} + \mathrm{H_l^{(0)\dagger}}\gamma_0 \mathrm{H_h^{(2)}} + \mathrm{H_l^{(2)\dagger}}\gamma_0 \mathrm{H_h^{(0)}} \right\} \right\rangle_G$$

The first contribution P gives us the tree level of the operator $f_{\mathrm{A}}^{\mathrm{stat}}$. Q always vanishes. This can easily seen, because $H^{(1)}(x)$ is proportional to $q_\mu(y)$ whereas $H^{(0)}(x)$ does not depend on $q_\mu(y)$. As we know that $< q_\mu >_G = 0$, it follows that $Q = 0$. Finally, R gives us the one-loop contributions to $f_{\mathrm{A}}^{\mathrm{stat}}$ which are a bit more involved and will be discussed in the following.

At this point, we want to consider specific quantities in their Fourier transformed shape which eases or makes even possible many considerations. In the SF, we miss translation invariance in the temporal direction. Therefore, we cannot Fourier-transform our quantities as usual. However, we are able to perform a spatial Fourier transformation (SFT) as translation invariance is given in the spatial directions. Doing this for the H-matrix, we obtain

$$H(x, \mathbf{p}) = a^3 \sum_{\mathbf{y}} e^{i\mathbf{py}} \frac{\delta \Psi_{cl}(x)}{\delta \rho(\mathbf{y})} \tag{3.50}$$

and for $f_{\mathrm{A}}^{\mathrm{stat}}$:

$$f_{\mathrm{A}}^{\mathrm{stat}}(x_0, \mathbf{p}) = -a^6 \sum_{\mathbf{y},\mathbf{z}} e^{i\mathbf{p}(\mathbf{y}-\mathbf{z})} \frac{1}{2} \left\langle A_0^{stat}(x) \bar{\zeta}_h(\mathbf{y}) \gamma_5 \zeta_l(\mathbf{z}) \right\rangle \tag{3.51}$$
$$= -\frac{1}{2} < \mathrm{tr}\left\{ \mathrm{H_l(x, p)}\gamma_0 \mathrm{H_h(x, p)} \right\} >_{\mathrm{G}}$$

A pertubative expansion of the H-matrices immediately yields

$$H^{(k)}(x, \mathbf{p}) = a^3 \sum_{\mathbf{y}} e^{i\mathbf{py}} \frac{\delta \Psi_{cl}^{(k)}(x)}{\delta \rho(\mathbf{y})} \tag{3.52}$$

It is now convenient to define the matrix $\chi(x_0, \mathbf{p})$ as the SFT of $H^{(0)}(x)$. $\chi(x_0, \mathbf{p})$ describes the quark propagator from the SF boundary to the interior point x_0 with momentum $\mathbf{p}$ at tree level:

$$\chi(x_0, \mathbf{p}) = e^{i\mathbf{px}} H^{(0)}(x, \mathbf{p}) \tag{3.53}$$

Furthermore, the SFT of the quark propagator $S(x, y)$ is needed:

$$\tilde{S}(x_0, y_0, \underline{\mathrm{p}}) = a^3 \sum_{\mathbf{x}} e^{i\mathbf{p}(\mathbf{x}-\mathbf{y})} S(x, y) \tag{3.54}$$

With above definition and referring to Eq. (A.37), the static quark propagator at tree level reduces to

$$\tilde{S}_h^{(0)} = P_+ \tag{3.55}$$

This allows us to express the tree level of f_A^{stat} as per Eq. (3.49) as

$$f_{\mathrm{A}}^{\mathrm{stat}\,(0)}(x_0, \mathbf{p}) = -\frac{1}{2} N \mathrm{tr}\left[\chi(\mathrm{x_0, p})^\dagger \gamma_0 \mathrm{P_+} \right] \tag{3.56}$$

where $N = 3$ is the number of colours in QCD. From now on, the trace is to be taken over Dirac indices only.
$f_{\mathrm{A}}^{\mathrm{stat}\,(0)}$ depends on the bare quark mass m_0 which has a functional dependence upon the bare coupling g_0. In order to reflect this fact, a mass shift $df_A^{stat(0)}$ has to be taken into account when computing f_A^{stat}:

$$\frac{df_{\mathrm{A}}^{\mathrm{stat}\,(0)}(x_0,\mathbf{p},m_0(g_0^2))}{dg_0^2}|_{g_0^2=0} = -\frac{1}{2}N\mathrm{tr}\left\{\frac{\mathrm{d}\chi(\mathrm{x}_0,\mathbf{p})^\dagger}{\mathrm{dm}_0}\overbrace{\frac{dm_0}{dg_0^2}|_{g_0^2=0}}^{=\mathrm{m}_0^{(1)}}\gamma_0\mathrm{P}_+\right\} \tag{3.57}$$

$$\begin{aligned}&= -\frac{1}{2}Nm_0^{(1)}\mathrm{tr}\left\{\frac{\mathrm{d}\chi(\mathrm{x}_0,\mathbf{p})^\dagger}{\mathrm{dm}_0}\gamma_0\mathrm{P}_+\right\}\\ &= \frac{1}{2}Nm_0^{(1)}\sum_{u_0=a}^{T-a}\mathrm{tr}\left\{\chi(\mathrm{u}_0,\mathbf{p})^\dagger\tilde{\mathrm{S}}^{(0)\dagger}(\mathrm{x}_0,\mathbf{p})\gamma_0\mathrm{P}_+\right\}\end{aligned} \tag{3.58}$$

Later, we will set m_0 to ist critical value $m_c = m_c^{(1)}g_0^2 + \mathcal{O}(g_0^4)$.

In the following, a set of ingredients will be described allowing us to express equation (3.49) in a more descriptive way. Further related formulae and derivations can be found in [8]. In the following, we adopt the notation and sketch the underlying ideas.

Firstly, we define vertices $V^{(1)}$ and $V^{(2)}$ for the relativistic quark-gluon emission/absorption. Basically, those vertices will, besides causing an additional factor in the correlation functions, induce a shift in the contracted gluon propagators as well as in the relativistic propagators. These factors and shifts arise from the expansion of the improved Dirac Wilson operator can be read off Tables 7 and 8 in Appendix B.
$V^{(1)}$ describes the relativistic three-point quark-gluon vertex, e.g. a gluon with momentum $\mathbf{k}$ ist emitted or absorbed by a propagating quark with momentum $\mathbf{p}$. $V^{(2)}$ denotes the relativistic four-point quark-gluon vertex. A quark with momentum $\mathbf{p}$ can emit or absorb gluons with momentum $\mathbf{k}$ and $\mathbf{q}$. Figures 2 and 3 show the basic vertices.

Considering equation (3.49) anew, the contained matrix $H^{(2)}$ can be split to get the resulting Feynman diagrams. We distinguish between the light (relativistic) case $H_l^{(2)}$ and heavy (static) case $H_h^{(2)}$ because in the light case, $H_l^{(2)}$ contains the improvement term $H_{bi}^{(2)}(x,\mathbf{p})$ arising from the improvement term δD_b, see Eq. (3.23). If we for simplicity set the boundary fields to zero, this contribution takes the form

$$\begin{aligned}H^{(2)}(x,\mathbf{p})_{bi} = -\tilde{c}_t e^{i\mathbf{px}}\big(&\tilde{S}^{(0)}(x_0,a;\mathbf{p})\left[\chi(a;\mathbf{p}) - P_+\right]\\ &+ \tilde{S}^{(0)}(x_0,T-a;\mathbf{p})\chi(T-a;\mathbf{p})\big)\end{aligned} \tag{3.59}$$

Accordingly, $H_l^{(2)}$ can be split into three contributions [8]

$$H_l^{(2)}(x,\mathbf{p}) = H_{l,tp}^{(2)}(x,\mathbf{p}) + H_{l,ss}^{(2)}(x,\mathbf{p}) + H_{bi}^{(2)}(x,\mathbf{p}) \tag{3.60}$$

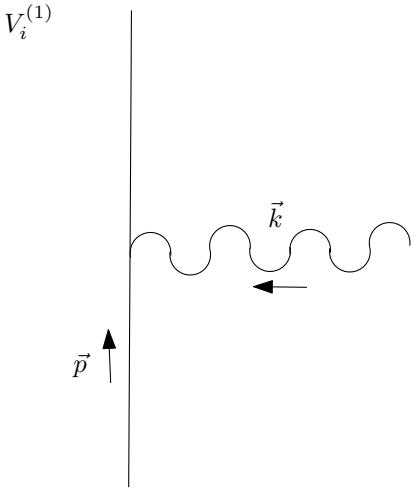

Figure 2: three-point quark-gluon vertex

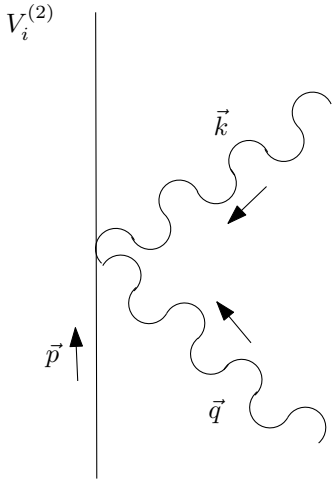

Figure 3: four-point quark-gluon vertex

The subscripts *bi* denote the boundary improvement contribution whereas *tp* stands for *tadpole* and *ss* for *setting sun*, i.e. the self energy. For the the static case, $H_h^{(2)}$ contains only the two components

$$H_h^{(2)}(x,\mathbf{p}) = H_{h,tp}^{(2)}(x,\mathbf{p}) + H_{h,ss}^{(2)}(x,\mathbf{p}) \tag{3.61}$$

The H-matrices contain the above introduced vertices. That is, $H_{l,ss}$ arises from a quark line with two relativistic three-point quark-gluon vertices. It is constructed by summing up all possible vertices $V_i^{(1)}$ and $V_j^{(1)}$ bearing in mind their induced shifts and by summing over all possible combinations of emission/absorption points. The sum furthermore extends over all possible gluon momenta $\mathbf{p}$ and $\mathbf{q}$. If both gluons are emitted or absorbed at the same time, one has to consider a relativistic four-point quark-gluon vertex $V_i^{(2)}$ and $H_{l,tp}$ emerges after having summed up the emission/absorption points and the

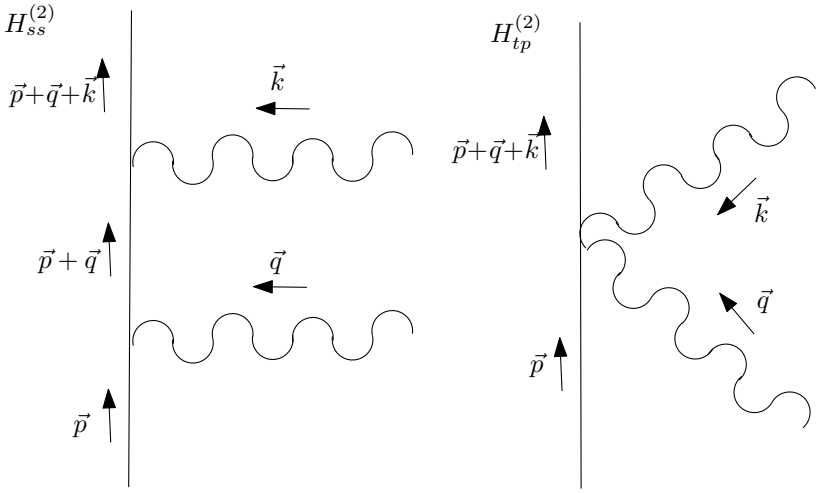

Figure 4: Self energy and tadpole contributions to $H^{(2)}$

momenta. One then gets the analytic expressions

$$H_l^{(2)}(x,\mathbf{p})_{tp} = -\frac{a}{L^6}\sum_{\mathbf{k},\mathbf{q}}\sum_{u_0=a}^{T-a} e^{i(\mathbf{k}+\mathbf{q}+\mathbf{p})\mathbf{x}}\tilde{S}^{(0)}(x_0,u_0;\mathbf{k}+\mathbf{q}+\mathbf{p}) \tag{3.62}$$
$$\times\sum_{i=1}^{5}\tilde{q}^a_{\mu(i)}(u_0+at(i);\mathbf{k})\tilde{q}^b_{\mu(i)}(u_0+at(i);\mathbf{q})T^aT^bV_i^{(2)}(\mathbf{k},\mathbf{q},\mathbf{p})\chi(u_0+as(i);\mathbf{p})$$

$$H_l^{(2)}(x,\mathbf{p})_{ss} = -\frac{a^2}{L^6}\sum_{\mathbf{k},\mathbf{q}}\sum_{u_0,v_0=a}^{T-a} e^{i(\mathbf{k}+\mathbf{q}+\mathbf{p})\mathbf{x}}\tilde{S}^{(0)}(x_0,u_0;\mathbf{k}+\mathbf{q}+\mathbf{p})$$
$$\times\sum_{i,j=1}^{16}\tilde{q}^a_{\mu(i)}(u_0+at(i);\mathbf{k})T^aV_i^{(1)}(\mathbf{k},\mathbf{q}+\mathbf{p})\tilde{S}^{(0)}(u_0+as(i),v_0;\mathbf{q}+\mathbf{p})$$
$$\times\tilde{q}^b_{\mu(j)}(v_0+at(j);\mathbf{q})T^bV_j^{(1)}(\mathbf{q},\mathbf{p})\chi(v_0+as(j);\mathbf{p})$$

The matrices $H_l^{(2)}(x,\mathbf{p})_{tp}$ and $H_l^{(2)}(x,\mathbf{p})_{ss}$ can be visualized as in figure 4.

A contraction of both gluons appearing in $H_l^{(2)}(x,\underline{\mathrm{p}})_{ss}$ yields a contribution to the self energy. If they are emitted and absorbed at the same point like in $H_l^{(2)}(x,\underline{\mathrm{p}})_{tp}$, a tadpole emerges when contracting both gluons.
Accordingly, we introduce new symbols N_l^i for the tadpole contraction and M_l^{ij} for the self-energy contraction resulting in

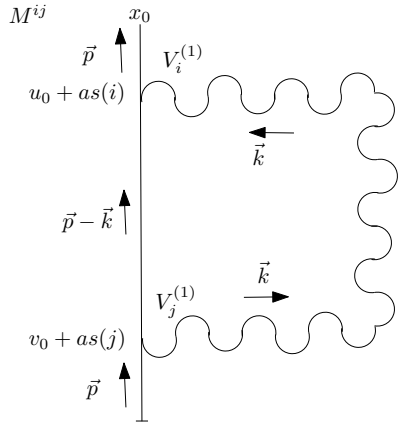

Figure 5: The Setting Sun Matrix M^{ij}

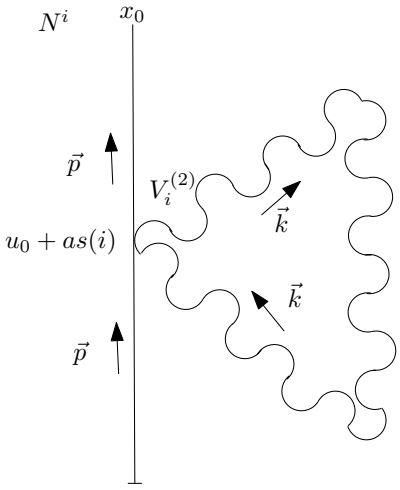

Figure 6: The Tadpole Matrix N^i

$$N_l^i(x_0, u_0, \mathbf{p}, \mathbf{k}) = \tilde{S}_l^{(0)}(x_0, u_0, \mathbf{p}) V_i^{(2)}(\mathbf{k}, -\mathbf{k}, \mathbf{p}) \chi_l(u_0 + as(i); \mathbf{p}) \tag{3.63}$$

$$\begin{aligned} M_l^{ij}(x_0, u_0, v_0; \mathbf{p}, \mathbf{k}) = \tilde{S}_l^{(0)}(x_0, u_0, \mathbf{p}) V_i^{(1)}(\mathbf{k}, \mathbf{p} - \mathbf{k}) \tilde{S}_l^{(0)}(u_0 + as(i), v_0, \mathbf{p} - \mathbf{k}) \\ \times V_j^{(1)}(-\mathbf{k}, \mathbf{p}) \chi_l(v_0 + as(j); \mathbf{p}) \end{aligned}$$

which look like figures 5 and 6. Due to their shape, diagrams containing a loop like in figure 5 are also called setting sun diagrams. For the static quark, it holds

$$\begin{aligned} N_h^i(x_0, u_0, \mathbf{p}, \mathbf{k}) &= P_+ \Theta(x_0 - u_0) \\ M_h^{ij}(x_0, u_0, v_0; \mathbf{p}, \mathbf{k}) &= P_+ \Theta(x_0 - u_0) \Theta(u_0 - v_0 - a) \end{aligned} \tag{3.64}$$

where $\Theta(x)$ is the Heavyside function. One then finds

$$H_h^{(2)}(x, \mathbf{p})_{tp} = \frac{a^2}{2L^6} \sum_{\mathbf{k},\mathbf{q}} \sum_{u_0=a}^{T-a} e^{i(\mathbf{k}+\mathbf{q}+\mathbf{p})\mathbf{x}} \Theta(x_0 - u_0) \tilde{q}_0^a(u_0 - a; \mathbf{k}) \tilde{q}_0^b(u_0 - a; \mathbf{q}) T^a T^b P_+ \tag{3.65}$$

$$\begin{aligned} H_h^{(2)}(x, \mathbf{p})_{ss} = \frac{a^2}{L^6} \sum_{\mathbf{k},\mathbf{q}} \sum_{u_0, v_0=a}^{T-a} e^{i(\mathbf{k}+\mathbf{q}+\mathbf{p})\mathbf{x}} \Theta(x_0 - u_0) \Theta(u_0 - v_0 - a) \\ \times \tilde{q}_0^a(u_0 - a; \mathbf{k}) \tilde{q}_0^b(v_0 - a; \mathbf{q}) T^a T^b P_+ \end{aligned}$$

The expressions $\mathrm{tr}\left\{\mathrm{H_l^{(0)\dagger}} \gamma_0 \mathrm{H_h^{(2)}}\right\}$ and $\mathrm{tr}\left\{\mathrm{H_l^{(2)\dagger}} \gamma_0 \mathrm{H_h^{(0)}}\right\}$ in (3.49) can now basically be expressed by the above introduced auxiliary quantities N_l^i and M_l^{ij}. They result in two diagrams at a time. We now get the first four Feynman diagrams describing $f_{\mathrm{A}}^{\mathrm{stat}(1)}$ in figures 7 to 10. Using above introduced notation,

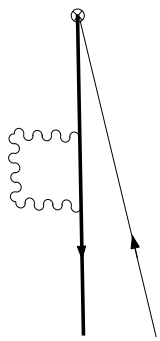

Figure 7: $f^{stat}_{A,ss-a}$

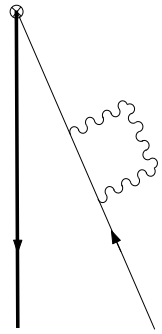

Figure 8: $f^{stat}_{A,ss-b}$

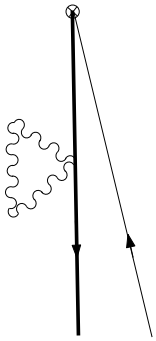

Figure 9: $f^{stat}_{A,tp-a}$

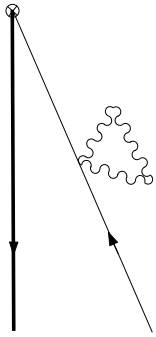

Figure 10: $f^{stat}_{A,tp-b}$

the diagrams are described by the expressions[5]

$$f^{stat}_{A,ss-a}(x_0,\mathbf{p}) = NC_F\frac{a^2}{2L^3}\sum_{\mathbf{k}}\sum_{u_0=a}^{x_0}\sum_{v_0=a}^{u_0-a} d_{00}(u_0-a,v_0-a;\mathbf{k}) \tag{3.66}$$
$$\times\,\mathrm{tr}\left[\chi_1(\mathrm{x_0};\mathbf{p})^\dagger\gamma_0\mathrm{P_+}\right]$$
$$f^{stat}_{A,ss-b}(x_0,\mathbf{p}) = NC_F\frac{a^2}{2L^3}\sum_{\mathbf{k}}\sum_{u_0,v_0=a}^{T-a}\sum_{i,j=1}^{16} d_{\mu(i)\mu(j)}(u_0+at(i),v_0+at(j);\mathbf{k}) \tag{3.67}$$
$$\times\,\mathrm{tr}\left[\mathrm{M_l^{ij}}(\mathrm{x_0},\mathrm{u_0},\mathrm{v_0};\mathbf{p},\mathbf{k})^\dagger\gamma_0\mathrm{P_+}\right]$$
$$f^{stat}_{A,tp-a}(x_0,\mathbf{p}) = NC_F\frac{a^2}{4L^3}\sum_{\mathbf{k}}\sum_{u_0=a}^{x_0} d_{00}(u_0-a,u_0-a;\mathbf{k}) \tag{3.68}$$
$$\times\,\mathrm{tr}\left[\chi_1(\mathrm{x_0};\mathbf{p})^\dagger\gamma_0\mathrm{P_+}\right]$$
$$f^{stat}_{A,tp-b}(x_0,\mathbf{p}) = -NC_F\frac{a^2}{2L^3}\sum_{\mathbf{k}}\sum_{u_0=a}^{T-a}\sum_{i=1}^{5} d_{\mu(i)\mu(j)}(u_0+at(i),u_0+at(i);\mathbf{k}) \tag{3.69}$$
$$\times\,\mathrm{tr}\left[\mathrm{N_l^i}(\mathrm{x_0},\mathrm{u_0};\mathbf{p},\mathbf{k})^\dagger\gamma_0\mathrm{P_+}\right]$$

Finally, the contribution $\mathrm{tr}\left\{\mathrm{H_l^{(1)\dagger}}\gamma_0\mathrm{H_h^{(1)}}\right\}$ in (3.49) describes a gluon exchange between heavy and relativistic quark. $H_l^{(1)}$ contains a three-point quark-gluon

[5] C_F denotes the Casimir number, i.e. $C_F = \frac{4}{3}$ for SU(3)

vertex and takes the form

$$H_l^{(1)}(x,\mathbf{p}) = -\frac{a}{L^3}\sum_{\mathbf{k}}\sum_{u_0=a}^{T-a} e^{i(\mathbf{k}+\mathbf{p})\mathbf{x}}\tilde{S}^{(0)}(x_0,u_0;\mathbf{k}+\mathbf{p}) \tag{3.70}$$
$$\times\sum_{i=1}^{16}\tilde{q}^a_{\mu(i)}(u_0+at(i);\mathbf{k})T^aV_i^{(1)}(\mathbf{k},\mathbf{p})\chi(u_0+as(i);\mathbf{p})$$

The corresponding auxiliary quantity $M_l^i(x_0,u_0,\mathbf{p},\mathbf{k})$ for the relativistic quark consists of a quark propagator from the boundary to the interior u_0. It emits or absorbs a gluon in a three-point quark-gluon vertex and then propagates further to x_0. The process reads

$$M_l^i(x_0,u_0,\mathbf{p},\mathbf{k}) = \tilde{S}_l^{(0)}(x_0,u_0,\mathbf{p}+\mathbf{k})V_i^{(1)}(\mathbf{k},\mathbf{p})\chi_l(u_0+as(i);\mathbf{p}) \tag{3.71}$$

The static counterpart

$$H_h^{(1)}(x,\mathbf{p}) = -\frac{a}{L^3}\sum_{\mathbf{k}}\sum_{u_0=a}^{T-a} e^{i(\mathbf{k}+\mathbf{p})\mathbf{x})}\Theta(x_0-u_0)\tilde{q}_0^a(u_0-a;\mathbf{k})T^aP_+ \tag{3.72}$$

contains

$$M_h = P_+\Theta(x_0-u_0) \tag{3.73}$$

and we can write down

$$f_{A,ge}^{stat}(x_0,\mathbf{p}) = -NC_F\frac{a^2}{2L^3}\sum_{\mathbf{k}}\sum_{u_0=a}^{T-a}\sum_{v_0=a}^{x_0}\sum_{i=1}^{16} d_{0\mu(i)}(u_0+at(i),v_0-a;\mathbf{k}) \tag{3.74}$$
$$\times\,\mathrm{tr}\left[\mathrm{M_l^i}(\mathrm{x_0},\mathrm{u_0};\mathbf{p},\mathbf{k})\gamma_0\mathrm{P_+}\right]$$

where the subscript ge denotes the gluon exchange. This yields the last Feynman diagram for $f_{\mathrm{A}}^{\mathrm{stat}(1)}$ in figure 12. The contribution generated by the boundary improvement term proportional to $\tilde{c}_t^{(1)}$ takes the form

$$f_{A,bi}^{stat}(x_0,\mathbf{p}) = \tilde{c}_t^{(1)}N\mathrm{tr}\left[\mathrm{R_l^i}(\mathrm{x_0},\mathbf{p})\gamma_0\mathrm{P_+}\right]\ , \tag{3.75}$$
$$R_l^i(x_0,\mathbf{p}) = \tilde{S}_l^{(0)}(x_0,a,\mathbf{p})\left[\chi_l(a,\mathbf{p})-P_+\right] + S_l^{(0)}(x_0,T-a,\mathbf{p})\chi_l(T-a,\mathbf{p})$$

Above defined R-matrix contains explicit tree level contributions arising from the boundary links. In the interior of the SF, those boundary links are continued by the respective quark propagators.
To achieve complete $\mathcal{O}(a)$ improvement, the axial current improvement term arising from Eq. (2.49) has to be added to $f_{\mathrm{A}}^{\mathrm{stat}}$, i.e.

$$f_{\mathrm{A,impr}}^{\mathrm{stat}} = f_{\mathrm{A}}^{\mathrm{stat}} + ac_{\mathrm{A}}^{\mathrm{stat}}f_{\delta A}^{stat} \tag{3.76}$$

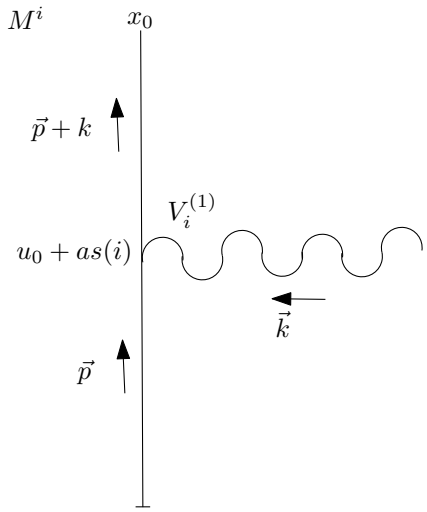

Figure 11: The Matrix M^i

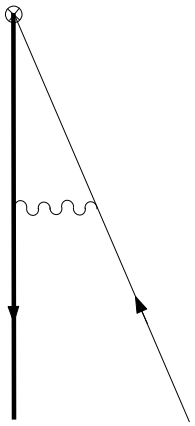

Figure 12: $f^{stat}_{A,ge}$

with

$$f^{\rm stat}_{\delta {\rm A}} = -a^6 \sum_{\mathbf{y},\mathbf{z}} < \overline{\Psi}_l \gamma_k \gamma_5 \frac{1}{2} (\overleftarrow{\nabla}_k + \overleftarrow{\nabla}^*_k) \Psi_h(x) \bar{\zeta}_h(\mathbf{y}) \gamma_5 \zeta_l(\mathbf{z}) > \tag{3.77}$$

$$= -a^6 \sum_{\mathbf{y},\mathbf{z}} < {\rm tr} \left\{ \left[\zeta_{\rm l}(\mathbf{z}) \overline{\Psi}_{\rm l}({\rm x}) \right]_{\rm F} \gamma_{\rm k} \gamma_5 \frac{1}{2} (\overleftarrow{\nabla}_{\rm k} + \overleftarrow{\nabla}^*_{\rm k}) \left[\Psi_{\rm h}({\rm x}) \bar{\zeta}_{\rm h}(\mathbf{y}) \right]_{\rm F} \gamma_5 \right\} >_{\rm G}$$

The above described discussion carries over to the second correlation function $f_1^{\rm stat}$ which we want to determine. In contrast to $f_{\rm A}^{\rm stat}$, it does not depend on x_0 and is defined by

$$f_1^{\rm stat} = -\frac{1}{2} \frac{a^{12}}{L^6} \sum_{\mathbf{u},\mathbf{v},\mathbf{y},\mathbf{z}} < \bar{\zeta}'_l(\mathbf{u}) \gamma_5 \zeta'_h(\mathbf{v}) \bar{\zeta}_h(\mathbf{y}) \gamma_5 \zeta_(\mathbf{z}) >_G \tag{3.78}$$

$$= \frac{1}{2} < {\rm tr} \left\{ {\rm K}_{\rm l}^\dagger {\rm K}_{\rm h} \right\} >_{\rm G}$$

and its Fourier transformed shape, where the momenta $\mathbf{p}$ and $\mathbf{p}$ describe the momenta of the boundary fields:

$$f_1^{\rm stat}(\mathbf{p},\mathbf{q}) = -\frac{1}{2} \frac{a^{12}}{L^6} \sum_{\mathbf{u},\mathbf{v},\mathbf{y},\mathbf{z}} e^{i\mathbf{p}(\mathbf{u}-\mathbf{v})} e^{i\mathbf{q}(\mathbf{y}-\mathbf{z})} < \bar{\zeta}'_l(\mathbf{u}) \gamma_5 \zeta'_h(\mathbf{v}) \bar{\zeta}_h(\mathbf{y}) \gamma_5 \zeta_(\mathbf{z}) >_G \tag{3.79}$$

$$= \frac{1}{2} < {\rm tr} \left\{ {\rm K}_{\rm l}(\mathbf{p},\mathbf{q})^\dagger {\rm K}_{\rm h}(\mathbf{p},\mathbf{q}) \right\} >_{\rm G}$$

In analogy to $f_{\rm A}^{\rm stat}$ and its H-matrix, above representation contains a K-matrix defined by

$$K_l(\mathbf{p},\mathbf{q}) = \tilde{c}_t \frac{a^3}{L^3} \sum_{\mathbf{x}} \left\{ P_+ e^{i\mathbf{px}} U_0(x)^{-1} H_l(x,\mathbf{q}) \right\} |_{x_0=T-a} \tag{3.80}$$
$$K_h(\mathbf{p},\mathbf{q}) = \tilde{c}_t \frac{a^3}{L^3} \sum_{\mathbf{x}} \left\{ P_+ e^{i\mathbf{px}} U_0(x)^{-1} H_h(x,\mathbf{q}) \right\} |_{x_0=T-a}$$

Again, we end up with

$$f_1^{\mathrm{stat}\,(0)}(\mathbf{p},\mathbf{q}) = -\frac{1}{2} \left\langle \mathrm{tr} \left\{ \mathrm{K_l^{(0)\dagger}}(\mathbf{p},\mathbf{q}) \mathrm{K_h^{(0)}}(\mathbf{p},\mathbf{q}) \right\} \right\rangle_G \tag{3.81}$$
$$f_1^{\mathrm{stat}\,(1)}(\mathbf{p},\mathbf{q}) = -\frac{1}{2} \left\langle \mathrm{tr} \left\{ \mathrm{K_l^{(1)\dagger}}(\mathbf{p},\mathbf{q}) \mathrm{K_h^{(1)}}(\mathbf{p},\mathbf{q}) + \mathrm{K_l^{(0)\dagger}}(\mathbf{p},\mathbf{q}) \mathrm{K_h^{(2)}}(\mathbf{p},\mathbf{q}) + \mathrm{K_l^{(2)\dagger}}(\mathbf{p},\mathbf{q}) \mathrm{K_h^{(0)}}(\mathbf{p},\mathbf{q}) \right\} \right\rangle_G$$

Considering the pertubative expansion of K, one obtains for the tree level

$$K_l^{(0)}(\mathbf{p},\mathbf{q}) = P_+ \delta_{\mathbf{p},\mathbf{q}} \chi_l(T-a,\mathbf{p}) \tag{3.82}$$
$$K_h^{(0)}(\mathbf{p},\mathbf{q}) = P_+ \delta_{\mathbf{p},\mathbf{q}} \chi_h(T-a,\mathbf{p})$$

which describes the respective quarks propagating between the the boundaries of the SF.
The first two oders of K can be split into [8]

$$\begin{aligned}
K_l^{(1)}(\mathbf{p},\mathbf{q}) &= K_l^{(1)}(\mathbf{p},\mathbf{q})_{bulk} + K_l^{(1)}(\mathbf{p},\mathbf{q})_{bound} \\
K_h^{(1)}(\mathbf{p},\mathbf{q}) &= K_h^{(1)}(\mathbf{p},\mathbf{q})_{bulk} + K_h^{(1)}(\mathbf{p},\mathbf{q})_{bound} \\
K_l^{(2)}(\mathbf{p},\mathbf{q}) &= K_l^{(2)}(\mathbf{p},\mathbf{q})_{ss,bulk} + K_l^{(2)}(\mathbf{p},\mathbf{q})_{ss;bound} + \\
&\quad + K_l^{(2)}(\mathbf{p},\mathbf{q})_{tp,bulk} + K_l^{(2)}(\mathbf{p},\mathbf{q})_{tp,bound} + K^{(2)}(\mathbf{p},\mathbf{q})_{bi} \\
K_h^{(2)}(\mathbf{p},\mathbf{q}) &= K_h^{(2)}(\mathbf{p},\mathbf{q})_{ss,bulk} + K_h^{(2)}(\mathbf{p},\mathbf{q})_{ss;bound} + \\
&\quad + K_h^{(2)}(\mathbf{p},\mathbf{q})_{tp,bulk} + K_h^{(2)}(\mathbf{p},\mathbf{q})_{tp,bound}
\end{aligned} \tag{3.83}$$

This splitting reflects the appearance of the boundary link in the definition of K. $K^{(1)}$ and $K^{(2)}$ can be found by expanding (3.80) in terms of g_0 and by reusing the expansions of the H-matrices. The resulting formulae can be rearranged according to (3.83) and then be inserted into (3.81). Adopting the auxiliary quantities from the former section, this gives the final relations for the Feynman diagrams for f_1^{stat}. It is worth mentioning that like for $f_{\mathrm{A}}^{\mathrm{stat}}$, there is no boundary improvement term for the heavy case.

For the tree level of f_1^{stat}, one gets

$$f_1^{\mathrm{stat}\,(0)}(\mathbf{p},\mathbf{q}) = \frac{1}{2} N \delta_{\mathbf{pq}} \mathrm{tr} \left[\chi_{\mathrm{l}}(\mathrm{T}-\mathrm{a},\mathbf{p})^\dagger \mathrm{P}_+ \right] \tag{3.84}$$

The mass shift in analogy to Eq. (3.57) is then given by

$$df_1^{\mathrm{stat}\,(0)}(\mathbf{p}) = \frac{1}{2} N \sum_{u_0=1}^{T-1} \mathrm{tr} \left\{ \chi(\mathrm{u}_0,\mathbf{p})^\dagger \tilde{\mathrm{S}}^{(0)}(\mathrm{T}-1,\mathbf{p}) \mathrm{P}_+ \right\} \tag{3.85}$$

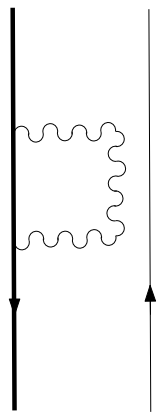

Figure 13: $f^{stat}_{1,ss-a}$

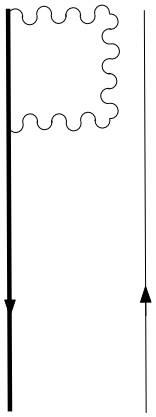

Figure 14: $f^{stat}_{1,ss-c}$

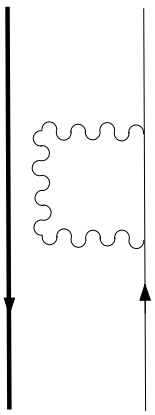

Figure 15: $f^{stat}_{1,ss-b}$

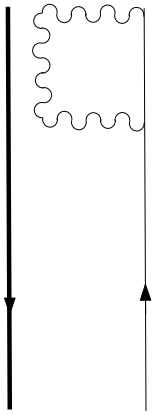

Figure 16: $f^{stat}_{1,ss-d}$

We are then having a look at at the diagrams for the self energy in which the gluon propagators have different emission and absorption points. Like for $f_{\mathrm{A}}^{\mathrm{stat}}$, the relativistic three-point quark-gluon vertices appear. They are expressed as

$$
\begin{aligned}
f^{stat}_{1,ss-a}(\mathbf{p},\mathbf{q}) &= -NC_F\frac{a^2}{2L^3}\delta_{\mathbf{pq}}\sum_{\mathbf{k}}\sum_{u_0=a}^{T-a}\sum_{v_0=a}^{u_0-a} d_{00}(u_0-a,v_0-a;\mathbf{k}) \\
&\quad\times \mathrm{tr}\left[\chi_1(\mathrm{T}-\mathrm{a};\mathbf{p})^\dagger \mathrm{P}_+\right] \\
f^{stat}_{1,ss-c}(\mathbf{p},\mathbf{q}) &= -NC_F\frac{a^2}{2L^3}\delta_{\mathbf{pq}}\sum_{\mathbf{k}}\sum_{u_0=a}^{T-a} d_{00}(T-a,u_0-a;\mathbf{k}) \\
&\quad\times \mathrm{tr}\left[\chi_1(\mathrm{T}-\mathrm{a};\mathbf{p})^\dagger \mathrm{P}_+\right] \\
f^{stat}_{1,ss-b}(\mathbf{p},\mathbf{q}) &= -NC_F\frac{a^2}{2L^3}\delta_{\mathbf{pq}}\sum_{\mathbf{k}}\sum_{u_0,v_0=a}^{T-a}\sum_{i,j=1}^{16} d_{\mu(i)\mu(j)}(u_0+at(i),v_0+at(j);\mathbf{k}) \\
&\quad\times \mathrm{tr}\left[\mathrm{M}_1^{\mathrm{ij}}(\mathrm{T}-\mathrm{a},\mathrm{u}_0,\mathrm{v}_0,\mathbf{p},\mathbf{k})^\dagger \mathrm{P}_+\right] \\
f^{stat}_{1,ss-d}(\mathbf{p},\mathbf{q}) &= -NC_F\frac{a^2}{2L^3}\delta_{\mathbf{pq}}\sum_{\mathbf{k}}\sum_{u_0=a}^{T-a}\sum_{i=1}^{16} d_{\mu(i)0}(u_0+at(i),T-a;\mathbf{k}) \\
&\quad\times \mathrm{tr}\left[\mathrm{M}_1^{\mathrm{i}}(\mathrm{T}-\mathrm{a},\mathrm{u}_0,\mathbf{p},\mathbf{k})^\dagger \mathrm{P}_+\right]
\end{aligned}
\tag{3.86}
$$

The formulae for the tadpole diagrams resemble the fromulae for the setting sun diagrams. The gluon propagators are contracted at the same emission and absorption points. The factor $\frac{1}{2}$ in below formulae arises from the expansion of the gauge links in terms g_0^2 causing a tadpole contribution to the self-energy. Accordingly, the relativistic four-point quark-gluon vertices are contained.

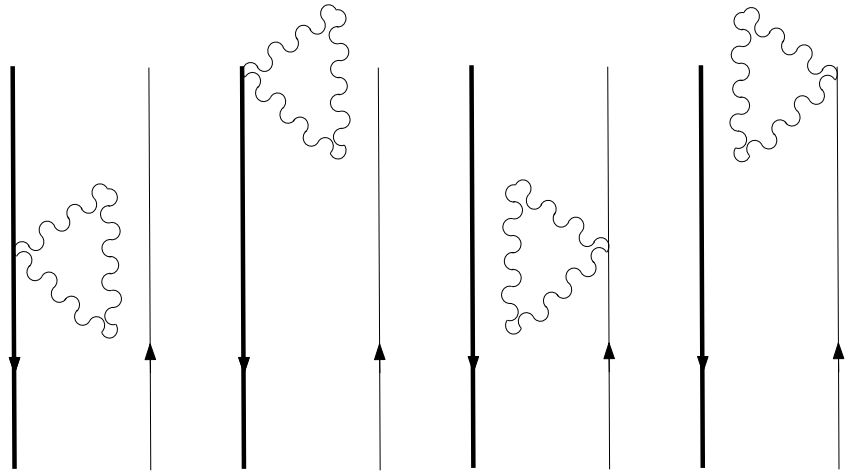

Figure 17: $f^{stat}_{1,tp-a}$

Figure 18: $f^{stat}_{1,tp-c}$

Figure 19: $f^{stat}_{1,tp-b}$

Figure 20: $f^{stat}_{1,tp-d}$

$$
\begin{aligned}
f^{stat}_{1,tp-a}(\mathbf{p},\mathbf{q}) &= -NC_F\frac{a^2}{4L^3}\delta_{\mathbf{pq}}\sum_{\mathbf{k}}\sum_{u_0=a}^{T-a} d_{00}(u_0-a,u_0-a;\mathbf{k}) \\
&\quad\times \mathrm{tr}\left[\chi_1(\mathrm{T}-\mathrm{a};\mathbf{p})^\dagger \mathrm{P}_+\right] \\
f^{stat}_{1,tp-c}(\mathbf{p},\mathbf{q}) &= -NC_F\frac{a^2}{4L^3}\delta_{\mathbf{pq}}\sum_{\mathbf{k}} d_{00}(T-a,T-a;\mathbf{k}) \\
&\quad\times \mathrm{tr}\left[\chi_1(\mathrm{T}-\mathrm{a};\mathbf{p})^\dagger \mathrm{P}_+\right] \\
f^{stat}_{1,tp-b}(\mathbf{p},\mathbf{q}) &= -NC_F\frac{a^2}{2L^3}\delta_{\mathbf{pq}}\sum_{\mathbf{k}}\sum_{u_0=a}^{T-a}\sum_{i=1}^{5} d_{\mu(i)\mu(i)}(u_0+at(i),u_0+at(i);\mathbf{k}) \\
&\quad\times \mathrm{tr}\left[\mathrm{N}^{\mathrm{i}}_1(\mathrm{T}-\mathrm{a},\mathrm{u}_0,\mathbf{p},\mathbf{k})^\dagger \mathrm{P}_+\right] \\
f^{stat}_{1,tp-d}(\mathbf{p},\mathbf{q}) &= -NC_F\frac{a^2}{4L^3}\delta_{\mathbf{pq}}\sum_{\mathbf{k}} d_{00}(T-a,T-a;\mathbf{k}) \\
&\quad\times \mathrm{tr}\left[\mathrm{N}^{\mathrm{i}}_1(\mathrm{T}-\mathrm{a},\mathbf{p})^\dagger \mathrm{P}_+\right]
\end{aligned}
\tag{3.87}
$$

For the boundary improvement term contribution,one gets

$$
f^{stat}_{1,bi}(\mathbf{p},\mathbf{q}) = \tilde{c}^{(1)}_t\left\{f^{stat(0)}_1(\mathbf{p},\mathbf{q}) - N\delta_{\mathbf{p},\mathbf{q}}\mathrm{tr}\left[\mathrm{R}^{\mathrm{i}}_1(\mathrm{T}-\mathrm{a},\mathbf{p})^\dagger \mathrm{P}_+\right]\right\} \tag{3.88}
$$

with the R-matrix defined in (3.75). We are now left in specifying the diagrams for the gluon exchange. If we again distinguish between bulk and boundary contributions according to (3.83), four further diagrams emerge like shown in Figures (21) to (24) Only gluons with vanishing momentum $\mathbf{q} = \underline{0}$ are exchanged.

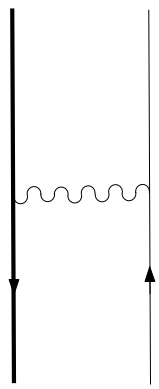

Figure 21: $f^{stat}_{1,ge-a}$

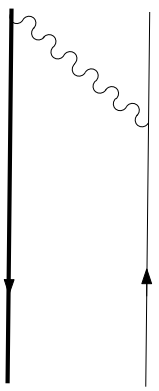

Figure 22: $f^{stat}_{1,ge-b}$

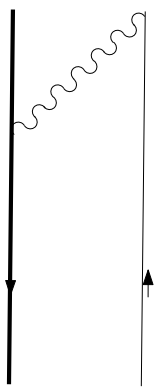

Figure 23: $f^{stat}_{1,ge-c}$

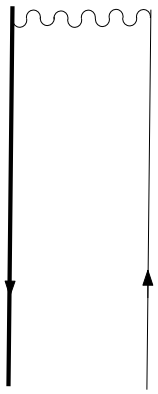

Figure 24: $f^{stat}_{1,ge-d}$

An analytic description of the diagrams reads

$$f^{stat}_{1,ge-a}(\mathbf{p},\mathbf{q}) = NC_F\frac{a^2}{2L^3}\delta_{\mathbf{pq}}\sum_{\mathbf{k}}\sum_{u_0=a}^{T-a}\sum_{v_0=a}^{T-a}\sum_{i=1}^{16} d_{0\mu(i)}(u_0+at(i),v_0-a;\mathbf{k}) \\ \times \mathrm{tr}\left[\mathrm{M}_1^{\mathrm{i}}(\mathrm{T}-\mathrm{a},\mathrm{u}_0,\mathbf{p},\underline{0})^\dagger \mathrm{P}_+\right] \tag{3.89}$$

$$f^{stat}_{1,ge-c}(\mathbf{p},\mathbf{q}) = NC_F\frac{a^2}{2L^3}\delta_{\mathbf{pq}}\sum_{\mathbf{k}}\sum_{u_0=a}^{T-a}\sum_{i=1}^{16} d_{0\mu(i)}(u_0+at(i),T-a;\underline{0})\mathrm{tr}\left[\mathrm{M}_1^{\mathrm{i}}(\mathrm{T}-\mathrm{a},\mathrm{u}_0,\mathbf{p},\mathbf{k})^\dagger \mathrm{P}_+\right]$$

$$f^{stat}_{1,ge-b}(\mathbf{p},\mathbf{q}) = NC_F\frac{a^2}{2L^3}\delta_{\mathbf{pq}}\sum_{\mathbf{k}}\sum_{u_0=a}^{T-a} d_{00}(T-a,u_0-a;\mathbf{k})\mathrm{tr}\left[\chi_{\mathrm{l}}(\mathrm{T}-\mathrm{a},\mathbf{p})^\dagger \mathrm{P}_+\right]$$

$$f^{stat}_{1,ge-d}(\mathbf{p},\mathbf{q}) = NC_F\frac{a^2}{2L^3}\delta_{\mathbf{pq}}\sum_{\mathbf{k}} d_{00}(T-a,T-a;\mathbf{k})\mathrm{tr}\left[\chi_{\mathrm{l}}(\mathrm{T}-\mathrm{a},\mathbf{p})^\dagger \mathrm{P}_+\right]$$

3.6 HYP links in the SF

The preceeding considerations can be reviewed when taking into account temporal HYP links for the static quark as introduced in chapter 2. Obviously, only the diagrams for the heavy quark and the gluon exchange between light and heavy quark are affected by this new point-of-view whereas the diagrams for the light quark remain unchanged. In the following, the Feynman rules are derived for the SF with HYP smearing.
Following the introductory considerations of section 1, the smeared gauge fields are projected to SU(3) and thus the three levels of the HYP procedure can be defined according to

$$W_{\mu}^{(3)}(x) = e^{ag_0 B_{\mu}^{(3)}(x)}, \tag{3.90}$$

$$W_{\mu;\nu}^{(2)}(x) = e^{ag_0 B_{\mu;\nu}^{(2)}(x)}, \tag{3.91}$$

$$W_{\mu;\nu\rho}^{(1)}(x) = e^{ag_0 B_{\mu;\nu\rho}^{(1)}(x)}. \tag{3.92}$$

The aim is now to obtain the relation between the smeared and original gauge fields, i.e. between $B_{\mu}^{(3)}(x)$ and $q_{\mu}(x)$. This relation has been derived for a finite lattice with PBC and with HYP smearing in momentum space [11] as a function

$$\tilde{B}_{\mu}^{(3)}(p) = \sum_{\nu} f_{\mu\nu}(p)\tilde{q}_{\nu}(p) \ + \ \mathrm{O}(g_0) \ , \tag{3.93}$$

with $\tilde{q}_{\nu}(p)$ and $\tilde{B}_{\mu}^{(3)}(p)$ denoting the FT of $q(x)$ and $B_{\mu}^{(3)}(x)$. Above equation is diagonal in momentum space. The tensor $f_{\mu\nu}(p)$ is given by

$$f_{\mu\nu}(p) = \delta_{\mu\nu}\left[1 - \frac{\alpha_1}{6}\sum_{\rho}(a^2\hat{p}_{\rho}^2)\Omega_{\mu\rho}(p)\right] + \frac{\alpha_1}{6}(a\hat{p}_{\mu})(a\hat{p}_{\nu})\Omega_{\mu\nu}(p) \ , \tag{3.94}$$

$$\Omega_{\mu\nu}(p) = 1 + \alpha_2(1+\alpha_3) - \frac{\alpha_2}{4}(1+2\alpha_3)a^2(\hat{p}^2 - \hat{p}_{\mu}^2 - \hat{p}_{\nu}^2) + \frac{\alpha_2\alpha_3}{4}\prod_{\eta\neq\mu,\nu} a^2\hat{p}_{\eta}^2 \ . \tag{3.95}$$

For the SF, we want to gain an according representation in time-momentum space. This relation can be derived in a smart way by following a proposal of D.Guazzini [22] by taking the result of Eq. (3.93) in full momentum space with periodic boundary conditions and performing an anti-Fourier transformation in time. This is possible in presence of homogeneous Dirichlet boundary conditions which allow to continue the SF periodically to all times with no non-trivial tems at the boundaries. The approach shall be pointed out a bit more in detail in the following:

Under the assumption of periodic boundary conditions in space and time, the gauge field of the fundamental (and smeared) link admits a 4-dimensional Fourier transform

$$q_{\mu}(x) = \frac{1}{L^4}\sum_{p} \mathrm{e}^{ipx}\mathrm{e}^{i\frac{a}{2}p_{\mu}}\tilde{q}_{\mu}(p) \ , \qquad -\frac{\pi}{a} \leq p_{\mu} = \frac{2\pi}{L}n_{\mu} < \frac{\pi}{a} \ , \tag{3.96}$$

where L is the toroidal extension of the space-time dimensions and the additional phase shift in direction $\hat{\mu}$ is due to the very definition of the gauge fields,

which are supposed to live between neighbouring lattice points. Factorizing the loop-sums over the spatial directions allows to express the gauge field in time-momentum representation in terms of the full Fourier-transformed one, i.e.

$$q_0(x) = \frac{1}{L^3}\sum_{\mathbf{p}} \mathrm{e}^{i\mathbf{px}} \left[\frac{1}{L}\sum_{p_0} \mathrm{e}^{ip_0x_0}\mathrm{e}^{i\frac{a}{2}p_0}\tilde{q}_0(p)\right] = \frac{1}{L^3}\sum_{\mathbf{p}} \mathrm{e}^{i\mathbf{px}}\tilde{q}_0(x_0;\mathbf{p}) \ , \quad (3.97)$$

$$q_k(x) = \frac{1}{L^3}\sum_{\mathbf{p}} \mathrm{e}^{i\mathbf{px}}\mathrm{e}^{i\frac{a}{2}p_k} \left[\frac{1}{L}\sum_{p_0} \mathrm{e}^{ip_0x_0}\tilde{q}_k(p)\right] = \frac{1}{L^3}\sum_{\mathbf{p}} \mathrm{e}^{i\mathbf{px}}\mathrm{e}^{i\frac{a}{2}p_k}\tilde{q}_k(x_0;\mathbf{p}) \ . \quad (3.98)$$

By direct comparison, it follows

$$\tilde{q}_0(x_0;\mathbf{p}) = \frac{1}{L}\sum_{p_0} \mathrm{e}^{ip_0x_0}\mathrm{e}^{i\frac{a}{2}p_0}\tilde{q}_0(p) \ ,$$

$$\tilde{q}_k(x_0;\mathbf{p}) = \frac{1}{L}\sum_{p_0} \mathrm{e}^{ip_0x_0}\tilde{q}_k(p) \ . \quad (3.99)$$

We now consider Eq. (3.93), i.e. the Feynman rules in momentum representation. Since we are interested in the static propagator, we first consider $B_0^{(3)}$, for which we get

$$\tilde{B}_0^{(3)}(x_0;\mathbf{p}) = \frac{1}{L}\sum_{p_0} \mathrm{e}^{ip_0x_0}\mathrm{e}^{i\frac{a}{2}p_0} \left[f_{00}(p)\tilde{q}_0(p) + \sum_{k=1}^{3} f_{0k}(p)\tilde{q}_k(p)\right] \ , \quad (3.100)$$

We then observe that

$$f_{00}(p) = 1 - \frac{\alpha_1}{6}\sum_{k=1}^{3}(a^2\hat{p}_k^2)\Omega_{0k}(p) \ , \quad (3.101)$$

$$\Omega_{0k}(p) = 1 + \alpha_2(1+\alpha_3) - \frac{\alpha_2}{4}(1+2\alpha_3)(a^2\hat{p}_j^2 + a^2\hat{p}_l^2) + \quad (3.102)$$

$$+ \frac{\alpha_2\alpha_3}{4}(a^2\hat{p}_j^2)(a^2\hat{p}_l^2) \ , \qquad (\hat{j},\hat{l}) \perp \hat{k} \ , \quad (3.103)$$

$$f_{0k}(p) = \frac{\alpha_1}{6}(a\hat{p}_0)(a\hat{p}_k)\Omega_{0k}(p) \ . \quad (3.104)$$

The above equations show in particular that Ω_{0k} and f_{00} depend only upon the spatial components of the Fourier momentum. Therefore,

$$\tilde{B}_0^{(3)}(x_0;\mathbf{p}) = f_{00}(\mathbf{p})\tilde{q}_0(x_0;\mathbf{p}) + \\ + \frac{\alpha_1}{6}\sum_{k=1}^{3}(a\hat{p}_k)\Omega_{0k}(\mathbf{p})\frac{1}{L}\sum_{p_0} \mathrm{e}^{ip_0x_0}\mathrm{e}^{i\frac{a}{2}p_0} \ (a\hat{p}_0)\tilde{q}_k(p) \ + \ \mathrm{O}(g_0) \ . \quad (3.105)$$

i	$\mu_H(i)$	$s_H(i)$	$h_{0;i}(\mathbf{p})$
0	0	0	$1-\frac{\alpha_1}{6}\sum_{k=1}^{3} a^2\hat{p}_k^2\Omega_{0k}(\mathbf{p})$
1,2,3	i	0	$+\frac{i\alpha_1}{6}a\hat{p}_i\Omega_{0i}(\mathbf{p})$
4,5,6	$i-3$	1	$-\frac{i\alpha_1}{6}a\hat{p}_{\mu(i)}\Omega_{0\mu(i)}(\mathbf{p})$

Table 1: Feynman rules of the temporal HYP link in time-momentum representation

The second term on the right hand side of the previous equation can be easily worked out,

$$\frac{1}{L}\sum_{p_0} \mathrm{e}^{ip_0x_0}\mathrm{e}^{i\frac{a}{2}p_0}\ (a\hat{p}_0)\tilde{q}_k(p) = \frac{1}{L}\sum_{p_0} \mathrm{e}^{ip_0x_0}\mathrm{e}^{i\frac{a}{2}p_0}\ \frac{1}{i}\left[\mathrm{e}^{i\frac{a}{2}p_0}-\mathrm{e}^{-i\frac{a}{2}p_0}\right]\tilde{q}_k(p) =$$

$$= -\frac{i}{L^3}\sum_{p_0} \mathrm{e}^{ip_0x_0}\left[\mathrm{e}^{iap_0}-1\right]\tilde{q}_k(p) = -ia\partial_0\tilde{q}_k(x_0,\mathbf{p})\ , \tag{3.106}$$

and we finally obtain

$$\tilde{B}_0^{(3)}(x_0;\mathbf{p}) = f_{00}(\mathbf{p})\tilde{q}_0(x_0;\mathbf{p}) - \frac{i\alpha_1}{6}\sum_{k=1}^{3}(a\hat{p}_k)\Omega_{0k}(\mathbf{p})\partial_0\tilde{q}_k(x_0;\mathbf{p})\ . \tag{3.107}$$

A very compact way of writing the above Feynman rule is to introduce an effective vertex and some auxiliary indices, as first pursued in [6], i.e.

$$\tilde{B}_0^{(3)}(x_0;\mathbf{p}) = \sum_{i=0}^{6} h_{0;i}(\mathbf{p})\tilde{q}_{\mu(i)}(x_0+as(i);\mathbf{p})\ . \tag{3.108}$$

giving Table 1. A direct comparison of Table 1 and Table 4 of [13] shows that the Feyman rules of the APE gauge link can be obtained from those of the HYP link by just setting $\Omega_{0k}=1$.
The result was checked by direct construction upon representing the HYP smearing by F.Palombi as a lattice differential operator acting linearly on the fundamental gauge fields [22].

The H-matrices for the static quark introduced in the former section now take a new form, similiar as those for the APE action given in [13]. A difference consists in the projection of the HYP gauge links onto the SU(3) group. This SU(3) projection is not uniquely defined and the resulting HYP link depends in principle upon the chosen definition. Here we follow [13] and in concrete [22]: if A denotes a generic 3×3 complex matrix, its projection M is obtained via

$$M = \frac{X}{\sqrt[3]{(\det X)}}\ , \qquad X = \frac{A}{\sqrt{A^\dagger A}}\ , \tag{3.109}$$

where the matrix A is first unitarized, and then its determinant is rotated to one. Another very popular definition, used for instance by the staggered community,

goes through the maximization (minimization) of the real (imaginary) trace

$$T = \mathrm{Tr}(M^\dagger A) \ . \tag{3.110}$$

In this framework Weon-jong Lee has been able to prove two interesting theorems concerning the gauge field of the fat link, which allow for a substantial simplication of the perturbative calculations at one-loop order [16]. Although his proof is based on Eq. (3.110), these theorems are valid independently. A proof of them based on Eq. (3.109) is indeed straightforward. To fix the notation, we define the gauge field of the fundamental link via

$$U_\mu(x) = e^{ag_0 q^a_\mu(x) T^a}, \tag{3.111}$$

where $\{T^a\}_{a=1\ldots8}$ denotes an anti-hermitian representation of the Gell-Mann matrices. The unprojected APE-blocked links of Eqs. (2.15,2.16,2.17) can be written in the general form

$$V_\mu(x) = \ + ag_0 \sum_{\nu;y} f_{\mu\nu}(x,y) q_\nu(y) \ + a^2 g_0^2 \sum_{\nu\rho;yz} h_{\mu\nu\rho}(x,y,z) q_\nu(y) q_\rho(z) \ + \mathrm{O}(g_0^3) \ , \tag{3.112}$$

with real vertices f, h depending on the level of the HYP smearing. It should be observed that, since V_μ is not an SU(3) matrix, no gauge field can be associated with it. Projecting the link according to Eq. (3.109) leads to

$$\begin{aligned} \frac{V_\mu(x)}{\sqrt{V_\mu^\dagger(x) V_\mu(x)}} \ = \ & + \ ag_0 \sum_{\nu;y} f_{\mu\nu}(x,y) q_\nu(y) \\ & + \ \frac{a^2 g_0^2}{2} \sum_{\nu\rho;yz} h_{\mu\nu\rho}(x,y,z) [q_\nu(y), q_\rho(z)] \\ & + \ \frac{a^2 g_0^2}{2} \sum_{\nu\rho;yz} f_{\mu\nu}(x,y) f_{\mu\rho}(x,z) q_\nu(y) q_\rho(z) \\ & + \ \mathrm{O}(g_0^3) \ , \end{aligned} \tag{3.113}$$

and

$$\det \left[\frac{V_\mu(x)}{\sqrt{V_\mu^\dagger(x) V_\mu(x)}} \right] \ = \ 1 \ + \ \mathrm{O}(g_0^3) \ . \tag{3.114}$$

Now, the projected link $\mathcal{P}_{\mathrm{SU(3)}}[V_\mu(x)]$ is in SU(3) by construction. Consequently, we are allowed to introduce a smeared gauge field

$$\mathcal{P}_{\mathrm{SU(3)}}[V_\mu(x)] = \exp\{ag_0 v^a_\mu(x) T^a\} \ . \tag{3.115}$$

As a remark we also note that, since the perturbative expansion of the staples generates gauge fields at all orders in perturbation theory, B_μ cannot be assumed to be linear in q_μ, and will have to be perturbatively expanded in its turn, i.e.

$$v_\mu = v'_\mu \ + \ ag_0 v''_\mu \ + \ \mathrm{O}(g_0^2) \ . \tag{3.116}$$

Accordingly, Eq. (3.115) reads

$$\mathcal{P}_{\mathrm{SU(3)}}[V_\mu(x)] = \ + \ ag_0 v'_\mu \ + \ a^2 g_0^2 v''_\mu \ + \ \frac{a^2 g_0^2}{2} v'_\mu v'_\mu \ + \ \mathrm{O}(g_0^3) \ . \tag{3.117}$$

Equating Eq. (3.117) and Eq. (3.113) order by order in the bare coupling allows to express the smeared gauge field in terms of the unsmeared ones. In particular

$$\mathrm{O}(g_0^0): \qquad \mathbb{1} \;=\; \mathbb{1}, \tag{3.118}$$

$$\mathrm{O}(g_0^1): \qquad v'_\mu \;=\sum_{\nu;y} f_{\mu\nu}(x,y)q_\nu(y)\ , \tag{3.119}$$

$$\mathrm{O}(g_0^2): \qquad v''_\mu \;=\frac{1}{2}\sum_{\nu\rho;yz} h_{\mu\nu\rho}(x,y,z)[q_\nu(y),q_\rho(z)]\ . \tag{3.120}$$

Eqs. (3.119,3.120) correspond precisely to Theorems 1 and 2 of [16].

To summarize, Eqs. (3.119,3.120) tell us that if we stay at one-loop order in perturbation theory and the background field is switched off, the smeared gauge field can be taken as a linear function of the unsmeared ones. It is worth noting that the tadpole diagrams associated with Eq. (3.120) do not contribute to any one-loop perturbative calculation without background field, although they are $\mathrm{O}(g_0^2)$. Indeed

$$[T^a,T^b] = -f^{abc}T^c \tag{3.121}$$

is antisymmetric in $a \leftrightarrow b$, while the Wick contraction $\langle q^a q^b\rangle$ is symmetric making the product of both factors vanish. The vanishing of the above-mentioned tadpole contributions is not anymore true in presence of a background field, where perturbation theory is expected to be more involved. The effect of the SU(3) projection can be disregarded in the linear term, and non-linear contributions should be discarded when deriving the Feynman rules of the HYP link. Eqs. (3.119) then leads to the first contribution of the new H-Matrix

$$\begin{aligned} H_h^{(1)}(x,\mathbf{p}) = -\frac{a}{L^3}\sum_{\mathbf{k}}\sum_{u_0=a}^{T-a}\sum_{i=1}^{6} & e^{i(\mathbf{k}+\mathbf{p})\mathbf{x}}\Theta(x_0-u_0) \\ & \times h_{0;i}(\mathbf{p})\tilde{q}^a_{\mu(i)}(u_0-a+as_H(i);\mathbf{k})T^aP_+ \end{aligned} \tag{3.122}$$

containing the vertices $h_{0;i}(\mathbf{p})$ and shifts from Table 1.
One should avoid the conclusion that tadpoles do not contribute at all, because terms such as $v'_\mu(x)v'_\mu(x)$ have to be always considered leading to the tadpole contribution of the H-Matrix

$$\begin{aligned} H_h^{(2)}(x,\mathbf{p}) = \frac{a^2}{2L^6}\sum_{\mathbf{k},\mathbf{q}}\sum_{u_0=a}^{T-a}\sum_{i,j=1}^{6} & e^{i(\mathbf{k}+\mathbf{q}+\mathbf{p})\mathbf{x}}\Theta(x_0-u_0) \\ & \times h_{0;j}(\mathbf{p})\tilde{q}^a_{\mu(j)}(u_0-a+as_H(j);\mathbf{k})h_{0;i}(\mathbf{p})\tilde{q}^b_{\mu(i)}(u_0-a+as_H(i);\mathbf{q})T^aT^bP_+ \end{aligned} \tag{3.123}$$

Knowing the expansion of the new H-Matrix, the deduction of the Feynman rules is straightforward from the basic Eq. (3.49). The only new ingredients are the additional HYP vertices for the static fermion and in the induced HYP shifts repectively. To make the notation clearer, shifts induced by the HYP action appear as $s_H(i)$ whereas shifts caused by the three-point gluon vertex (which is part of $M_l^i(x_0,u_0,\mathbf{p},\mathbf{k})$) come as $t(i)$. In the gluon index, the values

$\mu_H(i)$ come from the HYP action, $\mu(i)$ from the three-point gluon vertex. The formulae for f_A^{stat} with HYP thus read

$$f^{stat}_{A,ss-a}(x_0,\mathbf{p}) = NC_F\frac{a^2}{2L^3}\sum_{\mathbf{k}}\sum_{u_0=1}^{x_0}\sum_{v_0=1}^{u_0-1}\sum_{i,j=0}^{6} d_{\mu_H(i)\mu_H(j)}(u_0-1+s_H(i),v_0-1+s_H(j),\mathbf{k}) \tag{3.124}$$
$$\times\ \mathrm{tr}\left[\chi_1(\mathrm{x}_0;\mathbf{p})^\dagger\gamma_0\mathrm{P}_+\right]$$

$$f^{stat}_{A,ss-b}(x_0,\mathbf{p}) = NC_F\frac{a^2}{2L^3}\sum_{\mathbf{k}}\sum_{u_0,v_0=a}^{T-a}\sum_{i,j=1}^{16} d_{\mu(i)\mu(j)}(u_0+at(i),v_0+at(j);\mathbf{k}) \tag{3.125}$$
$$\times\ \mathrm{tr}\left[\mathrm{M}_1^{\mathrm{ij}}(\mathrm{x}_0,\mathrm{u}_0,\mathrm{v}_0;\mathbf{p},\mathbf{k})^\dagger\gamma_0\mathrm{P}_+\right]$$

$$f^{stat}_{A,tp-a}(x_0,\mathbf{p}) = NC_F\frac{a^2}{4L^3}\sum_{\mathbf{k}}\sum_{u_0=1}^{x_0}\sum_{i,j=0}^{6} d_{\mu_H(i)\mu_H(j)}(u_0-1+s_H(i),u_0-1+s_H(j),\mathbf{k}) \tag{3.126}$$
$$\times\ h_{0;i}(\mathbf{k})h_{0;j}(-\mathbf{k})\ tr\left\{\chi_l(x_0,\underline{0})^\dagger\gamma_0 P_+\right\}$$

$$f^{stat}_{A,tp-b}(x_0,\mathbf{p}) = -NC_F\frac{a^2}{2L^3}\sum_{\mathbf{k}}\sum_{u_0=a}^{T-a}\sum_{i=1}^{5} d_{\mu(i)\mu(j)}(u_0+at(i),u_0+at(i);\mathbf{k}) \tag{3.127}$$
$$\times\ \mathrm{tr}\left[\mathrm{N}_1^{\mathrm{i}}(\mathrm{x}_0,\mathrm{u}_0;\mathbf{p},\mathbf{k})^\dagger\gamma_0\mathrm{P}_+\right]$$

Also for the gluon exchange, one has to take into account additional vertices for the quark propagator when switching to the HYP action. Shifts are therefore induced by the HYP action at the heavy side for the gluon emission (absorption) and, included in $M_l^i(x_0,u_0,\mathbf{p},\mathbf{k})$, by the three-point gluon vertex at the light side for the gluon absorption (emission). This yields:

$$f^{stat}_{A,ge}(x_0,\mathbf{p}) = -NC_F\frac{a^2}{2L^3}\sum_{\mathbf{k}}\sum_{u_0=1}^{T-1}\sum_{v_0=1}^{x_0}\sum_{i=1}^{16}\sum_{j=0}^{6} d_{\mu_H(j)\mu(i)}(u_0+t(i),v_0-1+s_H(j),\mathbf{k}) \tag{3.128}$$
$$h_{0;j}(\mathbf{k})\mathrm{tr}\left\{\mathrm{M}_1^{\mathrm{i}}(\mathrm{x}_0,\mathrm{u}_0,\mathbf{p},\mathbf{k})\gamma_0\mathrm{P}_+\right\}$$

The principle carries over to the computation of f_1^{stat} for the HYP action. In detail, one gets:

$$f^{stat}_{1,ss-a}(\mathbf{p},\mathbf{q}) = -NC_F\frac{a^2}{2L^3}\delta_{\mathbf{pq}}\sum_{\mathbf{k}}\sum_{u_0=a}^{T-a}\sum_{v_0=a}^{u_0-a}\sum_{i,j=1}^{6} d_{00}(u_0-a+s_H(i), v_0-a+s_H(j);\mathbf{k}) \tag{3.129}$$

$$\times\, h_{0;i}(\mathbf{k})h_{0;j}(-\mathbf{k})\; tr\left[\chi_1(T-a;\mathbf{p})^\dagger P_+\right]$$

$$f^{stat}_{1,ss-c}(\mathbf{p},\mathbf{q}) = -NC_F\frac{a^2}{2L^3}\delta_{\mathbf{pq}}\sum_{\mathbf{k}}\sum_{u_0=a}^{T-a}\sum_{i,j=1}^{6} d_{00}(T-a, u_0-a;\mathbf{k}) \tag{3.130}$$

$$\times\, h_{0;i}(\mathbf{k})h_{0;j}(-\mathbf{k})\; tr\left[\chi_1(T-a;\mathbf{p})^\dagger P_+\right]$$

$$f^{stat}_{1,ss-b}(\mathbf{p},\mathbf{q}) = -NC_F\frac{a^2}{2L^3}\delta_{\mathbf{pq}}\sum_{\mathbf{k}}\sum_{u_0,v_0=a}^{T-a}\sum_{i,j=1}^{16} d_{\mu(i)\mu(j)}(u_0+at(i), v_0+at(j);\mathbf{k}) \tag{3.131}$$

$$\times\, \mathrm{tr}\left[\mathrm{M}^{\mathrm{ij}}_{\mathrm{l}}(\mathrm{T}-\mathrm{a},\mathrm{u}_0,\mathrm{v}_0,\mathbf{p},\mathbf{k})^\dagger \mathrm{P}_+\right]$$

$$f^{stat}_{1,ss-d}(\mathbf{p},\mathbf{q}) = -NC_F\frac{a^2}{2L^3}\delta_{\mathbf{pq}}\sum_{\mathbf{k}}\sum_{u_0=a}^{T-a}\sum_{i=1}^{16} d_{\mu(i)0}(u_0+at(i), T-a;\mathbf{k}) \tag{3.132}$$

$$\times\, \mathrm{tr}\left[\mathrm{M}^{\mathrm{i}}_{\mathrm{l}}(\mathrm{T}-\mathrm{a},\mathrm{u}_0,\mathbf{p},\mathbf{k})^\dagger \mathrm{P}_+\right] \tag{3.133}$$

$$f^{stat}_{1,tp-a}(\mathbf{p},\mathbf{q}) = -NC_F\frac{a^2}{4L^3}\delta_{\mathbf{pq}}\sum_{\mathbf{k}}\sum_{u_0=a}^{T-a}\sum_{i,j=1}^{6} d_{\mu_H(i)\mu_H(j)}(u_0-a+s_H(i), u_0-a+s_H(j);\mathbf{k}) \tag{3.134}$$

$$\times\, h_{0;i}(\mathbf{k})h_{0;j}(-\mathbf{k})\; tr\left[\chi_1(T-a;\mathbf{p})^\dagger P_+\right]$$

$$f^{stat}_{1,tp-c}(\mathbf{p},\mathbf{q}) = -NC_F\frac{a^2}{4L^3}\delta_{\mathbf{pq}}\sum_{\mathbf{k}}\sum_{i,j=1}^{6} d_{\mu_H(i)\mu_H(j)}(T-a, T-a;\mathbf{k}) \tag{3.135}$$

$$\times\, h_{0;i}(\mathbf{k})h_{0;j}(-\mathbf{k})\; tr\left[\chi_1(T-a;\mathbf{p})^\dagger P_+\right]$$

$$f^{stat}_{1,tp-b}(\mathbf{p},\mathbf{q}) = -NC_F\frac{a^2}{2L^3}\delta_{\mathbf{pq}}\sum_{\mathbf{k}}\sum_{u_0=a}^{T-a}\sum_{i=1}^{5} d_{\mu(i)\mu(i)}(u_0+at(i), u_0+at(i);\mathbf{k}) \tag{3.136}$$

$$\times\, \mathrm{tr}\left[\mathrm{N}^{\mathrm{i}}_{\mathrm{l}}(\mathrm{T}-\mathrm{a},\mathrm{u}_0,\mathbf{p},\mathbf{k})^\dagger \mathrm{P}_+\right]$$

$$f^{stat}_{1,tp-d}(\mathbf{p},\mathbf{q}) = -NC_F\frac{a^2}{4L^3}\delta_{\mathbf{pq}}\sum_{\mathbf{k}} d_{00}(T-a, T-a;\mathbf{k}) \tag{3.137}$$

$$\times\, \mathrm{tr}\left[\mathrm{N}^{\mathrm{i}}_{\mathrm{l}}(\mathrm{T}-\mathrm{a},\mathbf{p})^\dagger \mathrm{P}_+\right] \tag{3.138}$$

$$f^{stat}_{1,ge-a}(\mathbf{p},\mathbf{q}) = NC_F\frac{a^2}{2L^3}\delta_{\mathbf{pq}}\sum_{\mathbf{k}}\sum_{u_0=a}^{T-a}\sum_{v_0=a}^{T-a}\sum_{i=1}^{16}\sum_{j=1}^{6} d_{\mu_H(j)\mu(i)}(u_0+at(i), v_0-a+s(j);\mathbf{k}) \tag{3.139}$$

$$\times\, h_{0;j}\ \mathrm{tr}\left[\mathrm{M}_1^{\mathrm{i}}(\mathrm{T}-\mathrm{a},\mathrm{u}_0,\mathbf{p},\mathbf{k})^\dagger \mathrm{P}_+\right]$$

$$f^{stat}_{1,ge-c}(\mathbf{p},\mathbf{q}) = NC_F\frac{a^2}{2L^3}\delta_{\mathbf{pq}}\sum_{\mathbf{k}}\sum_{u_0=a}^{T-a}\sum_{i=1}^{16}\sum_{j=1}^{6} d_{\mu_H(j)\mu(i)}(u_0+at(i), T-a+s_H(j);\mathbf{k}) \tag{3.140}$$

$$\times\, h_{0;j}\ h_{0;j}\mathrm{tr}\left[\mathrm{M}_1^{\mathrm{i}}(\mathrm{T}-\mathrm{a},\mathrm{u}_0,\mathbf{p},\mathbf{k})^\dagger \mathrm{P}_+\right]$$

$$f^{stat}_{1,ge-b}(\mathbf{p},\mathbf{q}) = NC_F\frac{a^2}{2L^3}\delta_{\mathbf{pq}}\sum_{\mathbf{k}}\sum_{u_0=a}^{T-a}\sum_{j=1}^{6} d_{0\mu_H(j)}(T-a, u_0-a+s_H(j);\mathbf{k}) \tag{3.141}$$

$$\times\, h_{0;j}\ \mathrm{tr}\left[\chi_{\mathrm{l}}(\mathrm{T}-\mathrm{a},\mathbf{p})^\dagger \mathrm{P}_+\right]$$

$$f^{stat}_{1,ge-d}(\mathbf{p},\mathbf{q}) = NC_F\frac{a^2}{2L^3}\delta_{\mathbf{pq}}\sum_{\mathbf{k}}\sum_{j=1}^{6} d_{0\mu_H(j)}(T-a, T-a+s_H(j);\mathbf{k}) h_{0;j}\mathrm{tr}\left[\chi_{\mathrm{l}}(\mathrm{T}-\mathrm{a},\mathbf{p})^\dagger \mathrm{P}_+\right] \tag{3.142}$$

3.7 Extension to spatial HYP links

In this subsection the spatial HYP inks are treated, i.e. a vertex table is given for the relation between the fields $\tilde{B}_k^{(3)}(x_0;\mathbf{p})$ and $\tilde{q}_\mu(x_0;\mathbf{p})$. Of course, the result does not affect the static-light current. The spatial links have to be taken into account when applying the HYP smearing to the light quark. e.g. to compute the light-light current with HYP smearing. Obviously, the situation then becomes a bit more involved because beside the shifts which are induced by the three-point quark-gluon vertex (see Table 7), additional shifts arising from the spatial HYP vertex appear (see Table 2).
We start from Eq. (3.93) and write it as

$$\tilde{B}_k^{(3)}(p) = f_{k0}(p)\tilde{q}_0(p) + \sum_{\eta\neq 0,k} f_{k\eta}(p)\tilde{q}_\eta(p) + f_{kk}(p)\tilde{q}_k(p) + \mathrm{O}(g_0)\,. \tag{3.143}$$

Contributions on the right hand side can be worked out separately using inverse Fourier transformation. A bit algebra leads to the expressions

$$\begin{aligned}\tilde{B}_k^{(3;1)}(x_0;\mathbf{p}) &\equiv \frac{1}{L}\sum_{p_0} \mathrm{e}^{ip_0x_0} f_{k0}(p)\tilde{q}_0(p) = \\ &= -i\frac{\alpha_1}{6}(a\hat{p}_k)\Omega_{k0}(\mathbf{p})a\partial_0^*\tilde{q}_0(x_0;\mathbf{p})\ ,\end{aligned} \tag{3.144}$$

$$\begin{aligned}\tilde{B}_k^{(3;2)}(x_0;\mathbf{p}) &\equiv \frac{1}{L}\sum_{p_0} \mathrm{e}^{ip_0x_0} \sum_{\eta\neq 0,k} f_{k\eta}(p)\tilde{q}_\eta(p) = \\ &= (a\hat{p}_k)\sum_{\eta\neq 0,k}\left[\Delta_{k\eta}^{(\mathrm{s})}(\mathbf{p}) + \Delta_{k\eta}^{(\mathrm{t})}(\mathbf{p})a^2\partial_0^*\partial_0\right]\tilde{q}_\eta(x_0;\mathbf{p})\ ,\end{aligned} \tag{3.145}$$

$$\begin{aligned}\tilde{B}_k^{(3;3)}(x_0;\mathbf{p}) &\equiv \frac{1}{L}\sum_{p_0} \mathrm{e}^{ip_0x_0} f_{kk}(p)\tilde{q}_k(p) = \\ &= \Bigg\{1 + \frac{\alpha_1}{6}\Omega_{k0}(\mathbf{p})a^2\partial_0^*\partial_0 - \\ &- \sum_{\eta\neq 0,k}(a\hat{p}_\eta)\left[\Delta_{k\eta}^{(\mathrm{s})}(\mathbf{p}) + \Delta_{k\eta}^{(\mathrm{t})}(\mathbf{p})a^2\partial_0^*\partial_0\right]\Bigg\}\tilde{q}_k(x_0;\mathbf{p})\ ,\end{aligned} \tag{3.146}$$

where we have introduced the symbols

$$\Delta_{k\eta}^{(\mathrm{s})}(\mathbf{p}) = \frac{\alpha_1}{6}(a\hat{p}_\eta)\Omega_{k\eta}^{(\mathrm{s})}(\mathbf{p})\ , \tag{3.147}$$

$$\Delta_{k\eta}^{(\mathrm{t})}(\mathbf{p}) = \frac{\alpha_1}{6}(a\hat{p}_\eta)\left[\frac{\alpha_2}{4}(1+2\alpha_3) - \frac{\alpha_2\alpha_3}{4}(a^2\hat{p}_{l;k\eta}^2)\right] \tag{3.148}$$

with

$$\Omega_{k\eta}^{(s)}(\mathbf{p}) = 1 + \alpha_2(1+\alpha_3) - \frac{\alpha_2}{4}(1+2\alpha_3)(a^2\hat{p}_{l;k\eta}^2)\,. \tag{3.149}$$

$$\tag{3.150}$$

i	$\mu(i)$	$s(i)$	$V_{k;i}(\mathbf{p})$
0	0	0	$-i\frac{\alpha_1}{6}\hat{p}_k\Omega_{k0}(\mathbf{p})$
1	0	-1	$+i\frac{\alpha_1}{6}\hat{p}_k\Omega_{k0}(\mathbf{p})$
2	k	0	$1-\frac{\alpha_1}{3}\Omega_{k0}(\mathbf{p})+\sum_{\eta\neq 0,k} a\hat{p}_\eta\,[2\Delta^{(\mathrm{t})}_{k\eta}(\mathbf{p})-\Delta^{(\mathrm{s})}_{k\eta}(\mathbf{p})]$
3	k	1	$\frac{\alpha_1}{6}\Omega_{k0}(\mathbf{p})-\sum_{\eta\neq 0,k} a\hat{p}_\eta\Delta^{(\mathrm{t})}_{k\eta}(\mathbf{p})$
4	k	-1	$\frac{\alpha_1}{6}\Omega_{k0}(\mathbf{p})-\sum_{\eta\neq 0,k} a\hat{p}_\eta\Delta^{(\mathrm{t})}_{k\eta}(\mathbf{p})$
5	$\eta;0k$	0	$a\hat{p}_k[\Delta^{(s)}_{k\eta}(\mathbf{p})-2\Delta^{(\mathrm{t})}_{k\eta}(\mathbf{p})]$
6	$\eta;0k$	-1	$a\hat{p}_k\Delta^{(\mathrm{t})}_{k\eta}(\mathbf{p})$
7	$\eta;0k$	1	$a\hat{p}_k\Delta^{(\mathrm{t})}_{k\eta}(\mathbf{p})$

Table 2: Feynman rules of the spatial HYP link in time-momentum representation.

Eqs.(3.144)-(3.146) can be written in the compact form

$$\tilde{B}^{(3)}_k(x_0;\mathbf{p})=\sum_{i=0}^{7} V_{k;i}(\mathbf{p})\tilde{q}_{\mu(i)}(x_0+as(i);\mathbf{p})\ . \tag{3.151}$$

where the vertex $V_{k;i}(\mathbf{p})$ and the auxiliary indices μ, s are collected in Table 2. A detailed derivation of above relations, especially the inverse Fourier transformation of the involved terms, can be found in Appendix A.5.

4 Determination of $c_{\mathrm{A}}^{\mathrm{stat}}$ for the static-light case

4.1 Theoretical Setup

Once f_1^{stat} and $f_{\mathrm{A}}^{\mathrm{stat}}$ are known for different lattice sizes, the improvement coefficient $c_{\mathrm{A}}^{\mathrm{stat}}$ can be determined by following the procedure described in [1]. The method shall be skteched a bit more in detail in the following.
First, the parameter m_q is introduced which denotes the bare subtracted mass of the light quark, which, however, in our treatment is zero for the light quark :

$$\begin{aligned} m_q &= m_0 - m_c \\ \Rightarrow\ m_0 &= m_c \quad \text{for } \mathrm{m_q} = 0 \end{aligned} \tag{4.1}$$

The meaning of above equation can be interpreted as follows: Due to the fact that chiral symmetry is broken on the lattice, the bare quark mass is not equal to zero for a vanishing physical quark mass. Therefore, the critical mass m_c has to be introduced which shifts the equality of light quark mass and bare mass for a specific amount. Different definitions are possible for the critical mass m_c differing by $\mathcal{O}(a^2)$ terms. For the following calculation, the critical mass is obtained by requiring the PCAC mass (see Eq. (2.10)) to be zero which results in the physical quark mass being zero up to $\mathcal{O}(a^2)$ effects.

$\mathcal{O}(a)$ improvement now means the cancellation of the diverging self energy δm by a counterterm. δm leads to an exponential factor even in the renormalized correlation functions

$$(f_{\mathrm{A}}^{\mathrm{stat}})_R(\frac{T}{2}) \propto e^{-\delta m \frac{T}{2}} \tag{4.2}$$

$$(f_1^{\mathrm{stat}})_R \propto e^{-\delta m T} \tag{4.3}$$

Now the ratio

$$X(g_0, \frac{L}{a}, \frac{T}{L}, \Theta) = \frac{f_{\mathrm{A}}^{\mathrm{stat}}}{\sqrt{f_1^{\mathrm{stat}}}} \tag{4.4}$$

can be defined in which δm cancels. In X, also the wave function renormalisation constants of the boundary fermion fields cancel so that the renormalised ratio X_R in the SF for the vanishing light quark mass can be written as

$$\begin{aligned} X_R &= Z_{\mathrm{A}}^{\mathrm{stat}}(1 + b_{\mathrm{A}}^{\mathrm{stat}} a m_q) X \\ &= Z_A^{stat} X \quad for\ m_q = 0 \end{aligned} \tag{4.5}$$

$Z_{\mathrm{A}}^{\mathrm{stat}}$ is the axial current renormalisation constant (see Eq. (2.50)) which is the only renormalisation which has to be taken into account. As we set the light quark mass to zero, neither mass renormalisation nor mass dependent improvement terms will arise. The renormalisation of the coupling constant enters only at tree level into our calculations with $Z_g = 1$ as we expand our correlation functions in one-loop pertubation theory to contributions up to order g_0^2. However, a mass shift has to be considered due to the non-vanishing critical mass. If we bring above relations onto the lattice, a divergency proportional to $\ln(\frac{\mathrm{a}}{\mathrm{L}})$ arises. This divergency can be cancelled by a so called minimal subtraction scheme which we will use as a possible renormalisation scheme in the following way: We require the coefficients of the renormalisation constant $Z_{A,lat}^{stat}$ to be

polynomials in $\ln(a\mu)$ without constant parts at each order of pertubation theory at a fixed renormalisation scale chosen to $\mu = \frac{1}{L}$. Doing so, we end up with the minimal sutracted ratio

$$X_{\mathrm{lat}} = Z^{stat}_{A,lat} X \tag{4.6}$$

and its coefficients

$$\begin{aligned} {X_{\mathrm{lat}}}^{(0)} &= X^{(0)} \\ {X_{\mathrm{lat}}}^{(1)} &= X^{(1)} - \frac{1}{4\pi^2}\ln(\frac{\mathrm{a}}{\mathrm{L}})\mathrm{X}^{(0)} \end{aligned} \tag{4.7}$$

with

$$\begin{aligned} X^{(0)} &= X_I|_{g_0=0} \\ &= \frac{{f_{\mathrm{A}}^{\mathrm{stat}}}^{(0)}}{\sqrt{{f_1^{\mathrm{stat}}}^{(0)}}} \end{aligned} \tag{4.8}$$

and

$$\begin{aligned} X^{(1)} &= \frac{\partial}{\partial g_0^2} X_I|_{g_0=0} \\ &= \Big(\frac{{f_{\mathrm{A}}^{\mathrm{stat}}}^{(1)}}{\sqrt{{f_{\mathrm{A}}^{\mathrm{stat}}}^{(0)}}} - \frac{1}{2}\frac{{f_1^{\mathrm{stat}}}^{(1)}}{\sqrt{{f_1^{\mathrm{stat}}}^{(0)}}}\Big) X^{(0)} \end{aligned} \tag{4.9}$$

Complete $\mathcal{O}(a)$ improvement of the correlation function $f_{\mathrm{A}}^{\mathrm{stat}}$ is achieved by adding a local counterterm $c_{\mathrm{A}}^{\mathrm{stat}} f_{\delta\mathrm{A}}^{\mathrm{stat}}(\frac{T}{2})$. This leads to the improved ratio

$$X_I(g_0, \frac{L}{a}, \frac{T}{L}, \Theta) = \frac{f_{\mathrm{A}}^{\mathrm{stat}}(\frac{T}{2}) + a c_{\mathrm{A}}^{\mathrm{stat}} f_{\delta\mathrm{A}}^{\mathrm{stat}}(\frac{T}{2})}{\sqrt{f_1^{\mathrm{stat}}}} \tag{4.10}$$

In order to ectract $c_{\mathrm{A}}^{\mathrm{stat}}$, X_I can now be expanded in terms of g_0^2:

$$\begin{aligned} X_I &= X_I^{(0)} + g_0^2 X_I^{(1)} + O(g_0^4) \\ &= X_I|_{g_0=0} + g_0^2 \frac{\partial}{\partial g_0^2} X_I|_{g_0=0} \end{aligned} \tag{4.11}$$

which leads to

$$\begin{aligned} X_I^{(0)} &= X_I|_{g_0=0} \\ &= \frac{{f_{\mathrm{A}}^{\mathrm{stat}}}^{(0)}}{\sqrt{{f_1^{\mathrm{stat}}}^{(0)}}} \end{aligned} \tag{4.12}$$

$$\begin{aligned} X_I^{(1)} &= \frac{\partial}{\partial g_0^2} X_I|_{g_0^2=0} \\ &= \frac{{f_{\mathrm{A}}^{\mathrm{stat}}}^{(1)}(\frac{T}{2})\sqrt{{f_1^{\mathrm{stat}}}^{(0)}} - \frac{1}{2}\frac{{f_{\mathrm{A}}^{\mathrm{stat}}}^{(0)}(\frac{T}{2})}{{f_1^{\mathrm{stat}}}^{\frac{3}{2}}} {f_1^{\mathrm{stat}}}^{(1)} + \frac{a c_{\mathrm{A}}^{\mathrm{stat}(1)} {f_{\delta\mathrm{A}}^{\mathrm{stat}}}^{(0)}}{(} \frac{T}{2})}{\sqrt{{f_1^{\mathrm{stat}}}^{(0)}}} \end{aligned} \tag{4.13}$$

Above result is obtained by expanding all contained expressions as

$$f_{\mathrm{A}}^{\mathrm{stat}}(\frac{T}{2}) = f_{\mathrm{A}}^{\mathrm{stat}\,(0)}(\frac{T}{2}) + g_0^2 f_{\mathrm{A}}^{\mathrm{stat}\,(1)}(\frac{T}{2}) + O(g_0^4) \tag{4.14}$$

as well as

$$f_1^{\mathrm{stat}} = f_1^{\mathrm{stat}\,(0)} + g_0^2 f_1^{\mathrm{stat}\,(1)} + O(g_0^4) \tag{4.15}$$

and

$$\begin{aligned} c_{\mathrm{A}}^{\mathrm{stat}} f_{\delta\mathrm{A}}^{\mathrm{stat}} &= g_0^2 c_{\mathrm{A}}^{\mathrm{stat}\,(1)}(f_{\delta\mathrm{A}}^{\mathrm{stat}\,(0)} + g_0^2 f_{\delta A}^{stat^{(1)}}) + O(g_0^4) \\ &= g_0^2 c_{\mathrm{A}}^{\mathrm{stat}\,(1)} f_{\delta A}^{stat^{(0)}} + O(g_0^4) \end{aligned} \tag{4.16}$$

.
The improved minimal subtracted ratio is complete analogue to the non-improved ratio X_{lat}:

$$X_{\mathrm{I,lat}} = Z_{\mathrm{A,lat}}^{\mathrm{stat}} X_I \tag{4.17}$$

with its coefficients

$$\begin{aligned} {X_{\mathrm{I,lat}}}^{(0)} &= X_I^{(0)} \\ {X_{\mathrm{I,lat}}}^{(1)} &= X_I^{(1)} - \gamma_0 \ln(\frac{\mathrm{a}}{\mathrm{L}})\mathrm{X}_{\mathrm{I}}^{(0)} \end{aligned} \tag{4.18}$$

Now, Eq. (4.13) is considered anew and decomposed into a volume and a boundary part where the boundary part is proportional to $(\tilde{c_t} - 1)$ and vanishes for $\tilde{c_t} = 1$. Knowing that ${\tilde{c_t}}^{(0)} = 1$, one gets

$$X_I^{(1)}(\frac{L}{a}) = X^{(1)}(\frac{L}{a})|_{\tilde{c_t}=1} + {\tilde{c_t}}^{(1)} a X_b^{(0)}(\frac{L}{a}) + c_{\mathrm{A}}^{\mathrm{stat}\,(1)} a {X_{\delta\mathrm{A}}}^{(0)} + O(a^2) \tag{4.19}$$

The aim is now to make the $\mathcal{O}(a)$ part of $X_I^{(1)}(\frac{L}{a})$ vanish for $a \to 0$ by the right choice of $c_{\mathrm{A}}^{\mathrm{stat}}$.
In order to do so, on has to consider the right-hand terms separately. $X_b^{(0)}(\frac{L}{a})$ and ${X_{\delta\mathrm{A}}}^{(0)}$ are finite values as no renormalisation is necessary at tree level. A divergency of $X_I^{(1)}(\frac{L}{a})$ comes from the term $X^{(1)}(\frac{L}{a})|_{\tilde{c_t}=1}$. Therefore, we adopt the renormalisation of $X^{(1)}$ and consider the $\mathcal{O}(a)$ part of ${X_{\mathrm{lat}}}^{(1)}$ which is not obvious at first sight. But expanding ${X_{\mathrm{lat}}}^{(1)}$ as

$${X_{\mathrm{lat}}}^{(1)} = \alpha + \frac{a}{L}\beta + O(\frac{a^2}{L^2}) \ , \tag{4.20}$$

one can extract its $\mathcal{O}(a)$ part β by applying the lattice derivatives

$$\partial_L X_{\mathrm{lat}}(\frac{L}{a}) = \frac{X(\frac{L+a}{a}) - X(\frac{L}{a})}{a} \tag{4.21}$$

and

$$\partial_L^* X_{\mathrm{lat}}(\frac{L}{a}) = \frac{X(\frac{L}{a}) - X(\frac{L-a}{a})}{a} \tag{4.22}$$

to ${X_{\text{lat}}}^{(1)}$. This gives

$$\begin{aligned}(\partial_L + \partial_L^*){X_{\text{lat}}}^{(1)}(\frac{L}{a}) &= \frac{1}{a}\big({X_{\text{lat}}}^{(1)}(\frac{L+a}{a}) - {X_{\text{lat}}}^{(1)}(\frac{L-a}{a})\big) \\ &= \frac{1}{a}\big(\alpha + \frac{a}{L+a}\beta - \alpha - \frac{a}{L-a}\beta + O(\frac{a^2}{L^2})\big) \\ &= \beta(\frac{1}{L+a} - \frac{1}{L-a}) + O(\frac{a^2}{L^2}) \\ &= \frac{\beta}{L}\frac{-2\frac{a}{L}}{1-\frac{a^2}{L^2}} + O(\frac{a^2}{L^2}) \\ &= -2\frac{a}{L^2}\beta + O(\frac{a^2}{L^2})\end{aligned} \tag{4.23}$$

implicating for the $\mathcal{O}(a)$ part of the ${X_{\text{lat}}}^{(1)}$ volume term

$$\beta|_{\tilde{c}_t=1} = \lim_{\frac{a}{L}\to 0} -\frac{L^2}{2a}(\partial_L + \partial_L^*)X_{\text{lat}}(\frac{L}{a})|_{\tilde{c}_t=1} \tag{4.24}$$

This yields the final expression for the improvement coefficient from equation(4.19)

$$c_{\text{A}}^{\text{stat}(1)} = \frac{lim_{\frac{a}{L}\to 0}\ \frac{L^2}{2a}(\partial + \partial^*){X_{\text{lat}}}^{(1)}(\frac{L}{a})|_{\tilde{c}_t=1} - lim_{\frac{a}{L}\to 0}\ \tilde{c_t}^{(1)} L X_b^{(1)}(\frac{L}{a})}{lim_{\frac{a}{L}\to 0}\ L{X_{\delta\text{A}}}^{(0)}(\frac{L}{a})} \tag{4.25}$$

4.2 Data analysis and Continuum limes

Now the one-loop Feynman diagrams of the boundary term $LX_b^{(1)}$ and the improvement counterterm $L{X_{\delta\text{A}}}^{(0)}$ can be fitted[6] against a general expansion [2]

$$f(\frac{a}{L}) = \sum_{m=0}^{\infty}\sum_{n=0}^{l}(\frac{a}{L})^m(\ln(\frac{a}{L}))^n \tag{4.26}$$

with l being the loop order. In our case we truncate at

$$f(\frac{a}{L}) = \alpha_1 + \alpha_2\frac{a}{L} + \alpha_3\frac{a}{L}\ln(\frac{a}{L}) + \alpha_4(\frac{a}{L})^2 \tag{4.27}$$

because the higher terms do not yield any improvement at the given number of points which was checked exemplary for the HYP2 action. The resulting diagrams for boundary and improvement term are sketched for the HYP1 action at $\Theta = 0.5$ in the figures 25 and 26. The asympotic expansion of the counterterm and the boundary term are perfectly known as both terms have been computed analytically for each lattice size. This reduces the systematic effects arising from lattice artefacts which shall be neglected in the following computations. [7]

[6] All Least square fits have been done in a numerical stable way by a Singular Value Decomposition (SVD)

[7] However, one can apply methods for removing cutoff effects [17] which are not considered here.

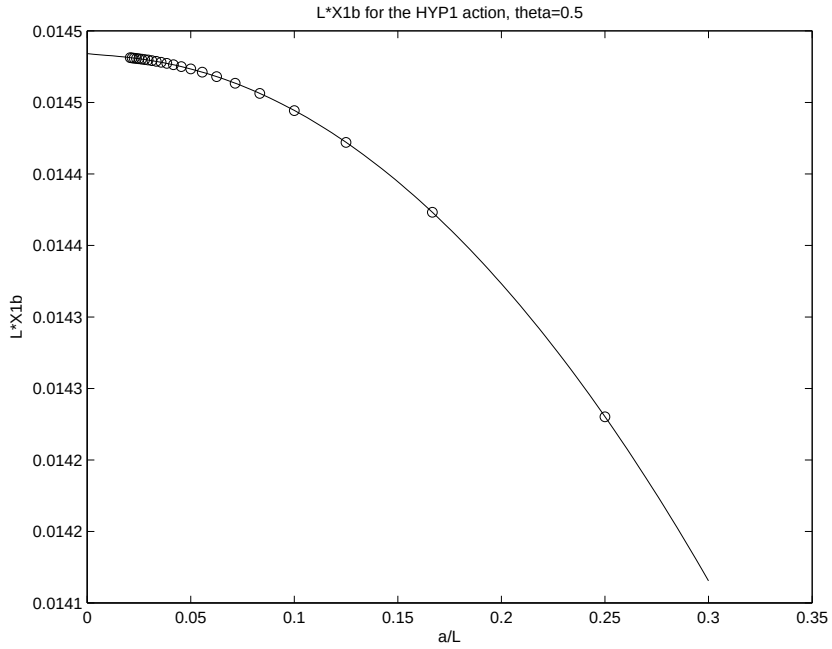

Figure 25: Boundary Term for the HYP1 action at $\Theta = 0.5$

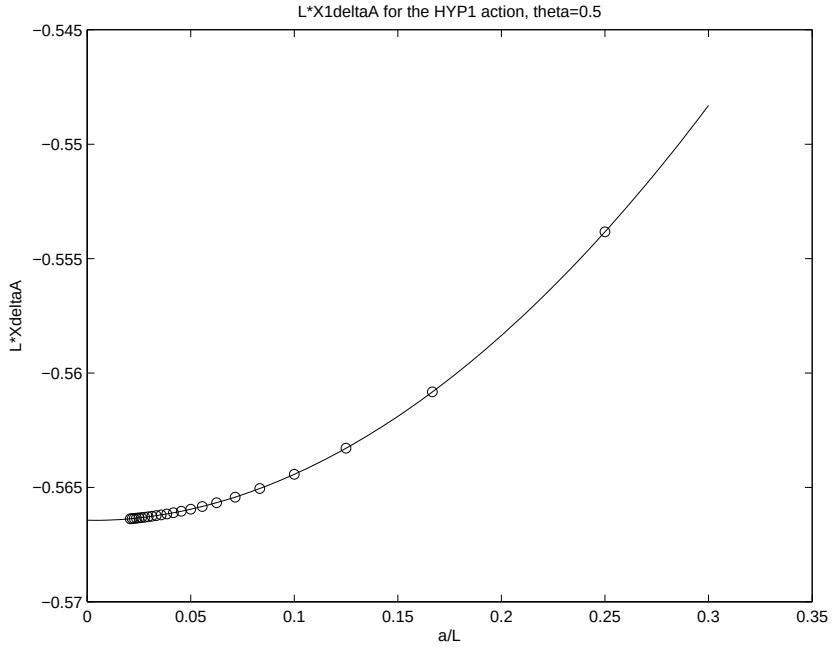

Figure 26: Counterterm for the HYP1 action at $\Theta = 0.5$

Building the continuum limes, the contribution α_1 will survive, so that:

$$\lim_{\frac{a}{L}\to 0} LX_b^{(1)} = \alpha_{1,LX_b}$$
$$\lim_{\frac{a}{L}\to 0} LX_{\delta \mathrm{A}}{}^{(0)} = \alpha_{1,LX_{\delta \mathrm{A}}{}^{(0)}} \tag{4.28}$$

Action	$c_{\mathrm{A}}^{\mathrm{stat}(1)}$
EH	-0.0833(2)
HYP1	0.0025(3)
HYP2	0.0516(3)

Table 3: Simulation Results for $c_{\mathrm{A}}^{\mathrm{stat}(1)}$

In Table 9 in Appendix C, the results for boundary and improvement term for the different actions are given. Those numerical values are used for the $c_{\mathrm{A}}^{\mathrm{stat}(1)}$ fits.
The values for $c_{\mathrm{A}}^{\mathrm{stat}(1)}$ are now determined for $\Theta = 0.5$ and $\Theta = 1.0$, first separately. As it is a priori not clear how much the higher terms affect the inaccuracy of the fit, this is done by taking into consideration a variable number of values. For $\frac{T}{a} = \frac{L}{a} = 48$ and $\Delta\frac{T}{a} = \Delta\frac{L}{a} = 2$, one starts with the first four values ($\frac{a}{L} < \frac{1}{38}$) up to all available values ($\frac{a}{L} < \frac{1}{4}$) and determines the respective average value of $c_{\mathrm{A}}^{\mathrm{stat}}(\frac{a}{L})$ and the goodness of the fit ($\chi^2(\frac{a}{L})$). The result is given in the tables 10 to 12 in Appendix C. All values with $\chi^2(\frac{a}{L}) < 10^{(-11)}$ are then taken into account to compute the average value. The so obtained values for $\Theta = 0.5$ and $\Theta = 1.0$ and then averaged anew as

$$c_{\mathrm{A}}^{\mathrm{stat}(1)} = \frac{1}{2}(c_{\mathrm{A}}{}_{\Theta=0.5}^{\mathrm{stat}(1)} + c_{\mathrm{A}}{}_{\Theta=1.0}^{\mathrm{stat}(1)}) \tag{4.29}$$

The error is estimated by the deviation of the fits

$$\sigma_{ges} = |c_{\mathrm{A}}{}_{\Theta=0.5}^{\mathrm{stat}(1)} - c_{\mathrm{A}}{}_{\Theta=1.0}^{\mathrm{stat}(1)}| \tag{4.30}$$

The results are collected in Table 3.

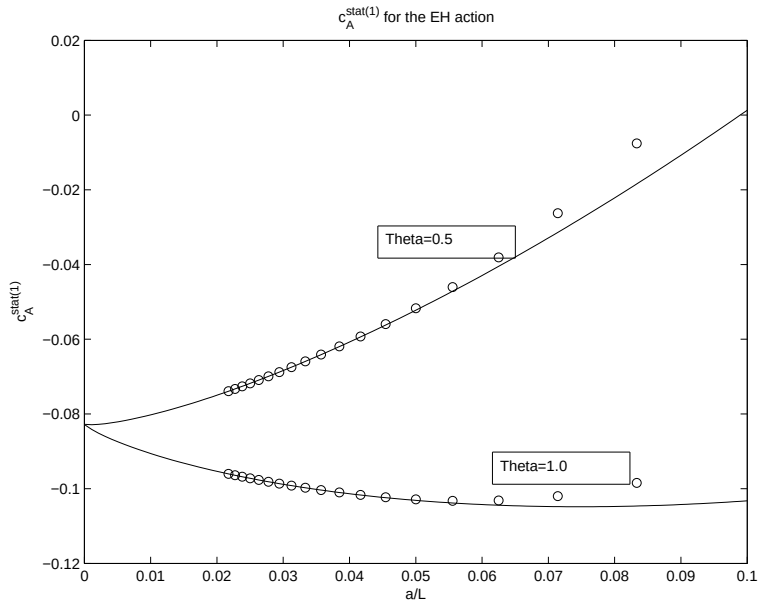

Figure 27: $c_{\mathrm{A}}^{\mathrm{stat}(1)}$ for the EH action at $\Theta \in [0.5, 1.0]$

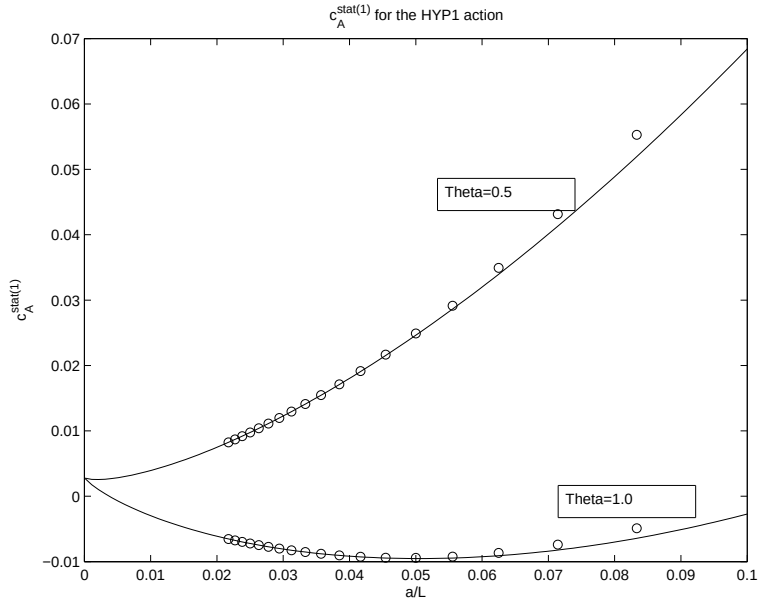

Figure 28: $c_{\mathrm{A}}^{\mathrm{stat}(1)}$ for the HYP1 action at $\Theta \in [0.5, 1.0]$

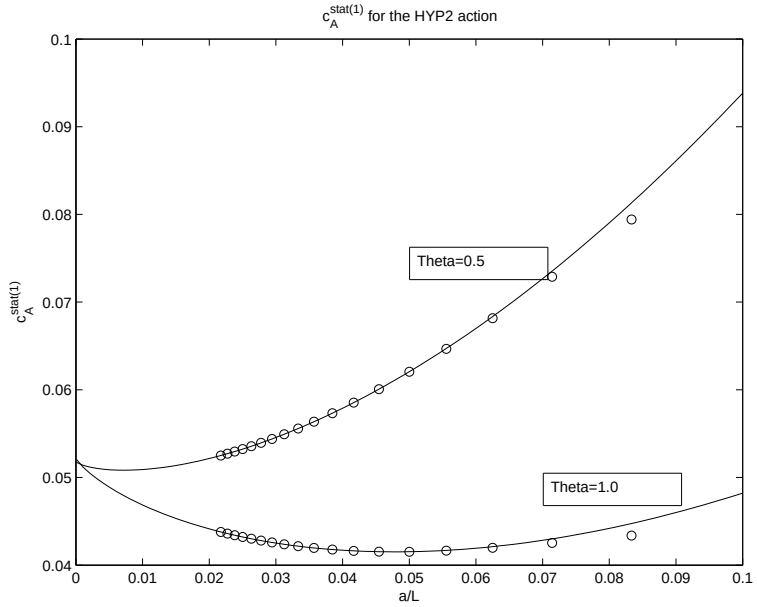

Figure 29: $c_{\mathrm{A}}^{\mathrm{stat}\,(1)}$ for the HYP2 action at $\Theta \in [0.5, 1.0]$

5 The static self-energy

5.1 Computation of the self-energy

The static self-energy can be used as a check of the obtained Feynman diagrams, i.e. the one-loop diagrams of a correlator can be used to extract the one-loop coefficient of the static self-energy and compare it with known results [11].

Let us first consider the correlation functions $f_{\mathrm{A}}^{\mathrm{stat}}(x_0)$ and f_{1}^{stat}. They are expected to fulfil the properties

$$f_{\mathrm{A}}^{\mathrm{stat}}(x_0) \propto e^{-E_{\mathrm{stat}} x_0} \tag{5.1}$$

$$f_{1}^{\mathrm{stat}} \propto e^{-E_{\mathrm{stat}}\, T} \tag{5.2}$$

where E_{stat} is the binding energy of the static-light system. It diverges approximately linearly in the lattice spacing [13] as

$$E_{\mathrm{stat}} \propto E_{\mathrm{self}} + \mathcal{O}(a^0) \tag{5.3}$$

E_{self} may then be expanded in pertubation theory as

$$E_{\mathrm{self}} = {E_{\mathrm{stat}}}^{(1)} g_0^2 + \mathcal{O}(g_0^4) \quad \text{with} \tag{5.4}$$

$${E_{\mathrm{stat}}}^{(1)} = \frac{1}{a} e^{(1)} + \mathcal{O}(a^0)\ . \tag{5.5}$$

The $\frac{1}{a}$ dependence appears in terms of a $\frac{L}{a}$ dependence in the SF. It is important to understand that the self-energy and thus the coefficient $e^{(1)}$, which represents an ultraviolet property of the static action, depends only on the action. For HYP1 and HYP2, $e^{(1)}$ has been computed in [10] and appears as $r^{(1)}$ in Table 1 of [13] for different actions. The different notation is caused by the fact that in smearing procedures without $SU(3)$ projections (like APE), $r^{(1)}$ does not equal $e^{(1)}$.

The self energy does neither depend on the correlator used to determine it nor on the imposed boundary conditions. We are going to use f_1^{stat} and sum up the one-loop diagrams of f_1^{stat} where the light quark is kept at tree-level and normalise them against the tree level value of f_1^{stat}:

$$\frac{f_{1,\,\mathrm{self}}^{\mathrm{stat}(1)}}{f_1^{\mathrm{stat}(0)}} = (f_1^{\mathrm{stat}(0)})^{-1} \left[f_{1,ss-a}^{stat} + f_{1,ss-c}^{stat} + f_{1,tp-a}^{stat} + f_{1,tp-c}^{stat} \right] \tag{5.6}$$

Taking into account Eq. (5.5), we will have to determine

$$e^{(1)} = -\lim_{\frac{a}{T}\to 0} \left\{ \frac{a}{T} \frac{f_{1,\,\mathrm{self}}^{\mathrm{stat}(1)}}{f_1^{\mathrm{stat}(0)}} \right\} \tag{5.7}$$

$e^{(1)}$ is the assumed to have the structure

$$e^{(1)} = \sum_{m=0}^{\infty} \sum_{n=0}^{l} (\frac{a}{T})^m (\ln(\frac{\mathrm{a}}{\mathrm{T}}))^{\mathrm{n}} \tag{5.8}$$

with l being the loop order. Here, we truncate at $m = 2$ and, by performing the fitting procedure with values $T \in [4, 48]$ in Eq. (5.7), obtain the results in Table 4.

The results are in good agreement with Table 1 in [13], the difference amounts less than 0.3%.

Action	$e^{(1)}$
EH	0.168502(1)
HYP1	0.048631(1)
HYP2	0.035559(1)

Table 4: Simulation results for the self energy extracted from the one-loop order expansion of $f_1^{\rm stat}$

5.2 Minimisation of the self-energy

The coefficient $e^{(1)}$ has a functional dependence on the HYP smearing parameters, namely

$$e^{(1)} = \sum_{k1,k2,k3=0}^{2} e^{(1)}_{k_1k_2k_3} \alpha_1^{k_1}\alpha_2^{k_2}\alpha_3^{k_3} \tag{5.9}$$

The coefficients $e^{(1)}_{k_1k_2k_3}$ can be determined analytically from the Feynman diagrams for $f_1^{\rm stat}$ as shown below. The static self-energy is a multivariate polynomial of $(\alpha_1, \alpha_2, \alpha_3)$ whose structure is triangular, i.e. only the coefficients fulfilling $0 \le k_3 \le k_2 \le k_1 \le 2$ are non-zero. This is an obvious consequence of how the the HYP link is constructed.

Expanding $f_1^{\rm stat}$ at one-loop order of pertubation theory allows to write the coefficient $e^{(1)}$, see Eq. (5.7), as

$$\begin{aligned} e^{(1)} = &- \lim_{a/L\to 0} C_F \frac{a}{L^4} \sum_{\mathbf{p}} a^2 \sum_{u_0=a}^{T} \sum_{v_0=a}^{u_0} b(u_0,v_0) \sum_{i,j=0}^{6} \delta_{\mu(i)\mu(j)} V_{0;i}(\mathbf{p}) V_{0;j}(-\mathbf{p}) \times \\ &\times d_{\mu(i)\mu(j)}(u_0 - a + as(i), v_0 - a + as(j); \mathbf{p}) \;= \\ \equiv &- \lim_{a/L\to 0} C_F \frac{1}{L^3} \sum_{\mathbf{p}} a^2 \sum_{u_0=a}^{T} \sum_{v_0=a}^{u_0} b(u_0,v_0) \mathcal{V}(u_0,v_0,\mathbf{p}) \;, \end{aligned} \tag{5.10}$$

where $d_{\mu\nu}(x_0, y_0, \mathbf{p})$ denotes the gluon propagator in time-momentum representation. The weight-coefficient $b(u_0, v_0)$ is given by

$$b(u_0,v_0) = \begin{cases} 1/2 & u_0 = v_0 \;, \\ 1 & \text{otherwise} \;, \end{cases} \tag{5.11}$$

and the interaction blob

$$\mathcal{V}(u_0,v_0,\mathbf{p}) = \sum_{i,j=0}^{6} \delta_{\mu(i)\mu(j)} V_{0;i}(\mathbf{p}) V_{0;j}(-\mathbf{p}) d_{\mu(i)\mu(j)}(u_0 - a + as(i), v_0 - a + as(j); \mathbf{p}) \tag{5.12}$$

denotes a HYP gluon propagating on the lattice from time u_0 to time v_0 with spatial momentum $\mathbf{p}$. The above expression can be simplified by using spatial rotational invariance, i.e. $d_{11} = d_{22} = d_{33}$ and $d_{ij} = 0$ if $i \neq j$. Accordingly, the

vertex reads

$$\begin{aligned}\mathcal{V}(u_0, v_0, \mathbf{p}) = |V_{0;0}(\mathbf{p})|^2 d_{00}(u_0 - a, v_0 - a; \mathbf{p}) + \\ + \left[|V_{0;1}(\mathbf{p})|^2 + |V_{0;2}(\mathbf{p})|^2 + |V_{0;3}(\mathbf{p})|^2\right] \times \\ \times \left[d_{kk}(u_0 - a, v_0 - a; \mathbf{p}) + d_{kk}(u_0, v_0; \mathbf{p}) - \right. \\ \left. - d_{kk}(u_0, v_0 - a; \mathbf{p}) - d_{kk}(u_0 - a, v_0; \mathbf{p})\right] . \end{aligned} \tag{5.13}$$

From Eq. (5.13), we conclude that the HYP vertex $V_{0;j}(\mathbf{p})$ enters the coefficient $e^{(1)}$ only in the rotationally symmetric combinations

$$\begin{aligned} h_{\mathrm{t}}(\mathbf{p}) &= |V_{0;0}(\mathbf{p})|^2 , \\ h_{\mathrm{s}}(\mathbf{p}) &= |V_{0;1}(\mathbf{p})|^2 + |V_{0;2}(\mathbf{p})|^2 + |V_{0;3}(\mathbf{p})|^2 . \end{aligned} \tag{5.14}$$

These quantities are multivariate polynomials of the HYP smearing parameters, i.e.

$$h_{\mathrm{t,s}}(\mathbf{p}) = \sum_{k_1 k_2 k_3 = 0}^{2} w_{\mathrm{t,s}}^{k_1 k_2 k_3}(\mathbf{p}) \alpha_1^{k_1} \alpha_2^{k_2} \alpha_3^{k_3} , \qquad w_{\mathrm{t,s}}^{k_1 k_2 k_3} = \frac{1}{k_1! k_2! k_3!} \frac{\partial^{k_1+k_2+k_3} h_{\mathrm{t,s}}}{\partial \alpha_1^{k_1} \partial \alpha_2^{k_2} \partial \alpha_3^{k_3}} . \tag{5.15}$$

The coefficients $w_{\mathrm{t,s}}^{k_1 k_2 k_3}$ have been written according to the Taylor expansion in several variables. They can be algebraically evaluated, the non-vanishing ones are collected in Appendix A.7.

Upon inserting Eq. (5.15) into Eq. (5.13) and Eq. (5.13) into Eq. (5.10), the final result represented by Eq. (5.9) is obtained with coefficients

$$\begin{aligned} e_{k_1 k_2 k_3}^{(1)} = \lim_{a/L \to 0} C_F \frac{a}{L^4} \sum_{\mathbf{p}} a^2 \sum_{u_0 = a}^{T} \sum_{v_0 = a}^{u_0} b(u_0, v_0) \times \\ \times \left\{ w_{\mathrm{t}}^{k_1 k_2 k_3}(\mathbf{p}) d_{\mathrm{t}}(u_0 - a, v_0 - a; \mathbf{p}) + \right\} \\ + w_{\mathrm{s}}^{k_1 k_2 k_3}(\mathbf{p}) \left[d_{\mathrm{s}}(u_0 - a, v_0 - a; \mathbf{p}) + d_{\mathrm{s}}(u_0, v_0; \mathbf{p}) - \right. \\ \left. - d_{\mathrm{s}}(u_0, v_0 - a; \mathbf{p}) - d_{\mathrm{s}}(u_0 - a, v_0; \mathbf{p})\right] \right\} . \end{aligned} \tag{5.16}$$

The coefficients $e_{k_1 k_2 k_3}^{(1)}$ can be found in Table 5[8].

A check of the obtained results can be performed by extracting the static self energy from the one-loop expansion of the static potential [11]. The respective integrals (see Appendix A.6, Eq. (A.77)) have been computed in Mathematica [9] and lead to the coefficients in Table 6. They confirm he results won by the pertubative expansion of f_1^{stat}.

[8] Thanks to F.Palombi for computing Table 5

[9] Thanks to R.Hoffman for sharing his program code with us, whereby the numerical precision of the provided code was improved to $3 * 10^8$ iteration steps to obtain a significant check

$[i,j,k]$	$e^{(1)}_{ijk}$
$[0,0,0]$	0.168487(1)
$[1,0,0]$	−0.222222(1)
$[1,1,0]$	−0.041164(1)
$[1,1,1]$	−0.015484(1)
$[2,0,0]$	0.111111(1)
$[2,2,0]$	0.023521(1)
$[2,2,1]$	−0.002620(1)
$[2,2,2]$	0.019055(1)

Table 5: Coefficients of the static self-energy at one-loop order of PT extracted from $f_1^{\rm stat}$.

$[i,j,k]$	$e^{(1)}_{ijk}$
$[0,0,0]$	0.16848(1)
$[1,0,0]$	−0.222222(1)
$[1,1,0]$	−0.041164(1)
$[1,1,1]$	−0.015484(1)
$[2,0,0]$	0.111111(1)
$[2,2,0]$	0.023521(1)
$[2,2,1]$	−0.002620(1)
$[2,2,2]$	0.019055(1)

Table 6: Coefficients of the static self-energy extracted from the one-loop expansion of the static potential.

Once the dependence of the self energy from the smearing parameters is known, the global minimum can be determined, e.g. by a short MATLAB routine. The result is

$$\begin{aligned} \vec{\alpha}^* &= (\alpha_1^*,\ ,\alpha_2^*,\ \alpha_3^*) \qquad (5.17)\\ &= (1.0000,\ 0.9011,\ 0.5196) \quad \text{with} \\ e^{(1)}(\vec{\alpha}^*) &= 0.03520(1) \qquad (5.18) \end{aligned}$$

A 3D plot for $e^{(1)}(\vec{\alpha})$ at $\alpha_1 = 1$ can be found in Figure 30.

Remarkably, the choice of the parameters minimising the self-energy is close to HYP2 which has been won by non-pertubative considerations [13]. One can therefore conclude that the self energy is dominated by pertubation theory as intuitively expected. A pertubative comparison between Eq. (5.18) and HYP2 is also possible. For HYP2, one finds the value $e^{(1)}(\vec{\alpha}_{HYP2}) = 0.03544(1)$ which is slightly higher than the reuslt in Table 1 of [13] and differs bei 0.7% of the pertubative minimum.

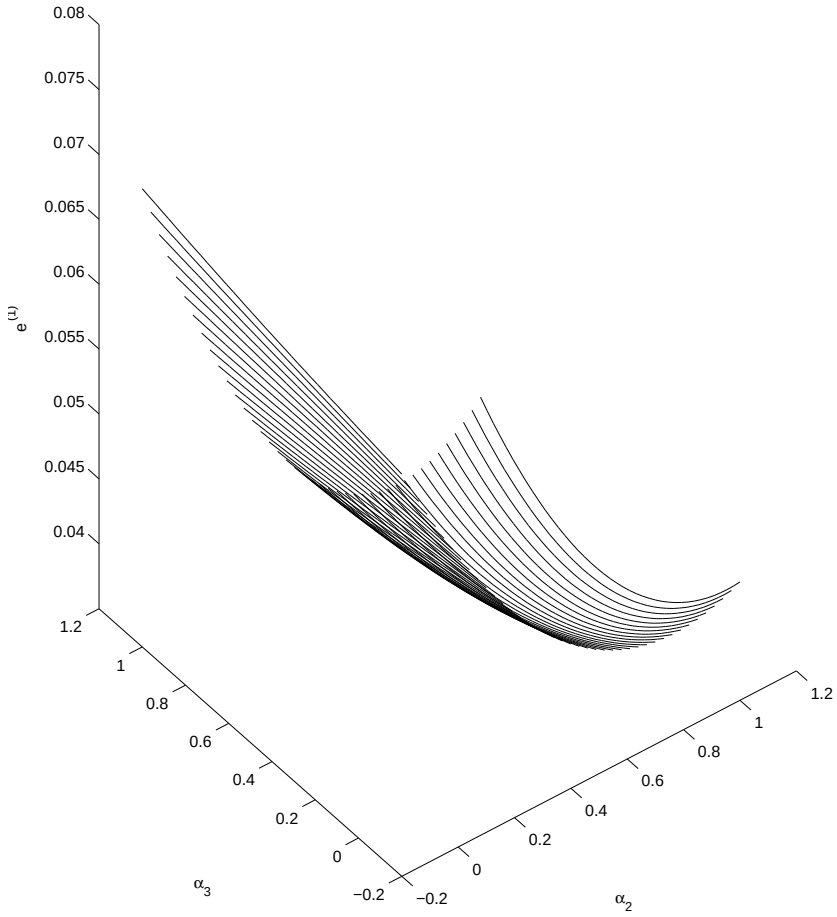

Figure 30: The coefficient $e^{(1)}$ as a function of the smearing parameters at $\alpha_1 = 1$

6 Conclusion

In this thesis, the $\mathcal{O}(a)$ improvement of the static-light axial current with light Wilson fermions and static fermions with smeared actions was studied at one-loop order in PT. The hypercubic smearing (HYP) with different smearing parameters was applied to the static fermion. Hereby, the initial situation was the existence of estimated values given by hybrid methods for the effective one-loop improvement coefficient $c_{\mathrm{A}}^{\mathrm{stat}(1)}$ [13]. The one-loop coefficient $c_{\mathrm{A}}^{\mathrm{stat}(1)}$ was determined by using the methodology of the Schrödinger functional.

In this framework, the fermionic correlation functions for light fermions in the SF were reproduced in detail and computed explicitly for the static fermion. The Feynman rules for the correlators $f_{\mathrm{A}}^{\mathrm{stat}}$ and f_1^{stat} in time-momentum representation, which play a role for computing $c_{\mathrm{A}}^{\mathrm{stat}(1)}$, were presented in the SF. This was done at one-loop order in PT without and with HYP smearing whereby the Feynman rules of the HYP link in time-momentum representation in the SF werde derived by inverse Fourier transformation of known results on the full torus. This method also yields the vertex for the spatial HYP link in time-momentum representation which was computed in detail and may become important for simulating HYP smeared relativistic fermions. In this context, theoretical considerations have shown that the smeared gauge field can be taken as a linear function of the unsmeared one at one-loop order in PT without background field.

Based on an existing C + + program package[10], the Feynman diagrams could be calculated and extended to the HYP action. A MATLAB progam was developed to extract $c_{\mathrm{A}}^{\mathrm{stat}(1)}$ from the diagrams. The known one-loop value for the EH action could be reproduced. For the HYP action, the one-loop coefficients compared with the effective values won by the hybrid method show the presence of non-negligible $\mathcal{O}(g_0^4)$ effects.

Based on the Feynman diagrams for f_1^{stat}, the static self-energy was computed and agreed with the value of the static self-energy which previously had been computed at one-loop order in PT on the full torus [11]. The self-energy, which diverges in the continuum limit, could be minimised by evaluating its minimal value w.r.t. the HYP smearing parameters. The minimum was identified to be in the vicinity of the HYP2 action whose value is based on non-pertubative estimations. This is interpreted as the self-energy being dominated by pertubation theory.

The results of this thesis are published in [22]. They are inputs for high precision lattice computations of B-meson transition amplitudes which play a role in tests of the Standard Model and discovery of new physics [23].

[10] Many thanks to F.Palombi for providing his code

A Appendix

A.1 Definitions

A.1.1 Euclidean field theory

We use lower greek indices for space-time coordinates and lower Latin indices for pure spatial coordinates. The Euclidean QCD emerges by a Wick rotation from the Minkowski metric, i.e. we perform the substitutions

$$x_0^E = -ix_4 \tag{A.1}$$
$$p_0^E = ip_4 \tag{A.2}$$

The Euclidean gamma matrices are obtained by

$$\gamma_4^E = \gamma^0 \tag{A.3}$$
$$\gamma_j^E = -i\gamma^j, \quad j \in [1,2,3] \tag{A.4}$$
$$\gamma_5^E = \gamma_0^E \gamma_1^E \gamma_2^E \gamma_3^E \tag{A.5}$$

which leads to

$$\left\{\gamma_\mu^E, \gamma_\nu^E\right\} = 2\delta_{\mu\nu} \tag{A.6}$$

and

$$\gamma_5^E = \gamma_5^{E\dagger} \tag{A.7}$$
$$(\gamma_5^E)^2 = \mathbb{1} \tag{A.8}$$

We define the hermitian matrices

$$\sigma_{\mu\nu}^E = \frac{i}{2}\left[\gamma_\mu^E, \gamma_\nu^E\right] \tag{A.9}$$

The upper index E is omitted in this work. Unless otherwise specified, Wick rotated quantities are used.

A.1.2 Euclidean space-time lattice

We introduce an isotropic lattice with finite extent L, volume $V = L^4$ and periodic boundary conditions (PBC). The coordinates and momenta are obtained by

$$x_i = an_i \tag{A.10}$$
$$p_i = \frac{2\pi}{La} l_i \tag{A.11}$$

with some integer values $n_i, l_i \in [0, L-1]$. The lattice distance a has the dimension of an inverse mass. We define the Fourier transformation by

$$\tilde{\Psi}(p) = \sum_x a^4 e^{ipx} \Psi(x) \tag{A.12}$$
$$\Psi(x) = \frac{1}{a^4 V} \sum_x e^{-ipx} \tilde{\Psi}(p) \tag{A.13}$$

In the limit to an inifinite extent, we obtain the continious momentum spectrum. The ordinary lattice derivatives are given by

$$\begin{aligned} \partial_\mu f(x) &= \frac{1}{a}[f(x+a\hat{\mu}) - f(x)] \\ \partial^*_\mu f(x) &= \frac{1}{a}[f(x) - f(x-a\hat{\mu})] \end{aligned} \tag{A.14}$$

with $\hat{\mu}$ being the unit vector in direction μ. Imposing PBC is equivalent to

$$\Psi(x + L\hat{\mu}) = e^{i\Theta_\mu}\Psi(x) \tag{A.15}$$

$$\overline{\Psi}(x + L\hat{\mu}) = \overline{\Psi}(x)e^{-i\Theta_\mu} \tag{A.16}$$

In the SF, PBC are only applied to the spatial coordinates, i.e. $\Theta_0 = 0$. With

$$\lambda_\mu = e^{ia\Theta_\mu/L}, \quad -\pi < \Theta_\mu \leq \pi \ , \tag{A.17}$$

we define covariant lattice derivatives by

$$\nabla_\mu \Psi(x) = \frac{1}{a}[\lambda_\mu U_\mu(x)\Psi(x+a\hat{\mu}) - \Psi(x)] \tag{A.18}$$

$$\nabla^*_\mu \Psi(x) = \frac{1}{a}[\Psi(x) - \lambda_\mu^{-1} U_\mu(x-a\hat{\mu})^{-1}\Psi(x-a\hat{\mu})] \tag{A.19}$$

$$\overline{\Psi}(x)\overleftarrow{\nabla}_\mu = \frac{1}{a}[\overline{\Psi}(x+a\mu)U_\mu(x)^{-1}\lambda_\mu^{-1} - \overline{\Psi}(x)] \tag{A.20}$$

$$\overline{\Psi}(x)\overleftarrow{\nabla}^*_\mu = \frac{1}{a}[\overline{\Psi}(x) - \overline{\Psi}(x-a\mu)U_\mu(x-a\mu)\lambda_\mu] \tag{A.21}$$

For an inifinite lattice, it holds $\lambda_\mu = \mathbb{1}$.
The gauge links are elements of the SU(3) group with

$$\begin{aligned} U_\mu(x) &= e^{iag_0 A_\mu(x+a\mu/2)} \\ &= 1 + iag_0 A_\mu(x + a\mu/2) + \mathcal{O}(a^2) \end{aligned} \tag{A.22}$$

It holds

$$U_{-\mu}(x) = U\mu^\dagger(x - a\mu) \tag{A.23}$$

The vector fields A_μ can be expanded from the Gell-Mann matrices λ_a with reel phases ζ_a as

$$A_\mu(x + a\mu/2) = \sum_{a=1}^{8} \zeta_a(x + a\mu/2)\frac{\lambda_a}{2} \tag{A.24}$$

A.2 Basic light correlation functions

Recall that

$$\ln \mathcal{Z}_f = ln\mathcal{Z}_f|_{\rho'..\eta=0} - S_{F,impr}\left[U, \overline{\Psi}_{cl}, \Psi_{cl}\right] + (\bar{\eta}, \Psi_{cl}) + (\overline{\Psi}_{cl}, \eta) + (\bar{\eta}, (D+m)^{-1}\eta)$$

Here, the scalar product $(\bar{\eta}, \Psi)$ is defined by

$$(\bar{\eta}, \Psi) = a^4 \sum_{0<x_0<T} \sum_{\mathbf{x}} \bar{\eta}(x)\Psi(x)$$

giving an explicit expression for

$$(\bar{\eta}, (D+m)^{-1}\eta) = a^8 \sum_{0<x_0,y_0<T} \sum_{\mathbf{x},\mathbf{y}} \bar{\eta}(x)S(x,y)\eta(y)$$

This allows us to compute the basic light two-point functions in the SF including gauge fields as

$$\begin{aligned}
[\Psi(x)\overline{\Psi}(y)]_F &= \frac{\delta}{\delta\bar{\eta}(x)}(-\frac{\delta}{\delta\eta(y)})e^{-S_{F,impr}\left[U,\overline{\Psi}_{cl},\Psi_{cl}\right]+(\bar{\eta},\Psi_{cl})+(\overline{\Psi}_{cl},\eta)+(\bar{\eta},(D+m)^{-1}\eta)}|_{\bar{\rho}'=\ldots=\eta=0} \\
&= \frac{\delta}{\delta\eta(y)}\frac{\delta}{\delta\bar{\eta}(x)}(\bar{\eta}, (D+m)^{-1}\eta) \\
&= S(x,y)
\end{aligned} \tag{A.25}$$

$$\begin{aligned}
[\Psi(x)\bar{\zeta}(\mathbf{y})]_F &= -\frac{\delta}{\delta\bar{\eta}(x)}\frac{\delta}{\delta\rho(\mathbf{y})}e^{-S_{F,impr}\left[U,\overline{\Psi}_{cl},\Psi_{cl}\right]+(\bar{\eta},\Psi_{cl})+(\overline{\Psi}_{cl},\eta)+(\bar{\eta},(D+m)^{-1}\eta)}|_{\bar{\rho}'=\ldots=\eta=0} \\
&= \frac{\delta}{\delta\rho(\mathbf{y})}\frac{\delta}{\delta\bar{\eta}(x)}(\bar{\eta}, \Psi_{cl}(x)) \\
&= \frac{\delta}{\delta\rho(\mathbf{y})}\Psi_{cl}(x) \\
&= \tilde{c}_t S(x,y)U(y-a\hat{0})^{-1}P_+|_{y_0=a}
\end{aligned} \tag{A.26}$$

$$\begin{aligned}
[\Psi(x)\bar{\zeta}'(\mathbf{y})]_F &= -\frac{\delta}{\delta\bar{\eta}(x)}\frac{\delta}{\delta\rho'(\mathbf{y})}e^{-S_{F,impr}\left[U,\overline{\Psi}_{cl},\Psi_{cl}\right]+(\bar{\eta},\Psi_{cl})+(\overline{\Psi}_{cl},\eta)+(\bar{\eta},(D+m)^{-1}\eta)}|_{\bar{\rho}'=\ldots=\eta=0} \\
&= \frac{\delta}{\delta\rho'(\mathbf{y})}\frac{\delta}{\delta\bar{\eta}(x)}(\bar{\eta}, \Psi_{cl}(x)) \\
&= \frac{\delta}{\delta\rho'(\mathbf{y})}\Psi_{cl}(x) \\
&= \tilde{c}_t S(x,y)U(y,0)P_-|_{y_0=T-a}
\end{aligned} \tag{A.27}$$

$$\begin{aligned}
[\zeta(\mathbf{x})\overline{\Psi}(y)]_F &= -\frac{\delta}{\delta\bar{\rho}(\mathbf{x})}\frac{\delta}{\delta\eta(\mathbf{y})}e^{-S_{F,impr}\left[U,\overline{\Psi}_{cl},\Psi_{cl}\right]+(\bar{\eta},\Psi_{cl})+(\overline{\Psi}_{cl},\eta)+(\bar{\eta},(D+m)^{-1}\eta)}|_{\bar{\rho}'=\ldots=\eta=0} \\
&= -\frac{\delta}{\delta\bar{\rho}(\mathbf{x})}\frac{\delta}{\delta\eta(\mathbf{y})}(\overline{\Psi}_{cl}, \eta) \\
&= \frac{\delta}{\delta\bar{\rho}(\mathbf{x})}(\overline{\Psi}_{cl}(x)) \\
&= \tilde{c}_t P_- U(x-a\hat{0},0)S(x,y)|_{x_0=a}
\end{aligned} \tag{A.28}$$

$$
\begin{aligned}
[\zeta'(\mathbf{x})\overline{\Psi}(y)]_F &= -\frac{\delta}{\delta\bar{\rho}'(\mathbf{x})}\frac{\delta}{\delta\eta(\mathbf{y})}e^{-S_{F,impr}\left[U,\overline{\Psi}_{cl},\Psi_{cl}\right]+(\bar{\eta},\Psi_{cl})+(\overline{\Psi}_{cl},\eta)+(\bar{\eta},(D+m)^{-1}\eta)}|_{\bar{\rho}'=\ldots=\eta=0} \\
&= -\frac{\delta}{\delta\bar{\rho}'(\mathbf{x})}\frac{\delta}{\delta\eta(\mathbf{y})}(\overline{\Psi}_{cl},\eta) \\
&= \frac{\delta}{\delta\bar{\rho}'(\mathbf{x})}(\overline{\Psi}_{cl}(x)) \\
&= \tilde{c_t}P_+U(x,0)^{-1}S(x,y)|_{x_0=T-a} \qquad \text{(A.29)}
\end{aligned}
$$

$$
\begin{aligned}
[\zeta(\mathbf{x})\bar{\zeta}(\mathbf{y})]_F &= -\frac{\delta}{\delta\bar{\rho}(\mathbf{x})}\frac{\delta}{\delta\rho(\mathbf{y})}e^{-S_{F,impr}\left[U,\overline{\Psi}_{cl},\Psi_{cl}\right]+(\bar{\eta},\Psi_{cl})+(\overline{\Psi}_{cl},\eta)+(\bar{\eta},(D+m)^{-1}\eta)}|_{\bar{\rho}'=\ldots=\eta=0} \\
&= \frac{\delta}{\delta\bar{\rho}(\mathbf{x})}\frac{\delta}{\delta\rho(\mathbf{y})}S_{F,impr}\left[U,\overline{\Psi}_{cl},\Psi_{cl}\right] \\
&= -\frac{1}{2}\tilde{c_s}P_-\gamma_k(\nabla_k+\nabla_k^*)P_+a^{-2}\delta_{\mathbf{xy}} + \frac{\delta}{\delta\rho(\mathbf{y})}\frac{\delta}{\delta\bar{\rho}(\mathbf{x})}\left[\tilde{c_t}\bar{\rho}(\mathbf{x})U(x-a\hat{0},0)\Psi_{cl}(x)|_{x_0=a}\right] \\
&= -\frac{1}{2}\tilde{c_s}P_-\gamma_k(\nabla_k+\nabla_k^*)a^{-2}\delta_{\mathbf{xy}} + \frac{\delta}{\delta\rho(\mathbf{y})}\left[\tilde{c_t}P_-U(x-a\hat{0},0)\Psi_{cl}(x)|_{x_0=a}\right] \\
&= -\frac{1}{2}\tilde{c_s}P_-\gamma_k(\nabla_k+\nabla_k^*)a^{-2}\delta_{\mathbf{xy}} + \tilde{c_t}^2P_-U(x-a\hat{0},0)S(x,y)U(y-a\hat{0},0)^{-1}P_+|_{x_0=y_0=a} \\
& \qquad \text{(A.30)}
\end{aligned}
$$

In the proceeding calculation, the anticommutation relation $\gamma_k P_+ = P_-\gamma_k$ is used to eliminate the projector P_+.

$$
\begin{aligned}
[\zeta'(\mathbf{x})\bar{\zeta}'(\mathbf{y})]_F &= -\frac{\delta}{\delta\bar{\rho}'(\mathbf{x})}\frac{\delta}{\delta\rho'(\mathbf{y})}e^{-S_{F,impr}\left[U,\overline{\Psi}_{cl},\Psi_{cl}\right]+(\bar{\eta},\Psi_{cl})+(\overline{\Psi}_{cl},\eta)+(\bar{\eta},(D+m)^{-1}\eta)}|_{\bar{\rho}'=\ldots=\eta=0} \\
&= \frac{\delta}{\delta\bar{\rho}'(\mathbf{x})}\frac{\delta}{\delta\rho'(\mathbf{y})}S_{F,impr}\left[U,\overline{\Psi}_{cl},\Psi_{cl}\right] \\
&= -\frac{1}{2}\tilde{c_s}P_+\gamma_k(\nabla_k+\nabla_k^*)P_-a^{-2}\delta_{\mathbf{xy}} + \frac{\delta}{\delta\rho'(\mathbf{y})}\frac{\delta}{\delta\bar{\rho}'(\mathbf{x})}\left[\tilde{c_t}\bar{\rho}'(\mathbf{x})U(x,0)^{-1}\Psi_{cl}(x)|_{x_0=T-a}\right] \\
&= -\frac{1}{2}\tilde{c_s}P_+\gamma_k(\nabla_k+\nabla_k^*)a^{-2}\delta_{\mathbf{xy}} + \frac{\delta}{\delta\rho'(\mathbf{y})}\left[\tilde{c_t}P_+U(x,0)^{-1}\Psi_{cl}(x)|_{x_0=T-a}\right] \\
&= -\frac{1}{2}\tilde{c_s}P_+\gamma_k(\nabla_k+\nabla_k^*)a^{-2}\delta_{\mathbf{xy}} + \tilde{c_t}^2P_+U(x,0)^{-1}S(x,y)U(y,0)P_-|_{x_0=y_0=T-a} \\
& \qquad \text{(A.31)}
\end{aligned}
$$

$$
\begin{aligned}
[\zeta(\mathbf{x})\bar{\zeta}'(\mathbf{y})]_F &= -\frac{\delta}{\delta\bar{\rho}(\mathbf{x})}\frac{\delta}{\delta\rho'(\mathbf{y})}e^{-S_{F,impr}\left[U,\overline{\Psi}_{cl},\Psi_{cl}\right]+(\bar{\eta},\Psi_{cl})+(\overline{\Psi}_{cl},\eta)+(\bar{\eta},(D+m)^{-1}\eta)}|_{\bar{\rho}'=\ldots=\eta=0} \\
&= \frac{\delta}{\delta\bar{\rho}(\mathbf{x})}\frac{\delta}{\delta\rho'(\mathbf{y})}S_{F,impr}\left[U,\overline{\Psi}_{cl},\Psi_{cl}\right] \\
&= \frac{\delta}{\delta\rho'(\mathbf{y})}\frac{\delta}{\delta\bar{\rho}(\mathbf{x})}\left[\tilde{c_t}\bar{\rho}(\mathbf{x})U(x-a\hat{0},0)\Psi_{cl}(x)|_{x_0=a}\right] \\
&= \frac{\delta}{\delta\rho'(\mathbf{y})}\left[\tilde{c_t}P_-U(x-a\hat{0},0)\Psi_{cl}(x)|_{x_0=a}\right] \\
&= \tilde{c_t}^2P_-U(x-a\hat{0},0)S(x,y)U(y,0)P_-|_{x_0=a,y_0=T-a} \qquad \text{(A.32)}
\end{aligned}
$$

$$
\begin{aligned}
[\zeta'(\mathbf{x})\bar{\zeta}(\mathbf{y})]_F &= -\frac{\delta}{\delta\bar{\rho}'(\mathbf{x})}\frac{\delta}{\delta\rho(\mathbf{y})} e^{-S_{F,impr}\left[U,\overline{\Psi}_{cl},\Psi_{cl}\right]+(\bar{\eta},\Psi_{cl})+(\overline{\Psi}_{cl},\eta)+(\bar{\eta},(D+m)^{-1}\eta)}|_{\bar{\rho}'=\ldots=\eta=0} \\
&= \frac{\delta}{\delta\bar{\rho}'(x)}\frac{\delta}{\delta\rho(\mathbf{y})} S_{F,impr}\left[U,\overline{\Psi}_{cl},\Psi_{cl}\right] \\
&= \frac{\delta}{\delta\rho(\mathbf{y})}\left[\tilde{c_t}P_+U(x,0)^{-1}\Psi_{cl}(x)|_{x_0=T-a}\right] \\
&= \tilde{c_t}^2 P_+U(x,0)^{-1}S(x,y)U(y-a\hat{0},0)^{-1}P_+|_{x_0=T-a,y_0=a} \qquad \text{(A.33)}
\end{aligned}
$$

A.3 Basic static correlation functions

For the static quark, it holds

$$
S\left[U,\overline{\Psi}_{cl,h},\Psi_{cl,h}\right]=0 \qquad \text{(A.34)}
$$

and

$$
\frac{\delta}{\delta\rho_h(\mathbf{x})}\overline{\Psi}_{cl,h}(x) = U_0(x-a\hat{0})^{-1}..U_0(x-x_0\hat{0})^{-1}P_+ \qquad \text{(A.35)}
$$

$$
\frac{\delta}{\delta\bar{\rho}'_h(\mathbf{x})}\overline{\Psi}_{cl,h}(x) = P_+U_0(x)^{-1}|_{x_0=T-a\hat{0}}..U_0(x)^{-1} \qquad \text{(A.36)}
$$

$$
\Psi_{h,cl}(x) = U_0(x-a\hat{0})^{-1}...U_0(x-x_0\hat{0})^{-1}\rho_h(\mathbf{x}) \qquad \text{(A.37)}
$$

$$
\overline{\Psi}_{h,cl}(x) = \bar{\rho}_h(\mathbf{x})'U_0(x)^{(-1)}|_{x_0=T-a\hat{0}}...U_0(x)^{(-1)} \qquad \text{(A.38)}
$$

This yields the basic static correlation functions

$$
\begin{aligned}
[\Psi(x)\overline{\Psi}(y)]_F &= \frac{\delta}{\delta\bar{\eta}(x)}(-\frac{\delta}{\delta\eta(y)})e^{(\bar{\eta},\Psi_{cl})+(\overline{\Psi}_{cl},\eta)+(\bar{\eta},(D+m)^{-1}\eta)}|_{\bar{\rho}'=\ldots=\eta=0} \\
&= \frac{\delta}{\delta\eta(y)}\frac{\delta}{\delta\bar{\eta}(x)}(\bar{\eta},(D+m)^{-1}\eta) \\
&= S(x,y) \qquad \text{(A.39)}
\end{aligned}
$$

$$
\begin{aligned}
[\Psi(x)\bar{\zeta}(\mathbf{y})]_F &= -\frac{\delta}{\delta\bar{\eta}(x)}\frac{\delta}{\delta\rho(\mathbf{y})}e^{(\bar{\eta},\Psi_{cl})+(\overline{\Psi}_{cl},\eta)+(\bar{\eta},(D+m)^{-1}\eta)}|_{\bar{\rho}'=\ldots=\eta=0} \\
&= \frac{\delta}{\delta\rho(\mathbf{y})}\frac{\delta}{\delta\bar{\eta}(x)}(\bar{\eta},\Psi) \\
&= \frac{\delta}{\delta\rho(\mathbf{y})}\Psi_{cl}(x) \\
&= \delta_{\mathbf{xy}}U_0(x-a\hat{0})^{-1}..U_0(x-x_0\hat{0})^{-1}P_+ \qquad \text{(A.40)}
\end{aligned}
$$

$$
\begin{aligned}
[\zeta'(\mathbf{x})\overline{\Psi}(y)]_F &= -\frac{\delta}{\delta\bar{\rho}'(\mathbf{x})}\frac{\delta}{\delta\eta(\mathbf{y})}e^{(\bar{\eta},\Psi_{cl})+(\overline{\Psi}_{cl},\eta)+(\bar{\eta},(D+m)^{-1}\eta)}|_{\bar{\rho}'=\ldots=\eta=0} \\
&= -\frac{\delta}{\delta\bar{\rho}'(\mathbf{x})}\frac{\delta}{\delta\eta(\mathbf{y})}(\overline{\Psi}_{cl},\eta) \\
&= \frac{\delta}{\delta\bar{\rho}'(\mathbf{x})}\overline{\Psi}_{cl}(x) \\
&= P_+U_0(x)^{-1}|_{x_0=T-a\hat{0}}..U_0(x)^{-1}
\end{aligned} \tag{A.41}
$$

$$
\begin{aligned}
[\zeta'(\mathbf{x})\bar{\zeta}(\mathbf{y})]_F &= -\frac{\delta}{\delta\bar{\rho}'(\mathbf{x})}\frac{\delta}{\delta\rho(\mathbf{y})}e^{(\bar{\eta},\Psi_{cl})+(\overline{\Psi}_{cl},\eta)+(\bar{\eta},(D+m)^{-1}\eta)}|_{\bar{\rho}'=\ldots=\eta=0} \\
&= \frac{\delta}{\delta\bar{\rho}'(\mathbf{x})}\overline{\Psi}_{cl}(x)\frac{\delta}{\delta\rho(\mathbf{y})}\Psi_{cl}(x) \\
&= \delta_{\mathbf{xy}}P_+U_0(x)^{-1}|_{x_0=T-a\hat{0}}..U_0(x)^{-1}U_0(x-a\hat{0})^{-1}..U_0(x-x_0\hat{0})^{-1}P_+
\end{aligned} \tag{A.42}
$$

A.4 The classical free action in the SF

The classical free action in the Schrödinger functional is derived, the result sounds

$$
\begin{aligned}
S_F[\overline{\Psi}_{cl},\Psi_{cl}] = a^4\sum_x \frac{1}{2}\big(\bar{\rho}(\vec{x})\gamma_k(\nabla_k+\nabla_k^*)\rho(\vec{x}) + \bar{\rho}'(\vec{x})\gamma_k(\nabla_k+\nabla_k^*)\rho'(\vec{x})\big) \\
-a^3\sum_x \bar{\rho}(\vec{x})\Psi_{cl}(x)|_{x_0=a} \\
-a^3\sum_x \bar{\rho}'(\vec{x})\Psi_{cl}(x)|_{x_0=T-a}
\end{aligned}
$$

Proof:
The action is defined as

$$
\begin{aligned}
&S[\overline{\Psi}_{cl},\Psi_{cl}] \\
&= a^4\sum_x \overline{\Psi}_{cl}(x)(D+m)\Psi_{cl}(x) \\
&= a^4\sum_x \underbrace{\overline{\Psi}_{cl}(\vec{x},x_0=0)}_{\bar{\rho}(\vec{x})}(D+m)\Psi_{cl}(x)|_{x_0=0} + a^4\sum_x \underbrace{\overline{\Psi}_{cl}(\vec{x},x_0=T)}_{\bar{\rho}'(\vec{x})}(D+m)\Psi_{cl}(x)|_{x_0=T}
\end{aligned} \tag{A.43}
$$

Please note that the entire expression $(D+m)\Psi_{cl}(x)$ is evaluated at the position x_0 which prevents to get rid of $\Psi_{cl}(x)$ by e.g. plugging in a boundary field like for $\overline{\Psi}_{cl}(x)$ at x_0.

Now consider

$$
\begin{aligned}
&(D+m)\Psi_{cl}(x)|_{x_0=0} \\
&= (\frac{1}{2}\gamma_\mu(\nabla_\mu+\nabla_\mu^*) - \frac{1}{2}\nabla_\mu\nabla_\mu^*)\Psi_{cl}(x)|_{x_0=0} \\
&= (\frac{1}{2}\gamma_k(\nabla_k+\nabla_k^*) - \frac{1}{2}\nabla_k\nabla_k^*)\underbrace{\Psi_{cl}(\vec{x},x_0=0)}_{\rho(\vec{x})} + (\frac{1}{2}\gamma_0(\nabla_0+\nabla_0^*) - \frac{1}{2}\nabla_0\nabla_0^*)\Psi_{cl}(x)|_{x_0=0}
\end{aligned}
\tag{A.44}
$$

The latter term can be written as

$$
\begin{aligned}
&(\frac{1}{2}\gamma_0(\nabla_0+\nabla_0^*) - \frac{1}{2}\nabla_0\nabla_0^*)\Psi_{cl}(x)|_{x_0=0} \\
&= \frac{1}{2a}\gamma_0(\Psi_{cl}(\vec{x},x_0=a) - \underbrace{\Psi_{cl}(\vec{x},x_0=-a))}_{=0} - \frac{1}{2a}(\Psi_{cl}(\vec{x},x_0=a) + \underbrace{\Psi_{cl}(\vec{x},x_0=-a)}_{=0} - 2\underbrace{\Psi_{cl}(\vec{x},x_0=0)}_{\rho(\vec{x})}) \\
&= \frac{1}{2a}(\gamma_0-1)\Psi_{cl}(\vec{x},x_0=a) + \frac{1}{a}\rho(\vec{x}) \\
&= -\frac{1}{a}P_-\Psi_{cl}(\vec{x},x_0=a) + \frac{1}{a}\rho(\vec{x})
\end{aligned}
\tag{A.45}
$$

Now while knowing that $\bar{\rho}(\vec{x})\rho(\vec{x})=0$ multiplying with $\bar{\rho}(\vec{x})$ one gets for

$$
\begin{aligned}
&a^4\sum_x \overline{\Psi}_{cl}(\vec{x},x_0=0)(D+m)\Psi_{cl}(x)|_{x_0=0} \\
&= a^4\sum_x \bar{\rho}(\vec{x})(\frac{1}{2}\gamma_k(\nabla_k+\nabla_k^*)\rho(\vec{x}) - a^3\sum_x \bar{\rho}(\vec{x})P_-\Psi_{cl}(\vec{x},x_0=a)
\end{aligned}
\tag{A.46}
$$

The term $\bar{\rho}(\vec{x})\frac{1}{2}\nabla_k\nabla_k^*\rho(\vec{x})$ vanishes because $\bar{\rho}(\vec{x})\rho(\vec{y})=0$.

Due to $\bar{\rho}(\vec{x}) = \overline{\Psi}(x)P_-$ it follows that $\bar{\rho}(\vec{x})P_- = \bar{\rho}(\vec{x})$, and the projector can be left out.

Analogously the second part can be written as

$$
\begin{aligned}
&a^4\sum_x \overline{\Psi}_{cl}(\vec{x},x_0=T)(D+m)\Psi_{cl}(x)|_{x_0=T} \\
&= a^4\sum_x \bar{\rho}'(\vec{x})(\frac{1}{2}\gamma_k(\nabla_k+\nabla_k^*)\rho'(\vec{x}) - a^3\sum_x \bar{\rho}'(\vec{x})P_+\Psi_{cl}(\vec{x},x_0=T-a)
\end{aligned}
\tag{A.47}
$$

while the projector P_+ is allowed to be omitted.

A.5 Derivation of HYP spatial links

The following deduction uses the method of anti-Fourier transformation from the known result [11] on the full torus. We work in units of the lattice spacing in order to simplify the notation. Let us start by observing that

$$\tilde{B}_k^{(3)}(p) = f_{k0}(p)\tilde{q}_0(p) + \sum_{\eta\neq 0,k} f_{k\eta}(p)\tilde{q}_\eta(p) + f_{kk}(p)\tilde{q}_k(p) + \mathrm{O}(g_0)\,. \tag{A.48}$$

The first term on the r.h.s. can be written as

$$f_{k0}(p)\tilde{q}_0(p) = \frac{\alpha_1}{6}\hat{p}_k\hat{p}_0\Omega_{k0}(\mathbf{p})\tilde{q}_0(p)\,, \tag{A.49}$$

where we remark again that Ω_{k0} does not depend upon p_0. Analogously, we have that for $\eta \neq 0, k$:

$$f_{k\eta}(p)\tilde{q}_\eta(p) = \frac{\alpha_1}{6}\hat{p}_k\hat{p}_\eta\Omega_{k\eta}(p)\tilde{q}_\eta(p)\,, \tag{A.50}$$

$$\Omega_{k\eta}(p) = 1 + \alpha_2(1+\alpha_3) - \frac{\alpha_2}{4}(1+2\alpha_3)\left[\hat{p}_0^2 + \hat{p}_{l;k\eta}^2\right] + \frac{\alpha_2\alpha_3}{4}\prod_{\omega\neq k,\eta}\hat{p}_\omega^2\,, \tag{A.51}$$

with $l; k\eta$ meaning that $\hat{l} \perp (\hat{k}, \hat{\eta}, \hat{0})$. Finally the third term on the r.h.s. of Eq. (A.48):

$$f_{kk}(p)\tilde{q}_k(p) = \left\{1 - \frac{\alpha_1}{6}\left[\hat{p}_0^2\Omega_{k0}(\mathbf{p}) + \sum_{\eta\neq k,0}\hat{p}_\eta^2\Omega_{k\eta}(p)\right]\right\}\tilde{q}_k(p)\,. \tag{A.52}$$

We now perform the Fourier anti-transform in time

$$\tilde{B}_k^{(3)}(x_0;\mathbf{p}) = \frac{1}{L}\sum_{p_0} \mathrm{e}^{ip_0x_0}\tilde{B}_k^{(3)}(p)\,, \tag{A.53}$$

by considering the first term (A.49),

$$\frac{1}{L}\sum_{p_0}\mathrm{e}^{ip_0x_0}f_{k0}(p)\tilde{q}_0(p) = \frac{\alpha_1}{6}\hat{p}_k\Omega_{k0}(\mathbf{p})\frac{1}{L}\sum_{p_0}\mathrm{e}^{ip_0x_0}\hat{p}_0\tilde{q}_0(p)\,. \tag{A.54}$$

We observe that

$$\begin{aligned}
\frac{1}{L}\sum_{p_0}\mathrm{e}^{ip_0x_0}\hat{p}_0\tilde{q}_0(p) &= \frac{1}{L}\sum_{p_0}\mathrm{e}^{ip_0x_0}2\sin(\frac{p_0}{2})\tilde{q}_0(p) \\
&= \frac{-i}{L}\sum_{p_0}\mathrm{e}^{ip_0x_0}\left(\mathrm{e}^{i\frac{p_0}{2}} - \mathrm{e}^{-i\frac{p_0}{2}}\right)\tilde{q}_0(p) \\
&= -i\tilde{q}_0(x_0;\mathbf{p}) + \frac{i}{L}\sum_{p_0}\mathrm{e}^{ip_0x_0}\mathrm{e}^{-i\frac{p_0}{2}}\tilde{q}_0(p) \\
&= -i(\tilde{q}_0(x_0;\mathbf{p}) - \tilde{q}_0(x_0-1,\mathbf{p})) = -i\partial_0^*\tilde{q}_0(x_0;\mathbf{p})\,.
\end{aligned} \tag{A.55}$$

so that we obtain for the contribution

$$\begin{aligned}
\tilde{B}_k^{(3;1)}(x_0;\mathbf{p}) &\equiv \frac{1}{L}\sum_{p_0}\mathrm{e}^{ip_0x_0}f_{k0}(p)\tilde{q}_0(p) = \\
&= -i\frac{\alpha_1}{6}\hat{p}_k\Omega_{k0}(\mathbf{p})\partial_0^*\tilde{q}_0(x_0;\mathbf{p})
\end{aligned} \tag{A.56}$$

The second term is a bit more involved

$$\frac{1}{L}\sum_{p_0} \mathrm{e}^{ip_0x_0} \sum_{\eta\neq 0,k} f_{k\eta}(p)\tilde{q}_\eta(p) = \frac{1}{L}\sum_{p_0} \mathrm{e}^{ip_0x_0} \sum_{\eta\neq 0,k} \frac{\alpha_1}{6}\hat{p}_k\hat{p}_\eta\Omega_{k\eta}(p)\tilde{q}_\eta(p)\,, \quad \text{(A.57)}$$

and we perform the decomposition

$$\Omega_{k\eta}(p) = \Omega^{(s)}_{k\eta}(\mathbf{p}) + \Omega^{(0)}_{k\eta}(p)\,, \quad \text{(A.58)}$$

$$\Omega^{(s)}_{k\eta}(\mathbf{p}) = 1 + \alpha_2(1+\alpha_3) - \frac{\alpha_2}{4}(1+2\alpha_3)\hat{p}^2_{l;k\eta}\,, \quad \text{(A.59)}$$

$$\Omega^{(0)}_{k\eta}(p) = -\frac{\alpha_2}{4}(1+2\alpha_3)\hat{p}_0^2 + \frac{\alpha_2\alpha_3}{4}\hat{p}_0^2\hat{p}^2_{l;k\eta}\,. \quad \text{(A.60)}$$

By noticing that

$$\hat{p}_0^2 = 4\sin^2(p_0/2) = 2(1-\cos(p_0)) = 2[1-(\mathrm{e}^{ip_0}+\mathrm{e}^{-ip_0})/2] = 2-(\mathrm{e}^{ip_0}+\mathrm{e}^{-ip_0})\,, \quad \text{(A.61)}$$

we can rewrite the term containing $\Omega^{(0)}$ as

$$\begin{aligned}\frac{1}{L}\sum_{p_0} \mathrm{e}^{ip_0x_0} \sum_{\eta\neq 0,k} \frac{\alpha_1}{6}\hat{p}_k\hat{p}_\eta\Omega^{(0)}_{k\eta}(p)\tilde{q}_\eta(p) &= \sum_{\eta\neq 0,k}(-\hat{p}_k\Delta^{(t)}_{k\eta})\frac{1}{L}\sum_{p_0}\mathrm{e}^{ip_0x_0}\hat{p}_0^2\tilde{q}_\eta(p)\\ &= \sum_{\eta\neq 0,k}(-\hat{p}_k\Delta^{(t)}_{k\eta})\cdot(2\tilde{q}_\eta(x_0;\mathbf{p}) - \tilde{q}_\eta(x_0+1,\mathbf{p}) - \tilde{q}_\eta(x_0-1,\mathbf{p}))\\ &= \sum_{\eta\neq 0,k}\hat{p}_k\Delta^{(t)}_{k\eta}\partial_0^*\partial_0\tilde{q}_\eta(x_0;\mathbf{p})\,, \quad \text{(A.62)}\end{aligned}$$

letting us get

$$\frac{1}{L}\sum_{p_0} \mathrm{e}^{ip_0x_0} \sum_{\eta\neq 0,k} f_{k\eta}(p)\tilde{q}_\eta(p) = \sum_{\eta\neq 0,k}(\hat{p}_k\Delta^{(s)}_{k\eta}(\mathbf{p}) + \hat{p}_k\Delta^{(t)}_{k\eta}(\mathbf{p})\partial_0^*\partial_0)\tilde{q}_\eta(x_0;\mathbf{p})\,, \quad \text{(A.63)}$$

with

$$\Delta^{(s)}_{k\eta}(\mathbf{p}) = \frac{\alpha_1}{6}\hat{p}_\eta\Omega^{(s)}_{k\eta}(\mathbf{p})\,, \quad \text{(A.64)}$$

$$\Delta^{(t)}_{k\eta}(\mathbf{p}) = \frac{\alpha_1}{6}\hat{p}_\eta(\frac{\alpha_2}{4}(1+2\alpha_3) - \frac{\alpha_2\alpha_3}{4}\hat{p}^2_{l;k\eta})\,. \quad \text{(A.65)}$$

We thus get for the second contribution

$$\begin{aligned}\tilde{B}^{(3;2)}_k(x_0;\mathbf{p}) \equiv \frac{1}{L}\sum_{p_0}\mathrm{e}^{ip_0x_0}\sum_{\eta\neq 0,k} f_{k\eta}(p)\tilde{q}_\eta(p) =\\ = \hat{p}_k\sum_{\eta\neq 0,k}\left[\Delta^{(\mathrm{s})}_{k\eta}(\mathbf{p}) + \Delta^{(\mathrm{t})}_{k\eta}(\mathbf{p})a^2\partial_0^*\partial_0\right]\tilde{q}_\eta(x_0;\mathbf{p}) \quad \text{(A.66)}\end{aligned}$$

The Fourier anti-transformed expression of the third term in the r.h.s. of Eq. (A.48) can be in turn decomposed into three terms (c.f. Eq. (A.52)). One of them is $\tilde{q}_k(x_0;\mathbf{p})$, the second

$$-\frac{1}{L}\sum_{p_0}\mathrm{e}^{ip_0x_0}\frac{\alpha_1}{6}\hat{p}_0^2\Omega_{k0}(\mathbf{p})\tilde{q}_k(p) = \frac{\alpha_1}{6}\Omega_{k0}(\mathbf{p})\partial_0^*\partial_0\tilde{q}_k(x_0;\mathbf{p})\,, \quad \text{(A.67)}$$

while the third term is a bit more involved. We rewrite it as

$$-\frac{1}{L}\sum_{p_0} \mathrm{e}^{ip_0x_0}\frac{\alpha_1}{6}\sum_{\eta\neq 0,k}\hat{p}_\eta^2\Omega_{k\eta}(p)\tilde{q}_k(p) = -\frac{\alpha_1}{6}\sum_{\eta\neq 0,k}\hat{p}_\eta^2\Big(\Omega^{(s)}_{k\eta}(\mathbf{p})\tilde{q}_k(x_0;\mathbf{p}) + \frac{1}{L}\sum_{p_0}\mathrm{e}^{ip_0x_0}\Omega^{(0)}_{k\eta}(p)\tilde{q}_k(p)\Big)\,, \quad \text{(A.68)}$$

and consider only the term proportional to $\Omega^{(0)}$:

$$\begin{aligned} &-\frac{\alpha_1}{6}\sum_{\eta\neq 0,k}\hat{p}_\eta^2\frac{1}{L}\sum_{p_0}\mathrm{e}^{ip_0x_0}\Omega^{(0)}_{k\eta}(p)\tilde{q}_k(p) \\ &\quad= \sum_{\eta\neq 0,k}\frac{\alpha_1}{6}\hat{p}_\eta^2\left[\frac{\alpha_2}{4}(1+2\alpha_3) - \frac{\alpha_2\alpha_3}{4}\hat{p}^2_{l;k\eta}\right]\frac{1}{L}\sum_{p_0}\mathrm{e}^{ip_0x_0}\hat{p}_0^2\tilde{q}_k(p) \\ &\quad= \sum_{\eta\neq 0,k} -\hat{p}_\eta\Delta^{(t)}_{k\eta}(\mathbf{p})\partial_0^*\partial_0\tilde{q}_k(x_0;\mathbf{p})\,. \end{aligned} \quad \text{(A.69)}$$

We thus end up with

$$\frac{1}{L}\sum_{p_0}\mathrm{e}^{ip_0x_0}f_{kk}(p)\tilde{q}_k(p) = \Big[1 - \sum_{\eta\neq 0,k}\Big(\hat{p}_\eta\Delta^{(s)}_{k\eta}(\mathbf{p}) + \hat{p}_\eta\Delta^{(t)}_{k\eta}(\mathbf{p})\partial_0^*\partial_0\Big)\Big]\tilde{q}_k(x_0;\mathbf{p}) \quad \text{(A.70)}$$

The last contribution is therefore

$$\begin{aligned} \tilde{B}^{(3;3)}_k(x_0;\mathbf{p}) &\equiv \frac{1}{L}\sum_{p_0}\mathrm{e}^{ip_0x_0}f_{kk}(p)\tilde{q}_k(p) = \\ &= \Big\{1 + \frac{\alpha_1}{6}\Omega_{k0}(\mathbf{p})\partial_0^*\partial_0 - \\ &- \sum_{\eta\neq 0,k}\hat{p}_\eta\left[\Delta^{(\mathrm{s})}_{k\eta}(\mathbf{p}) + \Delta^{(\mathrm{t})}_{k\eta}(\mathbf{p})\partial_0^*\partial_0\right]\Big\}\tilde{q}_k(x_0;\mathbf{p})\,, \end{aligned} \quad \text{(A.71)}$$

The final result is

$$\tilde{B}^{(3)}_k(x_0;\mathbf{p}) = \tilde{B}^{(3;1)}_k(x_0;\mathbf{p}) + \tilde{B}^{(3;2)}_k(x_0;\mathbf{p}) + \tilde{B}^{(3;3)}_k(x_0;\mathbf{p}) \quad \text{(A.72)}$$

with above introduced contributions.

In oder to build a vertex table, one can recall that $\partial_0^* q(x_0;\mathbf{p}) = q(x_0,\mathbf{p}) - q(x_0-a;\mathbf{p})$ and $\partial_0^*\partial_0 q(x_0;\mathbf{p}) = -2q(x_0,\mathbf{p}) + q(x_0-a;\mathbf{p}) + q(x_0+a;\mathbf{p})$. So one can rewrite above equations. Accordingly, the first contribution is dependent on $\tilde{q}_0$ and can be written as

$$\begin{aligned} \tilde{B}^{(3;1)}_k(x_0;\mathbf{p}) &= -i\frac{\alpha_1}{6}\hat{p}_k\Omega_{k0}(\mathbf{p})\partial_0^*\tilde{q}_0(x_0;\mathbf{p}) \\ &= -i\frac{\alpha_1}{6}\hat{p}_k\Omega_{k0}(\mathbf{p})\tilde{q}_0(x_0;\mathbf{p}) + i\frac{\alpha_1}{6}\hat{p}_k\Omega_{k0}(\mathbf{p})\tilde{q}_0(x_0-1;\mathbf{p}) \end{aligned} \quad \text{(A.73)}$$

The third contribution yields

$$\tilde{B}_k^{(3;3)}(x_0;\mathbf{p}) = \tilde{q}_k(x_0;\mathbf{p}) - \frac{\alpha_1}{3}\Omega_{k0}(\mathbf{p})\tilde{q}_k(x_0;\mathbf{p}) + \frac{\alpha_1}{6}\Omega_{k0}(\mathbf{p})\tilde{q}_k(x_0-1;\mathbf{p}) + \frac{\alpha_1}{6}\Omega_{k0}(\mathbf{p})\tilde{q}_k(x_0+1;\mathbf{p}) -$$
$$- \sum_{\eta\neq 0,k} \hat{p}_\eta \Delta_{k\eta}^{(s)} \tilde{q}_k(x_0;\mathbf{p}) + 2\sum_{\eta\neq 0,k} \hat{p}_\eta \Delta_{k\eta}^{(t)} \tilde{q}_k(x_0;\mathbf{p}) -$$
$$- \sum_{\eta\neq 0,k} \hat{p}_\eta \Delta_{k\eta}^{(t)} \tilde{q}_k(x_0-1;\mathbf{p}) - \sum_{\eta\neq 0,k} \hat{p}_\eta \Delta_{k\eta}^{(t)} \tilde{q}_k(x_0+1;\mathbf{p}) \qquad \text{(A.74)}$$

Finally, the middle term depends on the complementary $\tilde{q}_{\eta;k0}$:

$$\tilde{B}_k^{(3;2)}(x_0;\mathbf{p}) = \hat{p}_k \sum_{\eta\neq 0,k} \Delta_{k\eta}^{(\mathrm{s})}(\mathbf{p})\tilde{q}_\eta(x_0;\mathbf{p}) - 2\hat{p}_k \sum_{\eta\neq 0,k} \Delta_{k\eta}^{(\mathrm{t})}(\mathbf{p})\tilde{q}_\eta(x_0;\mathbf{p})$$
$$+ \hat{p}_k \sum_{\eta\neq 0,k} \Delta_{k\eta}^{(\mathrm{t})}(\mathbf{p})\tilde{q}_\eta(x_0+1;\mathbf{p}) + \hat{p}_k \sum_{\eta\neq 0,k} \Delta_{k\eta}^{(\mathrm{t})}(\mathbf{p})\tilde{q}_\eta(x_0-1;\mathbf{p}) \qquad \text{(A.75)}$$

This allows us to formulate Eq. (A.72) as

$$\tilde{B}_k^{(3)}(x_0;\mathbf{p}) = \sum_{i=0}^{7} V_{k;i}(\mathbf{p})\tilde{q}_{\mu(i)}(x_0 + as(i);\mathbf{p}) \ . \qquad \text{(A.76)}$$

with Table 2 given in section 2.7.

A.6 Integrals for the static potential at one-loop order in PT on the full torus

$$e^{(1)}_{000} = \frac{4}{3(2\pi^3)} \int_{-\pi}^{\pi}\int_{-\pi}^{\pi}\int_{-\pi}^{\pi} \frac{1}{\hat{x}^2+\hat{y}^2+\hat{z}^2} dxdydz \tag{A.77}$$

$$e^{(1)}_{100} = \frac{4}{3(2\pi^3)} \int_{-\pi}^{\pi}\int_{-\pi}^{\pi}\int_{-\pi}^{\pi} \frac{2c_1(x,y,z)}{\hat{x}^2+\hat{y}^2+\hat{z}^2} dxdydz \tag{A.78}$$

$$e^{(1)}_{110} = \frac{4}{3(2\pi^3)} \int_{-\pi}^{\pi}\int_{-\pi}^{\pi}\int_{-\pi}^{\pi} \frac{2c_2(x,y,z)}{\hat{x}^2+\hat{y}^2+\hat{z}^2} dxdydz \tag{A.79}$$

$$e^{(1)}_{111} = \frac{4}{3(2\pi^3)} \int_{-\pi}^{\pi}\int_{-\pi}^{\pi}\int_{-\pi}^{\pi} \frac{2c_3(x,y,z)}{\hat{x}^2+\hat{y}^2+\hat{z}^2} dxdydz \tag{A.80}$$

$$e^{(1)}_{200} = \frac{4}{3(2\pi^3)} \int_{-\pi}^{\pi}\int_{-\pi}^{\pi}\int_{-\pi}^{\pi} \frac{c_1(x,y,z)^2}{\hat{x}^2+\hat{y}^2+\hat{z}^2} ddxdydz \tag{A.81}$$

$$e^{(1)}_{220} = \frac{4}{3(2\pi^3)} \int_{-\pi}^{\pi}\int_{-\pi}^{\pi}\int_{-\pi}^{\pi} \frac{c_2(x,y,z)^2}{\hat{x}^2+\hat{y}^2+\hat{z}^2} dxdydz \tag{A.82}$$

$$e^{(1)}_{221} = \frac{4}{3(2\pi^3)} \int_{-\pi}^{\pi}\int_{-\pi}^{\pi}\int_{-\pi}^{\pi} \frac{2c_2(x,y,z)c_3(x,y,z)}{\hat{x}^2+\hat{y}^2+\hat{z}^2} ddxdydz \tag{A.83}$$

$$e^{(1)}_{222} = \frac{4}{3(2\pi^3)} \int_{-\pi}^{\pi}\int_{-\pi}^{\pi}\int_{-\pi}^{\pi} \frac{c_3(x,y,z)^2}{\hat{x}^2+\hat{y}^2+\hat{z}^2} dxdydz \tag{A.84}$$

with

$$c_1(x,y,z) = -\frac{1}{6}(\hat{x}^2+\hat{y}^2+\hat{z}^2)$$

$$c_2(x,y,z) = -\frac{1}{6}(\hat{x}^2+\hat{y}^2+\hat{z}^2) + \frac{1}{12}(\hat{x}^2\hat{y}^2+\hat{x}^2\hat{z}^2+\hat{y}^2\hat{z}^2)$$

$$c_3(x,y,z) = -\frac{1}{6}(\hat{x}^2+\hat{y}^2+\hat{z}^2) - \frac{1}{8}\hat{x}^2\hat{y}^2\hat{z}^2 + \frac{1}{6}(\hat{x}^2\hat{y}^2+\hat{x}^2\hat{z}^2+\hat{y}^2\hat{z}^2)$$

and, with a = 1

$$\hat{x} = 2\sin\frac{\mathrm{x}}{2}$$

$$\hat{y} = 2\sin\frac{\mathrm{y}}{2}$$

$$\hat{z} = 2\sin\frac{\mathrm{z}}{2}$$

A.7 Coefficients $w_{\mathrm{t,s}}^{k_1k_2k_3}$

$$w_{\mathrm{t}}^{000} = 1 \ , \tag{A.85}$$

$$w_{\mathrm{t}}^{100} = -\frac{1}{3}\left(\hat{p}_1^2+\hat{p}_2^2+\hat{p}_3^2\right) \ , \tag{A.86}$$

$$w_{\mathrm{t}}^{110} = -\frac{1}{3}\left(\hat{p}_1^2+\hat{p}_2^2+\hat{p}_3^2\right)+\frac{1}{6}\left(\hat{p}_1^2\hat{p}_2^2+\hat{p}_1^2\hat{p}_3^2+\hat{p}_2^2\hat{p}_3^2\right) \ , \tag{A.87}$$

$$w_{\mathrm{t}}^{111} = -\frac{1}{3}\left(\hat{p}_1^2+\hat{p}_2^2+\hat{p}_3^2\right)+\frac{1}{3}\left(\hat{p}_1^2\hat{p}_2^2+\hat{p}_1^2\hat{p}_3^2+\hat{p}_2^2\hat{p}_3^2\right)-\frac{1}{4}\,\hat{p}_1^2\hat{p}_2^2\hat{p}_3^2 \ , \tag{A.88}$$

$$w_{\mathrm{t}}^{200} = \frac{1}{36}\left(\hat{p}_1^4+\hat{p}_2^4+\hat{p}_3^4\right)+\frac{1}{18}\left(\hat{p}_1^2\hat{p}_2^2+\hat{p}_1^2\hat{p}_3^2+\hat{p}_2^2\hat{p}_3^2\right) \ , \tag{A.89}$$

$$\begin{aligned} w_{\mathrm{t}}^{210} = {} & \frac{1}{18}(\hat{p}_1^4+\hat{p}_2^4+\hat{p}_3^4)+\frac{1}{9}\left(\hat{p}_1^2\hat{p}_2^2+\hat{p}_1^2\hat{p}_3^2+\hat{p}_2^2\hat{p}_3^2\right)- \\ & -\frac{1}{36}\left(\hat{p}_1^4\hat{p}_2^2+\hat{p}_1^4\hat{p}_3^2+\hat{p}_2^4\hat{p}_1^2+\hat{p}_2^4\hat{p}_3^2+\hat{p}_3^4\hat{p}_1^2+\hat{p}_3^4\hat{p}_2^2\right)-\frac{1}{12}\,\hat{p}_1^2\hat{p}_2^2\hat{p}_3^2 \ , \end{aligned} \tag{A.90}$$

$$\begin{aligned} w_{\mathrm{t}}^{211} = {} & \frac{1}{18}\left(\hat{p}_1^4+\hat{p}_2^4+\hat{p}_3^4\right)+\frac{1}{9}\left(\hat{p}_1^2\hat{p}_2^2+\hat{p}_1^2\hat{p}_3^2+\hat{p}_2^2\hat{p}_3^2\right)- \\ & -\frac{1}{18}\left(\hat{p}_1^4\hat{p}_2^2+\hat{p}_1^4\hat{p}_3^2+\hat{p}_2^4\hat{p}_1^2+\hat{p}_2^4\hat{p}_3^2+\hat{p}_3^4\hat{p}_1^2+\hat{p}_3^4\hat{p}_2^2\right)-\frac{1}{6}\,\hat{p}_1^2\hat{p}_2^2\hat{p}_3^2+ \\ & +\frac{1}{24}\left(\hat{p}_1^4\hat{p}_2^2\hat{p}_3^2+\hat{p}_2^4\hat{p}_1^2\hat{p}_3^2+\hat{p}_3^4\hat{p}_1^2\hat{p}_2^2\right) \ , \end{aligned} \tag{A.91}$$

$$\begin{aligned} w_{\mathrm{t}}^{220} = {} & \frac{1}{36}\left(\hat{p}_1^4+\hat{p}_2^4+\hat{p}_3^4\right)+\frac{1}{18}\left(\,\hat{p}_1^2\hat{p}_2^2+\hat{p}_1^2\hat{p}_3^2+\hat{p}_2^2\hat{p}_3^2\right)-\frac{1}{12}\,\hat{p}_1^2\hat{p}_2^2\hat{p}_3^2- \\ & -\frac{1}{36}\left(\hat{p}_1^4\hat{p}_2^2+\hat{p}_1^4\hat{p}_3^2+\hat{p}_2^4\hat{p}_1^2+\,\hat{p}_2^4\hat{p}_3^2+\hat{p}_3^4\hat{p}_1^2+\hat{p}_3^4\hat{p}_2^2\right)+ \\ & +\frac{1}{72}\left(\hat{p}_1^4\hat{p}_2^2\hat{p}_3^2+\hat{p}_2^4\hat{p}_1^2\hat{p}_3^2+\hat{p}_3^4\hat{p}_1^2\hat{p}_2^2\right)+\frac{1}{144}\left(\hat{p}_1^4\hat{p}_2^4+\hat{p}_1^4\hat{p}_3^4+\hat{p}_2^4\hat{p}_3^4\right) \ , \end{aligned} \tag{A.92}$$

$$\begin{aligned} w_{\mathrm{t}}^{221} = {} & \frac{1}{18}\left(\hat{p}_1^4+\hat{p}_2^4+\hat{p}_3^4\right)+\frac{1}{9}\left(\hat{p}_1^2\hat{p}_2^2+\hat{p}_1^2\hat{p}_3^2+\hat{p}_2^2\hat{p}_3^2\right)- \\ & -\frac{1}{12}\left(\hat{p}_1^4\hat{p}_2^2+\hat{p}_1^4\hat{p}_3^2+\hat{p}_2^4\hat{p}_1^2+\hat{p}_2^4\hat{p}_3^2+\hat{p}_3^4\hat{p}_1^2+\hat{p}_3^4\hat{p}_2^2\right)-\frac{1}{4}\,\hat{p}_1^2\hat{p}_2^2\hat{p}_3^2+ \\ & +\frac{1}{36}\left(\hat{p}_1^4\hat{p}_2^4+\hat{p}_1^4\hat{p}_3^4+\hat{p}_2^4\hat{p}_3^4\right)+\frac{7}{72}\left(\hat{p}_1^4\hat{p}_2^2\hat{p}_3^2+\hat{p}_2^4\hat{p}_1^2\hat{p}_3^2+\hat{p}_3^4\hat{p}_1^2\hat{p}_2^2\right)- \\ & -\frac{1}{48}\left(\hat{p}_1^4\hat{p}_2^4\hat{p}_3^2+\hat{p}_1^4\hat{p}_3^4\hat{p}_2^2+\hat{p}_2^4\hat{p}_3^4\hat{p}_1^2\right) \ , \end{aligned} \tag{A.93}$$

$$\begin{aligned} w_{\mathrm{t}}^{222} = {} & \frac{1}{36}\left(\hat{p}_1^4+\hat{p}_2^4+\hat{p}_3^4\right)+\frac{1}{18}\left(\hat{p}_1^2\hat{p}_2^2+\hat{p}_1^2\hat{p}_3^2+\hat{p}_2^2\hat{p}_3^2\right)- \\ & -\frac{1}{6}\,\hat{p}_1^2\hat{p}_2^2\hat{p}_3^2-\frac{1}{18}\left(\hat{p}_1^4\hat{p}_2^2+\hat{p}_1^4\hat{p}_3^2+\hat{p}_2^4\hat{p}_1^2+\hat{p}_2^4\hat{p}_3^2+\hat{p}_3^4\hat{p}_1^2+\hat{p}_3^4\hat{p}_2^2\right)+ \\ & +\frac{1}{36}\left(\hat{p}_1^4\hat{p}_2^4+\hat{p}_1^4\hat{p}_3^4+\hat{p}_2^4\hat{p}_3^4\right)+\frac{7}{72}\left(\hat{p}_1^4\hat{p}_2^2\hat{p}_3^2+\hat{p}_2^4\hat{p}_1^2\hat{p}_3^2+\hat{p}_3^4\hat{p}_1^2\hat{p}_2^2\right)- \\ & -\frac{1}{24}\left(\hat{p}_1^4\hat{p}_2^4\hat{p}_3^2+\hat{p}_1^4\hat{p}_3^4\hat{p}_2^2+\hat{p}_2^4\hat{p}_3^4\hat{p}_1^2\right)\ +\frac{1}{64}\,\hat{p}_1^4\hat{p}_2^4\hat{p}_3^4 \ . \end{aligned} \tag{A.94}$$

$$w_{\rm s}^{200} = \frac{1}{18}\,(\hat{p}_1^2+\hat{p}_2^2+\hat{p}_3^2)\ , \tag{A.95}$$

$$w_{\rm s}^{210} = \frac{1}{9}\,(\hat{p}_1^2+\hat{p}_2^2+\hat{p}_3^2) - \frac{1}{18}\,(\hat{p}_1^2\hat{p}_2^2+\hat{p}_1^2\hat{p}_3^2+\hat{p}_2^2\hat{p}_3^2)\ , \tag{A.96}$$

$$w_{\rm s}^{211} = \frac{1}{9}\,(\hat{p}_1^2+\hat{p}_2^2+\hat{p}_3^2) - \frac{1}{9}(\,\hat{p}_1^2\hat{p}_2^2+\hat{p}_1^2\hat{p}_3^2+\hat{p}_2^2\hat{p}_3^2) + \frac{1}{12}\,\hat{p}_1^2\hat{p}_2^2\hat{p}_3^2\ , \tag{A.97}$$

$$\begin{aligned} w_{\rm s}^{220} = {}& \frac{1}{9}\,(\hat{p}_1^2+\hat{p}_2^2+\hat{p}_3^2) - \frac{1}{9}\,(\hat{p}_1^2\hat{p}_2^2+\hat{p}_1^2\hat{p}_3^2+\hat{p}_2^2\hat{p}_3^2) + \\ & + \frac{1}{144}\,(\hat{p}_1^4\hat{p}_2^2+\hat{p}_1^4\hat{p}_3^2+\hat{p}_2^4\hat{p}_1^2+\hat{p}_2^4\hat{p}_3^2+\hat{p}_3^4\hat{p}_1^2+\hat{p}_3^4\hat{p}_2^2) + \frac{1}{24}\,\hat{p}_1^2\hat{p}_2^2\hat{p}_3^2\ , \end{aligned} \tag{A.98}$$

$$\begin{aligned} w_{\rm s}^{221} = {}& \frac{2}{9}\,(\hat{p}_1^2+\hat{p}_2^2+\hat{p}_3^2) - \frac{1}{3}\,(\hat{p}_1^2\hat{p}_2^2+\hat{p}_1^2\hat{p}_3^2+\hat{p}_2^2\hat{p}_3^2) + \\ & + \frac{1}{36}\,(\hat{p}_1^4\hat{p}_2^2+\hat{p}_1^4\hat{p}_3^2+\hat{p}_2^4\hat{p}_1^2+\hat{p}_2^4\hat{p}_3^2+\hat{p}_3^4\hat{p}_1^2+\hat{p}_3^4\hat{p}_2^2) + \frac{1}{3}\,\hat{p}_1^2\hat{p}_2^2\hat{p}_3^2 - \\ & - \frac{1}{36}\,(\hat{p}_1^4\hat{p}_2^2\hat{p}_3^2+\hat{p}_2^4\hat{p}_1^2\hat{p}_3^2+\hat{p}_3^4\hat{p}_1^2\hat{p}_2^2)\ , \end{aligned} \tag{A.99}$$

$$\begin{aligned} w_{\rm s}^{222} = {}& \frac{2}{9}\,(\hat{p}_1^2+\hat{p}_2^2+\hat{p}_3^2) - \frac{4}{9}\,(\hat{p}_1^2\hat{p}_2^2+\hat{p}_1^2\hat{p}_3^2+\hat{p}_2^2\hat{p}_3^2) + \\ & + \frac{1}{18}\,(\hat{p}_1^4\hat{p}_2^2+\hat{p}_1^4\hat{p}_3^2+\hat{p}_2^4\hat{p}_1^2+\hat{p}_2^4\hat{p}_3^2+\hat{p}_3^4\hat{p}_1^2+\hat{p}_3^4\hat{p}_2^2) + \frac{2}{3}\,\hat{p}_1^2\hat{p}_2^2\hat{p}_3^2 + \\ & - \frac{1}{9}\,(\hat{p}_1^4\hat{p}_2^2\hat{p}_3^2+\hat{p}_2^4\hat{p}_1^2\hat{p}_3^2+\hat{p}_3^4\hat{p}_1^2\hat{p}_2^2) + \frac{1}{72}\,(\hat{p}_1^4\hat{p}_2^4\hat{p}_3^2+\hat{p}_1^4\hat{p}_3^4\hat{p}_2^2+\hat{p}_2^4\hat{p}_3^4\hat{p}_1^2)\ . \end{aligned} \tag{A.100}$$

B Appendix

The expansion of the Wilson-Dirac operator is given by

$$D\Psi(x) = \sum_{k=0}^{\infty} g_0^k (D^{(k)} + \delta D_V^{(k)})\Psi(x) \tag{B.1}$$

In time momentum representation, i.e. with

$$q_0^a(x) = L^{-3} \sum_{\mathbf{p}} e^{i\mathbf{px}} \tilde{q}_0^a(x_0, \mathbf{p}) \tag{B.2}$$

$$q_0^a(x) = L^{-3} \sum_{\mathbf{p}} e^{i\mathbf{px}} e^{\frac{i}{2}ap_k} \tilde{q}_0^a(x_0, \mathbf{p}) \tag{B.3}$$

$$\Psi(x) = L^{-3} \sum_{\mathbf{p}} e^{i\mathbf{px}} \tilde{\Psi}(x_0, \mathbf{p}) \tag{B.4}$$

the action of the first order correction to the Wilson-Dirac operator is given by

$$\begin{aligned} D^{(1)}\Psi(x) = L^{-6} \sum_{\mathbf{k},\mathbf{p}} e^{i(\mathbf{k}+\mathbf{p})\mathbf{x}} \sum_{i=1}^{5} \tilde{q}_{\mu(i)}^a(x_0 + at(i); \mathbf{k}) \\ \times T^a V_i^{(1)}(\mathbf{k}, \mathbf{p}) \tilde{\Psi}(x_0 + as(i); \mathbf{p}) \end{aligned} \tag{B.5}$$

$$\begin{aligned} \delta D_V^{(1)}\Psi(x) = L^{-6} \sum_{\mathbf{k},\mathbf{p}} e^{i(\mathbf{k}+\mathbf{p})\mathbf{x}} \sum_{i=6}^{16} \tilde{q}_{\mu(i)}^a(x_0 + at(i); \mathbf{k}) \\ \times T^a V_i^{(1)}(\mathbf{k}, \mathbf{p}) \tilde{\Psi}(x_0 + as(i); \mathbf{p}) \end{aligned} \tag{B.6}$$

$$\tag{B.7}$$

with the values $t(i)$, $s(i)$, $\mu(i)$ and $V_i^{(1)}$ given in Table 7.

The action of the second order term reads

$$\begin{aligned} D^{(2)}\Psi(x) = L^{-6} \sum_{\mathbf{k},\mathbf{p}} e^{i(\mathbf{k}+\mathbf{p})\mathbf{x}} \sum_{i=1}^{5} \tilde{q}_{\mu(i)}^a(x_0 + at(i); \mathbf{k}) \tilde{q}_{\mu(i)}^b(x_0 + at(i); \mathbf{k}) \\ \times T^a T^b V_i^{(2)}(\mathbf{k}, \mathbf{q}, \mathbf{p}) \tilde{\Psi}(x_0 + as(i); \mathbf{p}) \end{aligned} \tag{B.8}$$

$$\tag{B.9}$$

The data for this vertex are collected in Table 8.

i	$\mu(i)$	$t(i)$	$s(i)$	$V_i^{(1)}(\mathbf{p},\mathbf{k})$
1	0	0	1	$-\frac{1}{2}(\mathbb{1}-\gamma_0)$
2	0	-1	-1	$\frac{1}{2}(\mathbb{1}+\gamma_0)$
3	1	0	0	$\cos(\mathrm{ar}_1)\gamma_1 - \mathrm{i}\sin(\mathrm{ar}_1)\mathbb{1}$
4	2	0	0	$\cos(\mathrm{ar}_2)\gamma_2 - \mathrm{i}\sin(\mathrm{ar}_2)\mathbb{1}$
5	3	0	0	$\cos(\mathrm{ar}_3)\gamma_3 - \mathrm{i}\sin(\mathrm{ar}_3)\mathbb{1}$
6	0	0	0	$c_{sw}^{(0)}\frac{1}{4}\sigma_{0l}a\bar{k}_l$
7	0	-1	0	${c_{\mathrm{sw}}}^{(0)}\frac{1}{4}\sigma_{0l}a\bar{k}_l$
8	1	1	0	${c_{\mathrm{sw}}}^{(0)}\frac{i}{4}\sigma_{01}\cos(\frac{1}{2}\mathrm{ak}_1)$
9	2	1	0	${c_{\mathrm{sw}}}^{(0)}\frac{i}{4}\sigma_{01}\cos(\frac{1}{2}\mathrm{ak}_2)$
10	3	1	0	${c_{\mathrm{sw}}}^{(0)}\frac{i}{4}\sigma_{01}\cos(\frac{1}{2}\mathrm{ak}_3)$
11	1	-1	0	${c_{\mathrm{sw}}}^{(0)}\frac{i}{4}\sigma_{01}\cos(\frac{1}{2}\mathrm{ak}_1)$
12	2	-1	0	${c_{\mathrm{sw}}}^{(0)}\frac{i}{4}\sigma_{01}\cos(\frac{1}{2}\mathrm{ak}_2)$
13	3	-1	0	${c_{\mathrm{sw}}}^{(0)}\frac{i}{4}\sigma_{01}\cos(\frac{1}{2}\mathrm{ak}_3)$
14	1	0	0	${c_{\mathrm{sw}}}^{(0)}\frac{1}{2}\sigma_{0l}a\bar{k}_l\cos(\frac{1}{2}\mathrm{ak}_1)$
15	2	0	0	${c_{\mathrm{sw}}}^{(0)}\frac{1}{2}\sigma_{0l}a\bar{k}_l\cos(\frac{1}{2}\mathrm{ak}_1)$
16	3	0	0	${c_{\mathrm{sw}}}^{(0)}\frac{1}{2}\sigma_{0l}a\bar{k}_l\cos(\frac{1}{2}\mathrm{ak}_1)$

Table 7: Factors for the relativistic three-point quark-gluon vertex. The vertices 6 to 16 denote the SW improvement term in $\delta D_V^{(1)}$. $r_l = \frac{1}{2}k_l + p_l + \Theta_l/L$, $\bar{k} = \frac{1}{a}\sin(\mathrm{ak_l})$

i	$\mu(i)$	$t(i)$	$s(i)$	$\frac{2}{a}V_i^{(2)}(\mathbf{p},\mathbf{k},\mathbf{q})$
1	0	0	1	$-\frac{1}{2}(\mathbf{1}-\gamma_0)$
2	0	-1	-1	$-\frac{1}{2}(\mathbf{1}+\gamma_0)$
3	1	0	0	$i\sin(\mathrm{ar}_1)\gamma_1 - \cos(\mathrm{ar}_1)\mathbf{1}$
4	2	0	0	$i\sin(\mathrm{ar}_2)\gamma_2 - \cos(\mathrm{ar}_2)\mathbf{1}$
5	3	0	0	$i\sin(\mathrm{ar}_3)\gamma_3 - \cos(\mathrm{ar}_3)\mathbf{1}$

Table 8: Factors for the relativistic four-point quark-gluon vertex. $r_l = \frac{1}{2}(k_l + q_l) + p_l + \Theta_l/L$

C Appendix

	$LX_b^{(1)}$	$LX_{\delta A}^{(0)}$
EH, $\Theta = 0.5$	-0.56643046892042	0.01453419408366
EH, $\Theta = 1.0$	-1.71824482838356	0.02120541331543
HYP1, $\Theta = 0.5$	-0.56643046892042	0.01453419408366
HYP1, $\Theta = 1.0$	-1.71824482838356	0.02120541331543
HYP2, $\Theta = 0.5$	-0.56643046892042	0.01453419408366
HYP2, $\Theta = 1.0$	-1.71824482838356	0.02120541331543

Table 9: Simulation Results for boundary and improvement terms.

$\frac{T}{a}$	$\Theta = 0.5$	$\Theta = 1.0$
6	0.10587546124379	-0.03937388724916
8	0.07236792382030	-0.07176509596794
10	0.02314305322217	-0.08983254127042
12	-0.00757174459876	-0.09843610627536
14	-0.02625601334030	-0.10199380079393
16	-0.03807843126100	-0.10316294560661
18	-0.04602555182289	-0.10325215201789
20	-0.05169513424162	-0.10286932970777
22	-0.05594606338283	-0.10229260450018
24	-0.05925883372555	-0.10164920489914
26	-0.06191734585859	-0.10164920489914
28	-0.06409924564530	-0.10036335850358
30	-0.06592176144124	-0.09975846635136
32	-0.06746580022811	-0.09918674026393
34	-0.06878931813186	-0.09864878718531
36	-0.06993511884647	-0.09814355277797
38	-0.07093559747168	-0.09766922426179
40	-0.07181569671001	-0.09722373884971
42	-0.07259510372010	-0.09680496164796
44	-0.07328942449105	-0.09641078937692
46	-0.07391108923837	-0.09603929555343

Table 10: Simulation Results for $c_{\mathrm{A}}^{\mathrm{stat}(1)}$, EH action

$\frac{T}{a}$	$\Theta = 0.5$	$\Theta = 1.0$
6	0.11431925405843	0.02004430645987
8	0.10243955923002	0.00786933421361
10	0.07377175306511	-0.00021092775684
12	0.05527361311042	-0.00490048280899
14	0.04315057291348	-0.00740353669985
16	0.03493755970306	-0.00866492495002
18	0.02914437304804	-0.00923660768366
20	0.02489443002096	-0.00942505096930
22	0.02166690308152	-0.00939941293226
24	0.01914357856632	-0.00925404222636
26	0.01712301359960	-0.00904251117053
28	0.01547286006205	-0.00879586141039
30	0.01410302833119	-0.00853241823123
32	0.01295023891214	-0.00826314784015
34	0.01196874061646	-0.00799467237580
36	0.01112468155189	-0.00773095489854
38	0.01039245536252	-0.00747432588723
40	0.00975237059167	-0.00722611181359
42	0.00918896640921	-0.00698696069308
44	0.00869004245312	-0.00675710372029
46	0.00824587212013	-0.00653653820743

Table 11: Simulation Results for $c_{\mathrm{A}}^{\mathrm{stat}(1)}$, HYP1 action

$\frac{T}{a}$	$\Theta = 0.5$	$\Theta = 1.0$
6	0.11741337754619	0.04943795298004
8	0.10656005707018	0.04585703271613
10	0.08907324547597	0.04442539109683
12	0.07942390945063	0.04336520564278
14	0.07289030190505	0.04254126090744
16	0.06816407184843	0.04197802399245
18	0.06467377813074	0.04165861645970
20	0.06206021904560	0.04152985604260
22	0.06007276654325	0.04153525855129
24	0.05853563870254	0.04162923762923
26	0.05732636035165	0.04177901771530
28	0.05635954203736	0.04196229152533
30	0.05557514241833	0.04216428268900
32	0.05493039649333	0.04237534271438
34	0.05439430141166	0.04258920838812
36	0.05394404498936	0.04280187422691
38	0.05356251768684	0.04301080593755
40	0.05323669697001	0.04321441512898
42	0.05295648320754	0.04341179192899
44	0.05271403793332	0.04360245657414
46	0.05250317883117	0.04378617359738

Table 12: Simulation Results for $c_{\mathrm{A}}^{\mathrm{stat}\,(1)}$, HYP2 action

n_v	$c^{stat(1)}A, \Theta = 0.5(n_{values})$	$\chi^2_{\Theta=0.5}(n_{values})$	$c^{stat(1)}A, \Theta = 1.0(n_{values})$	$\chi^2_{\Theta=1.0}(n_{values})$
4	-8.216037e-02	4.923732e-26	-8.286116e-02	2.548602e-23
5	-8.271515e-02	6.934475e-16	-8.278339e-02	1.362813e-17
6	-8.310171e-02	4.140410e-15	-8.284896e-02	1.127918e-16
7	-8.329677e-02	9.157752e-15	-8.295707e-02	1.654282e-15
8	-8.349440e-02	3.087351e-14	-8.307056e-02	8.814330e-15
9	-8.374021e-02	1.474620e-13	-8.321349e-02	4.823367e-14
10	-8.406949e-02	7.810305e-13	-8.340867e-02	2.708344e-13
11	-8.453496e-02	4.247922e-12	-8.368127e-02	1.459923e-12
12	-8.521184e-02	2.284226e-11	-8.407309e-02	7.690505e-12
13	-8.620460e-02	1.184330e-10	-8.464624e-02	3.955225e-11
14	-8.765825e-02	5.861053e-10	-8.548943e-02	1.969032e-10
15	-8.974087e-02	2.699795e-09	-8.671602e-02	9.301084e-10
16	-9.255123e-02	1.095281e-08	-8.843107e-02	4.003663e-09
17	-9.581910e-02	3.444506e-08	-9.060901e-02	1.443850e-08
18	-9.810185e-02	5.833341e-08	-9.274443e-02	3.534273e-08
19	-9.502142e-02	1.488460e-07	-9.300937e-02	3.601228e-08
20	-7.723542e-02	6.483301e-06	-8.666260e-02	8.426097e-07
21	-5.248973e-03	2.293162e-04	-6.836198e-02	1.524417e-05

Table 13: EH action, $lim_{\frac{a}{L}\to 0} c_{\mathrm{A}}^{\mathrm{stat}\,(1)}(n_v)$ for different number of values n_v used for the fit

n_v	$c^{stat(1)}A, \Theta = 0.5(n_{values})$	$\chi^2_{\Theta=0.5}(n_{values})$	$c^{stat(1)}A, \Theta = 1.0(n_{values})$	$\chi^2_{\Theta=1.0}(n_{values})$
4	3.098172e-03	5.047339e-25	2.804598e-03	3.636957e-25
5	2.824599e-03	1.686250e-16	2.850314e-03	4.708825e-18
6	2.586748e-03	1.473611e-15	2.834554e-03	1.043795e-17
7	2.456087e-03	3.724973e-15	2.777080e-03	4.460532e-16
8	2.337974e-03	1.148107e-14	2.714752e-03	2.605842e-15
9	2.206514e-03	4.482701e-14	2.642865e-03	1.257734e-14
10	2.040216e-03	2.064285e-13	2.551244e-03	6.162929e-14
11	1.828736e-03	9.220796e-13	2.435325e-03	2.766474e-13
12	1.555937e-03	3.942300e-12	2.287543e-03	1.162975e-12
13	1.209253e-03	1.559957e-11	2.100666e-03	4.550197e-12
14	7.849463e-04	5.544492e-11	1.872007e-03	1.612173e-11
15	3.092126e-04	1.657389e-10	1.613945e-03	4.857602e-11
16	-1.111749e-04	3.504052e-10	1.378222e-03	1.066385e-10
17	-1.829306e-04	3.617321e-10	1.304983e-03	1.184384e-10
18	7.690444e-04	4.516236e-09	1.711369e-03	8.755256e-10
19	4.062309e-03	1.079686e-07	3.241987e-03	2.322262e-08
20	1.135251e-02	1.172189e-06	7.217617e-03	3.397157e-07
21	5.331423e-02	7.688763e-05	1.379604e-02	2.200610e-06

Table 14: HYP1 action, $lim_{\frac{a}{L}\to 0} c_{\mathrm{A}}^{\mathrm{stat}\,(1)}(n_v)$ for different number of values n_v used for the fit

n_v	$c^{stat(1)}A, \Theta = 0.5(n_{values})$	$\chi^2_{\Theta=0.5}(n_{values})$	$c^{stat(1)}A, \Theta = 1.0(n_{values})$	$\chi^2_{\Theta=1.0}(n_{values})$
4	5.194354e-02	4.204172e-25	5.176522e-02	3.566726e-24
5	5.179670e-02	4.857595e-17	5.185456e-02	1.798371e-17
6	5.161176e-02	8.376029e-16	5.186910e-02	2.285887e-17
7	5.150914e-02	2.226137e-15	5.183892e-02	1.429582e-16
8	5.144042e-02	4.851947e-15	5.181506e-02	4.596207e-16
9	5.139019e-02	9.720498e-15	5.179924e-02	9.424758e-16
10	5.134772e-02	2.025894e-14	5.178988e-02	1.453559e-15
11	5.132809e-02	2.642669e-14	5.179780e-02	2.455515e-15
12	5.135610e-02	5.826436e-14	5.183989e-02	7.435619e-14
13	5.148115e-02	1.575111e-12	5.194697e-02	1.186484e-12
14	5.178674e-02	2.224248e-11	5.217227e-02	1.242091e-11
15	5.240017e-02	2.056204e-10	5.260064e-02	1.018451e-10
16	5.348190e-02	1.428355e-09	5.335012e-02	6.888089e-10
17	5.513196e-02	7.417912e-09	5.453557e-02	3.780278e-09
18	5.705959e-02	2.445174e-08	5.611815e-02	1.526178e-08
19	5.776888e-02	2.925058e-08	5.753464e-02	3.440042e-08
20	5.345103e-02	4.025756e-07	5.746834e-02	3.448843e-08
21	7.317357e-02	1.712902e-05	5.399009e-02	5.547240e-07

Table 15: HYP2 action, $lim_{\frac{a}{L}\to 0} c_{\mathrm{A}}^{\mathrm{stat}\,(1)}(n_v)$ for different number of values n_v used for the fit

Acknowledgements

I would like to thank Francesco Knechtli for introducing me into lattice gauge theories and into theoretical physics at all.

I would also like to express my thanks to Filippo Palombi for providing his C++ program codes and for always having an open ear to my questions. Without his help, this thesis would not have been possible in this form. Thanks to Damiano Guazzini for his ingenious ideas and to Roland Hoffmann for providing his Mathematica code to me.

Cordial thanks to my family for supporting me, especially to Patty and Tiago for their patience.

References

[1] M. Kurth and R. Sommer [ALPHA Collaboration], "Renormalization and O(a)-improvement of the static axial current," Nucl. Phys. B **597**, 488 (2001) [arXiv:hep-lat/0007002].

[2] M. Luscher, R. Narayanan, P. Weisz and U. Wolff, "The Schrodinger functional: A Renormalizable probe for nonAbelian gauge," theories, Nucl. Phys. B **384** (1992) 168 [arXiv:hep-lat/9207009].

[3] M. Luscher, "Solution of the free Dirac equation on the lattice," unpublished notes, September 1995

[4] M. Luscher, S. Sint, R. Sommer and P. Weisz, "Chiral symmetry and O(a) improvement in lattice QCD," Nucl. Phys. B **478** (1996) 365 [arXiv:hep-lat/9605038].

[5] M. Luscher, "Advanced lattice QCD," arXiv:hep-lat/9802029.

[6] M. Lüscher, "Improved axial current at one-loop order in perturbation theory", private notes, April 1996

[7] R. Sommer, "Non-perturbative QCD: Renormalization, O(a)-improvement and matching to heavy quark effective theory," arXiv:hep-lat/0611020.

[8] C.Pena, DESY, "Perturbative renormalisation of two- and four-quark operators in SF schemes," Internal notes, October 2003

[9] M. Luscher and P. Weisz, "O(a) improvement of the axial current in lattice QCD to one-loop order of perturbation theory," Nucl. Phys. B **479** (1996) 429 [arXiv:hep-lat/9606016].

[10] A. Hasenfratz and F. Knechtli, "Flavor symmetry and the static potential with hypercubic blocking," Phys. Rev. D **64** (2001) 034504 [arXiv:hep-lat/0103029].

[11] A. Hasenfratz, R. Hoffmann and F. Knechtli, "The static potential with hypercubic blocking," Nucl. Phys. Proc. Suppl. **106** (2002) 418 [arXiv:hep-lat/0110168].

[12] M. Della Morte, N. Garron, M. Papinutto and R. Sommer, "Heavy quark effective theory computation of the mass of the bottom quark," JHEP **0701** (2007) 007 [arXiv:hep-ph/0609294].

[13] M. Della Morte, A. Shindler and R. Sommer, "On lattice actions for static quarks," JHEP **0508** (2005) 051 [arXiv:hep-lat/0506008].

[14] M. Della Morte, S. Durr, J. Heitger, H. Molke, J. Rolf, A. Shindler and R. Sommer [ALPHA Collaboration], "Lattice HQET with exponentially improved statistical precision," Phys. Lett. B **581** (2004) 93 [Erratum-ibid. B **612** (2005) 313] [arXiv:hep-lat/0307021].

[15] E. Eichten and B. R. Hill, "An Effective Field Theory for the Calculation of Matrix Elements Involving Heavy Quarks," Phys. Lett. B **234** (1990) 511.

[16] W. j. Lee, "Perturbative improvement of staggered fermions using fat links," Phys. Rev. D **66** (2002) 114504 [arXiv:hep-lat/0208032].

[17] F. Palombi, R. Petronzio and A. Shindler, "Moments of singlet parton densities on the lattice in the Schroedinger functional scheme," Nucl. Phys. B **637** (2002) 243 [arXiv:hep-lat/0203002].

[18] "I.Montvay, G.Muenster", Quantum fields on a lattice, Cambridge Univ. Press ,1997

[19] H.J.Rothe, ",Lattice gauge theories - An Introduction", World Scientific, Singapore, New Jersey, London, Hong Kong (1992)

[20] M.Creutz, "Quarks, gluons and lattices ", Cambridge Univ. Pr. , 1988

[21] S. Sint, "On the Schrodinger functional in QCD," Nucl. Phys. B **421** (1994) 135 [arXiv:hep-lat/9312079].

[22] A.Grimbach, D.Guazzini, F.Knechtli. F.Palombi, "O(a) improvement of the HYP static axial and vector currents at one-loop order of pertubation theory," [arXiv:0802.0862 [hep-lat]].

[23] M. Della Morte, "Standard Model parameters and heavy quarks on the lattice," PoS **LAT2007** (2007) 008 [arXiv:0711.3160 [hep-lat]].

[24] K. Symanzik "Some topics in quantum field theory" in: Mathematical problems in theoretical physics, eds. R.Schrader et al., Lecture notes in Physics, Vol 153 (springer, New York, 1982)

[25] K. Symanzik Nucl. Phys. B **226** (1993) 187 and 205